NOVEL NEUROBLASTOMA DIFFERENTIATING AGENTS

by

Breana Laguera, B.S.

A thesis submitted to the Graduate Council of
Texas State University in partial fulfillment
of the requirements for the degree of
Master of Science
with a Major in Biochemistry
May 2020

Committee Members:

Alexander Kornienko, Chair

Liqin Du

Tania Betancourt

COPYRIGHT

by

Breana Laguera

2020

FAIR USE AND AUTHOR'S PERMISSION STATEMENT

Fair Use

This work is protected by the Copyright Laws of the United States (Public Law 94-553, section 107). Consistent with fair use as defined in the Copyright Laws, brief quotations from this material are allowed with proper acknowledgement. Use of this material for financial gain without the author's express written permission is not allowed.

Duplication Permission

As the copyright holder of this work I, Breana Laguera, authorize duplication of this work, in whole or in part, for educational or scholarly purposes only.

ACKNOWLEDGEMENTS

Thank you to my research advisor, Dr. Alexander Kornienko, for the opportunity to work in his lab. I would like to thank my committee members, Dr. Tania Betancourt and Dr. Liqin Du, for their support and guidance throughout my project. I would also like to thank everyone in the Kornienko research group for their collaboration and support.

Thank you to the South Texas Doctoral Bridge Program Committee, Dr. Raquel Salinas, Dr. Carolyn Chang, Dr. Ronald Walter, Dr. Nicquet Blake, and Dr. Oyajobi for allowing me to be a part of this incredible program. Your continual support and advice have helped me navigate and prepare for my future studies. I am endlessly grateful.

TABLE OF CONTENTS

Page

ACKNOWLEDGEMENTS iv

LIST OF FIGURES vii

LIST OF SCHEMES viii

LIST OF ABBREVIATIONS x

ABSTRACT xi

CHAPTER

I. INTRODUCTION 1

a. Neuroblastoma is a deadly pediatric cancer 1
b. The origin of neuroblastoma 2
c. Differentiation therapy 3
d. Resistance to RA and MYCN amplification 4
e. Other neuroblastoma differentiating agents 6
f. Advantages of the use of small molecule-drugs for NB treatment 7
g. Small-molecule screening 8
h. Structure-Activity Relationship 11
i. Identifying a novel NB differentiating agent 12
j. Project aims 15

II. EXPERIMENTAL 17

a. Synthesis 17
b. Biological methods 32

III. RESULTS AND DISCUSSION 33

a. Synthesis 33
b. Biological evaluation and SAR analysis 39

IV. CONCLUSION AND FUTURE DIRECTIONS 43

APPENDIX SECTION.....45

REFERENCES 81

LIST OF FIGURES

Figure **Page**

1. Differentiation pathway 3

2. General structures for bromodomain inhibitors 7

3. BE(2)-C cell neurite outgrowth quantification 10

4. Example of privileged structures 11

5. Compound #3 13

6. Comparison of tested compounds in HCS 14

7. Biological activity of BL-X1 and compound #3 34

8. ChemBridge compounds 35

9. Synthesis of sulfonamides 37

10. Disulfonyl analogues 38

11. Dose-dependent neurite outgrowth curve of BL-X compounds 41

12. Dose-dependent cell viability curve of BL-X compounds 42

LIST OF SCHEMES

Scheme **Page**

1. Proposed synthetic method of BL-X1.....15

2. BL-01.....17

3. BL-02.....18

4. BL-X1.....18

5. BL-X2.....19

6. BL-X3.....20

7. BL-X4.....20

8. B2-X4.....21

9. BL-X5.....22

10. BL-X6.....22

11. BL-X7.....23

12. BL-X8.....24

13. BL-X10.....25

14. BL-X11.....25

15. BL-X12.....26

16. BL-X13.....27

17. BL-X14.....28

18. BL-X15.....28

19. BL-X16.....29

20. BL-X17 30

21. BL-X30 31

LIST OF ABBREVIATIONS

Abbreviation	Description
NB	Neuroblastoma
HCS	High Content Screening
RA	Retinoic Acid
SAR	Structure-Activity Relationship
INRG	International Neuroblastoma Risk Group
NCPC	Neural Crest Precursor Cells
tNCC	Trunk Neural Crest Cells
PNS	Peripheral Neural Crest Cells
ATRA	All-Trans Retinoic Acid
BBB	Blood-Brain-Barrier
CNS	Central Nervous System
BNB	Blood-Nerve-Barrier
NMR	Nuclear Magnetic Resonance
TLC	Thin Layer Chromatography
MHz	Megahertz
TMS	Tetramethylsilane
DMF	Dimethylformamide

ABSTRACT

Neuroblastoma (NB) is the 3rd most lethal pediatric cancer. In high-risk patients, the 5-year survival rate is 40-50% after treatment. The differentiation therapy with retinoic acid (RA) is at the forefront of approaches to treat neuroblastoma; however, more than half of patients experience recurrence suggesting resistance to RA. There is currently no alternative outside of chemotherapy for patients who have developed resistance to RA; therefore, the purpose of this research is to address this insufficiency by developing novel neuroblastoma differentiating agents. A promising agent will induce differentiation while reducing the cancer cell viability. A high-content screening (HCS) was conducted to identify hit compounds. This screening measured neurite outgrowth, a phenotypic change which has been described as a marker of differentiation in neuroblastoma cell lines. From this screening, three hits that induced the desired changes in cancer cells were identified.

In this work, we present analogues of a hit compound synthesized to increase potency. Currently, the mechanism of induced differentiation is unclear. However, by use of a Structure-Activity Relationship (SAR) study, the pharmacophore of the hit compound has begun to be elucidated. Understanding the chemical groups necessary for activity can give rise to more potent compounds as well as assist in future mode of action studies. Cell viability assays along with neurite outgrowth induced by the analogues of the hit compound are presented here to demonstrate the optimization of the compound potency in the BE(2)-C cell line.

I. INTRODUCTION

a. Neuroblastoma is a deadly pediatric cancer

Neuroblastoma is the 3rd most lethal pediatric cancer accounting for 15% of all childhood cancer-related deaths. [1] The median age of diagnosis is 22 months, and seventy-five percent of neuroblastoma cases occur before the age of five. [1, 2] The manifestation of neuroblastoma-related symptoms can vary widely between patients as tumor site location is found to be disproportionate along the sympathetic nervous system with 65% of primary tumors arising in the adrenal medulla abdomen. The other primary sites are the chest (5% of cases), the neck (1%), and the pelvis (1%). About 1% of patients do not have a clinically detectable primary tumor. [3] Additionally, two-thirds of patients already exhibit spread of the cancer either by lymphatic or hematogenous circulation at the time of diagnosis. The spread of cancer occurs by the detachment of the tumor cells from the primary site and intravasation into blood or lymphatic vessels. The circulating tumor cells then have the ability to exit the vessel at a distant site and, if the conditions are suitable, the cells can proliferate. This event of proliferation at a secondary site is referred to as distant metastasis and is the deadliest phase of cancer progression. [4]

Due to neuroblastoma's characteristic heterogeneity, assessing the patient's diagnosis and treatment has proved clinically challenging. To stage the disease and determine the prognosis, histological tests are performed according to the International Neuroblastoma Risk Group (INRG) classification system. [5] The INRG system, developed on the basis on survival analyses of pretreated patients, considers factors such as the tumors confinement, the involvement of vital structures, metastasis, and the age of the patient. [5] Patients are considered either low, intermediate or high-risk based on their

INRG stage, their age and their expression level of the MYCN oncogene. [6, 7] According to the long-term outcome cases, patients diagnosed before the age of 18 months have greater than an 85% chance of 5-year survival. In low and intermediate-risk patients, the outlook is generally favorable with a 90-95% survival rate. However, in high-risk patients the 5-year survival rate is 40-50% after treatments have been employed. [6]

b. The origin of neuroblastoma

As suggested by neuroblastoma's occurrence primarily in young children, the cancer is likely to be a result of genetic or epigenetic factors that disrupt the immature cells from engaging in normal embryonic development rather than mature cells that regress back to an immature state. [8] NB has been determined to arise from the failure of neural crest precursor cells (NCPC) to differentiate into mature neurons of the sympathetic nervous system (Figure 1). [3, 8, 9] The neural crest is a temporary structure present during early embryonic development. [10] The undifferentiated NB cell remains in a mesenchymal state where it continues to express genes necessary for cell growth and proliferation such as MYCN. [11] Within the neural crest, there are populations of cells that are ordered based on the cell types they differentiate into. The trunk neural crest cells (tNCC) give rise to the neurons of the peripheral nervous system (PNS) and secretory cells within the endocrine system. In normal development, the trunk neural crest cells are triggered to migrate along three distinct pathways. [12] Specific transcriptional factors have been identified to regulate the tNCC migration and differentiation; however, studies have also shown that their fate is heavily reliant on their external environment, particularly interacting structures and signaling molecules. [13, 14] The relationship between known tNCC differentiation pathways to mature cells and the clinically observed NB primary

sites suggests that pathogenesis may arise within this lineage; however, the exact cell state have not yet been conclusively identified. [5]

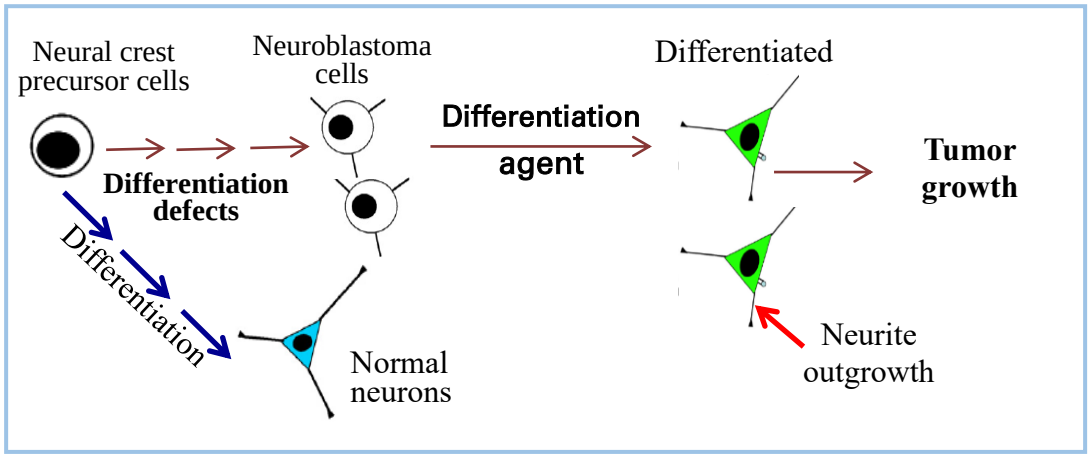

Figure 1. Differentiation pathway. Neuroblastoma cells arise from differentiation defects in neural crest precursor cells which results in a failure of proper differentiation to a normal neuron. Differentiation agents have the ability to induce an alternative route for differentiation into mature cells which results in tumor growth arrest. Image obtained from Dr. Du.

c. Differentiation therapy

NB has been clinically observed to have the highest rate of spontaneous regression of any human tumor. [15] Spontaneous regression is characterized by a decrease in size or disappearance of the tumor without therapeutic intervention. This characteristic of NB paired with the understanding that *ex vivo* biochemical signaling induces normal NCPC differentiation inspired the concept of differentiation therapy. [15-17] The goal of differentiation therapy is to direct the malignant cell to a non-malignant mature form by restoring its native pathways rather than killing the cancer cell. [18] Once differentiation is induced, tumor growth is arrested. [15] Currently, chemotherapy and radiation are the major forms of treatment for high-risk NB patients while differentiation therapies are used to treat the malignant cells that remain after major treatment methods are employed. [3, 9] The

current differentiation therapies available for patients are small molecules, 13-cis retinoic acid and all-trans retinoic acid (ATRA), with RA being the standard of care. Cytotoxic methods of targeting cancer cells primarily rely on the notion that cancer cells rapidly proliferate and therefore take up nutrients in their environment at a higher metabolic rate than normal cells. [19, 20] This assumption can be problematic when applied to the treatment of neuroblastoma as rates of proliferation have been reported to be slower than those of normal somatic cells leading to the loss of non-diseased cells. [21-23] Thus, differentiation therapy offers a milder form of cancer treatment in comparison to traditional methods of radiation and cytotoxic chemotherapy.

Desired cancer therapies are selective in targeting tumors cells while minimally affecting normal cells. Since the mid-20th century, a wide range of drug candidates have been investigated in hopes to identify a method to successfully induce differentiation. [24-26] Through the study of normal epithelial differentiation, endogenous compounds that induce differentiation were identified and tested *in vitro.* [23] Vitamin A and its derivatives known collectively as retinoids were found to be potent inducers of differentiation in NB [16]. Since its discovery, retinoic acids (RA) have been at the forefront of treatment and are considered the standard-of-care for post remission therapy. [27]

d. Resistance to RA and MYCN amplification

Low/intermediate-risk patients respond well to RA, however, more than half of patients experience recurrence which suggests resistance to RA. [28] This phenomenon is referred to as secondary resistance. Many high-risk patients do not respond to RA at all; this is known as primary resistance. [6, 11] One of the most robust ways to predict patient treatment response is by their MYCN amplification status as primary resistance has been

clinically well documented to occur in patients with amplified MYCN. [3, 16, 29]

The MYCN gene is a part of the Myelocytomatosis (Myc) proto-oncogene family of transcription factors and codes for the MYCN protein. [7, 11] MYCN expression is dependent on the developmental stage of the cell. In normal cells, it is expressed during embryogenesis and then downregulated and not significantly expressed after embryonic development which allows the cell to differentiate. [30] Studies have shown that the MYCN dependent signaling is necessary for normal cell cycle progression from G1 to S phase. [7] One way the MYCN protein promotes cell cycle progression is by forming a heterodimer with Max protein. The complex binds to gene promoters via the DNA gene sequence, enhancer box (E-box). [30, 31] When amplification of the MYCN gene is present, the protein becomes less specific and binds to more DNA sequences than its usual E-box promoter region. [32] The MYCN protein is not considered directly druggable due to its lack of hydrophobic pockets and inability to be targeted by small molecules when it forms large complexes with other transcription factors. [31, 33] There are many proposed genes that are targeted and expressed by the MYCN-Max complex which complicates drug targeting therapies for neuroblastoma.

RA exhibits its gene regulating effects by binding to retinoic acid receptor (RAR) and retinoic X receptor (RXR). [34, 35] The molecular mechanisms by which MYCN amplification confers RA resistance is not known. However, it is theorized that the key to the RA signaling pathway is believed to be ineffective in MYCN amplified cell lines due to opposing transcriptional regulation (up- or downregulation) by MYCN and RA. [6] There are currently no clinically approved alternative differentiation agents for patients who have developed resistance to RA. This lack of options for patients, particularly

those who are high-risk, calls for the discovery of additional differentiating agents.

e. Other neuroblastoma differentiating agents

Previous work demonstrates that RA increases cAMP levels in NB cells during induced differentiation. [36] cAMP then activates AMP-activated protein kinase (AMPK), a major regulator of cell growth and metabolic reprogramming. [37] It is suggested that the activation of the AMPK pathway is necessary for RA-induced differentiation in NB along with other regulatory pathways such as MAPK and Wnt. [6] Many key players of cell cycle regulation have been targeted using small molecules to induce differentiation in NB cells; inhibitors of glycogen synthase kinase-3 β (GSK-3 β) and phosphoinositide-dependent kinase-1 (PDK1) of the PI3K/Akt pathway and phosphodiesterase-5 have been reported in various NB cell lines. [38, 39] Cytochrome P450 (CYP) 26, the enzyme that oxidizes RA has also been the target of inhibition with the hopes of increasing RA levels; however, targeting the enzyme alone has resulted in the increase of MYCN expression which promotes cell growth and represses differentiation. [40] One of the most promising NB small-molecule differentiating agent for MYCN amplified cell lines may be inhibitors of bromodomain and extra-terminal domain (BET) proteins. [33, 41] BET proteins regulate gene expression and consequentially cell differentiation and proliferation by recognizing histone lysine acetylation sites and recruiting other transcription factors [42]. In a patent published in 2016, the bromodomain inhibitors were proposed to downregulate a gene linked to spontaneous differentiation in normal human embryonic cells (Figure 2). [41]

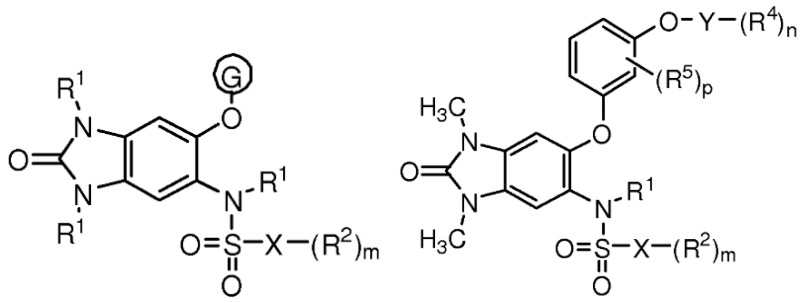

Figure 2. General structures of bromodomain inhibitors.

The predated body of work support this study's hypothesis that there are many potential small molecule targets that can mediate the induction of differentiation independent of RA. Unfortunately, *in vitro* and *in vivo* small-molecule differentiating agents in MYCN amplified neuroblastoma cell lines are still lacking. Additionally, over 90% of drug candidates fail the drug discovery process. [43] Thus, there remains a need to develop NB differentiating agents for MYCN amplified cells.

f. Advantages of the use of small molecule-drugs for NB treatment

Classical drug development utilizes small-molecule drugs (< 900 Daltons) to exert effects on a biological system as mediated by a target. [44] Small-molecules offer an advantage over other drug design methods such as biologics in some notable ways. First of all, biologics are large complex molecules that often require a clearly defined target. [45] Though this aspect of drug development can be powerful when the target is known, in the case of NB, the structure of the target is unrevealed and thus gives the advantage to the amenable small-molecule approach. [44, 46] Secondly, the more liberal abilities of small-molecules can also be the favorable approach when considering the full disposition of a pharmaceutical compound within an organism or ADME. [45]

ADME stands for absorption, distribution, metabolism and excretion and is a

defining component of pharmacokinetics. [45] ADME considers how the drug enters the body (A), how it is distributed (D), changes of the drug within the body (M), and the drug leaving the body (E). [47] Afforded by their molecular weights that are often less than 500 Daltons, small-molecule drugs are more readily able to cross membranes to get to their intended target than biologics. [45] Small-molecules have the ability to permeate the cell and elicit a response by binding to an intracellular target. This is an important factor to consider for the treatment of NB as the disease of the PNS. Similar to the blood-brain-barrier (BBB) of the central nervous system (CNS), the PNS has a blood-nerve-barrier (BNB) which guards the system from external influences. [48, 49] Biologics have a disadvantage regarding permeability due to not being readily available to cross membranes. Small molecules offer versatility and, given the appropriate physicochemical properties, can overcome permeability restraints that may be necessary for the treatment of NB.

g. Small-molecule screening

In drug design, the target does not have to be known to uncover a clinically relevant therapeutic small-molecule. Instead, a screening for a desired phenotypic change can be conducted. This approach is referred to as ‘classical pharmacology’ or ‘forward pharmacology’ and was the first way in which drugs were discovered. [50] Furthermore, analyses have found that phenotypic identification has contributed to a significant amount of new small-molecule cancer drugs approved by the Food and Drug Administration (FDA) in recent decades. [51] Overall, more drugs have been identified through screenings compared to designing a molecule based on a target relevant to the disease of interest. [50] A high content screening (HCS) is one such phenotypic drug discovery method that uses

automated microscopy, imaging processing and visualization tools to identify compounds with the ability to induce a specified phenotypic change in cell populations. [52] Neurite outgrowth is an established marker of differentiation in NB and can be used to quantify the potency of a compound. [53] In contrast, undifferentiated NB cells are characteristically small and circular with minimal projections. [54] SK-N-BE(2)-C is a NB cell line that shows easily detectable neurite outgrowth and reduced cell viability upon differentiation induced by all-trans retinoic acid (ATRA), an RA isomer (Figure 3). [27] The neurite elongation, induced by ATRA as a positive control, has been demonstrated to be quantifiable by means of measuring its length against the cells body area. [54] The induction of differentiation has been observed as being time and dose-dependent (Figure 3). The reduction in cell viability can be used as a second indicator to confirm differentiation (Figure 3E). The undifferentiated SK-N-BE(2)-C cell line is characteristically immortal and will continue to proliferate in adequate media conditions. Once differentiated, however, the NB cells have been demonstrated to no longer rapidly proliferate or persist. [55]

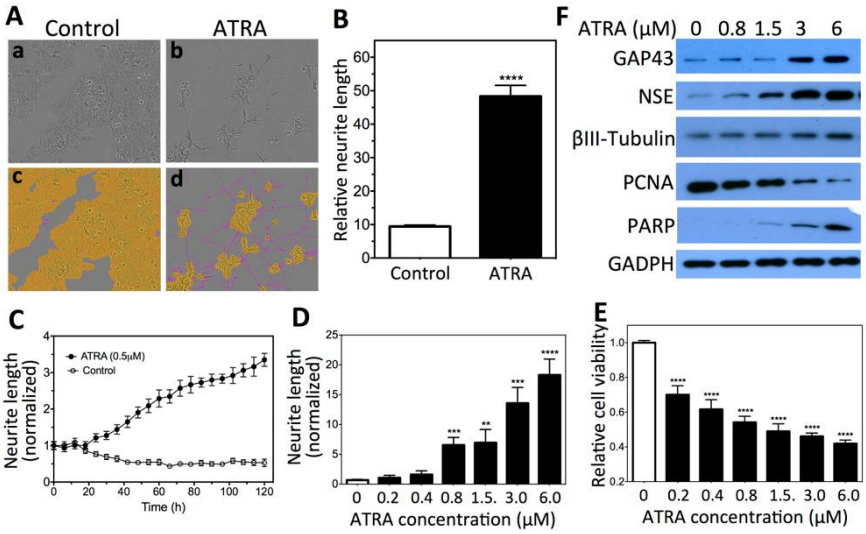

Figure 3. BE(2)-C cell neurite outgrowth quantification. Relative neurite length is defined as neurite length per cell body area. **A**, ATRA induces neurite outgrowth. **B**, Quantification of neurite outgrowth based on A. **C**, Relative neurite lengths increase in a time-dependent manner during ATRA treatment. Neurite lengths were normalized to the starting time point (0 h). **D**, Dose-dependent effect of ATRA on neurite outgrowth. **E,** Dose-dependent effect of ATRA on cell viability. **F,** Dose-dependent effect of ATRA on protein expression levels of cell differentiation, proliferation and apoptotic markers with GAPDH protein levels used as a loading control. Cells were treated with ATRA as above, and protein levels were determined by Western blots after 5 days. **, p<0.01; ***, p<0.001; ****, p<0.0001. Figure obtained from Dr. Du.

To identify small-molecule compounds with the ability to induce certain desired effects, commercial compound libraries are often screened. Compound libraries are collections of stored chemicals and include information such as the molecules structure and physical properties. Compound libraries often center either around target-oriented design or diversity-oriented design. Diversity oriented libraries possess compounds with a demonstrated broad range of biological activities which is correlated with structural diversity. The structural diversity refers to the arrangement of atoms within the molecule and is proportional to the chemical space occupied. [44] Thus, a wide range of structures within a library will increase the possible spaces in which the compound may make contact to a biological target.

In medicinal chemistry, certain moieties have been consistently found to have activity due to their versatile binding properties and thus have been termed ‘privileged’. [56] The pattern of ‘privilege’ can be understood by considering that macromolecules are often structured in a non-random pattern which is reflected in the small molecules that elicit biological effects (Figure 4). [57] Therefore, diverse small-molecule libraries endorsing known privilege structures are considered to be a good fit for phenotypic screenings. Once the screening is performed, compounds identified to have the desired activity are then referred to as ‘hits’.

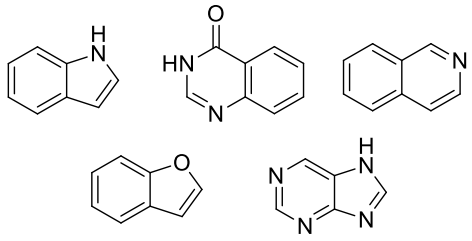

Figure 4. Example of privileged structures.

h. Structure-Activity Relationship

Hit compounds are great starting points for drug design as they have already been demonstrated to possess the desired activity through screening. [58] However, in order for a compound to move along the drug discovery process as a lead and ultimately a drug candidate, it must be potent at a pharmacological level, ideally in the sub-micromolar concentration range. [59, 60] This high potency requirement is important for preventing off-target effects as low potency drugs require higher concentrations to be effective which may result in the drug outcompeting other ligands at unintended receptors. [46] Additionally, high potency drugs are cost-efficient which is favorable when considering manufacturing. [58]

Increasing the potency of a hit compound can be achieved by uncovering which part of the molecule is responsible for binding to the biological target, also known as the molecule's pharmacophore. [61] Without knowing the target, the pharmacophore can be investigated by altering the molecule and observing how the change has affected the molecule's activity. The concept of exploring the molecule's structure as it relates with a biological activity is termed Structure Activity Relationship (SAR). [56, 62] SAR studies have been utilized since the 1800's and have been a consistently powerful tool for understanding the physiological action as it relates to the chemicals constitution. [62] The grounds for an SAR study are based on the understanding that similar molecules exhibit similar physical characteristics in a predictable way. Small changes to a molecule's structure can result in a change in how the molecule interacts with a binding pocket. The SAR's hallmark is the synthesis of many analogues of a hit or lead compound to then test the analogs for activity. With enough analogues, conclusions can be drawn about what sites on the molecule are important for binding making the molecule amenable for optimization. [56, 62]

i. Identifying a novel NB differentiating agent

The purpose of this study is the development of novel neuroblastoma differentiating agents. As previously mentioned, targets to induce differentiation are poorly understood and therefore the approach of this study is based on phenotypic changes within the NB SK-N-BE(2)-C cell line. To identify a differentiation agent, a compound library was purchased from ChemBridge Diverset^{TM} containing 10,000 compounds. [54] Previous studies have screened this same library and have identified compounds with anti-cancer and differentiation-inducing activity; however, the small-

molecule library had never been investigated for their differentiating effects in NB. [63-65] Compounds that elicited a predetermined threshold for activity were identified as 'hits'. From this screening, hit compounds that induced the desired changes in the cell line were identified.

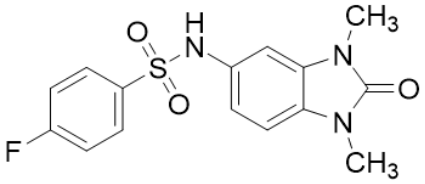

Formula	$C_{15}H_{14}FN_3O_3S$
Molecular Weight	335
LogP	2.34
LogSW	-3.65
Rotatable Bonds	2
Hdon	1
Hacc	3
tPSA	73.1
Form	Solid

Figure 5. Compound #3. Structure of compound #3 identified from the HCS that induced neurite outgrowth at a 25 µM concentration. Parameters of Compound #3. Molecular Formula, Molecular Weight (g/mol), Log P (Lipophilicity), Log SW (Aqueous Solubility), Rotatable Bonds, Hydrogen donors, Hydrogen acceptors, Topological Polar Surface Area ($Å^2$), Form.

One of the hit compounds from the HCS was identified for optimization through the investigation of its pharmacophore by use of a SAR study (Figure 5). The hit compound, Compound #3, was identified to induce neurite outgrowth at a 25 µM concentration by the HCS and was selected for further optimization that will be carried out in this Structure-Activity Relationship (SAR) study (Figure 5, 6).

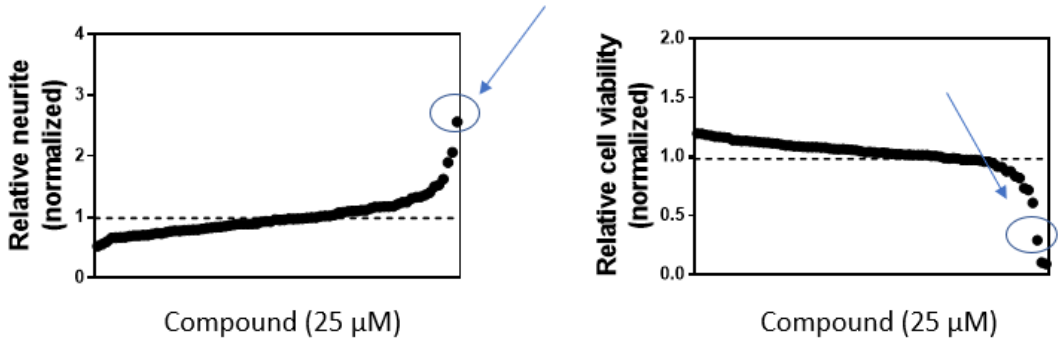

Figure 6. Comparison of tested compounds in HCS. Arrows indicate Compound #3. **a.** Relative neurite outgrowth of each compound ranked from least to greatest effect (left to right), normalized to the control. **b.** Relative cell viability ranked from least to greatest effect (left to right), normalized to the control.

Compound #3 is a promising starting point for the synthesis of analogues with differentiation-inducing activity in NB due to its favorable parameters (Figure 5b). The Partition Coefficient (P) is an established molecular characteristic that expresses how lipophilic or hydrophilic a molecule is. Log P is often used in medicinal chemistry to make predictions about how a molecule will distribute within an organism. Molecules with higher log P values favor hydrophobic compartments and are more likely to pass through the lipid bilayer of a cell. [66] Conversely, if the log P value is too high, the molecule will not be soluble and therefore not orally available. The Lipinski "rule of five" for drug-like molecules states that the log P value should be less than 5. [67] Additionally, a low molecular weight (<500 g/mol), less than 5 hydrogen bond donors, less than 10 hydrogen bond acceptors, less than 10 rotatable bonds and a low polar surface area (tPSA <140 $Å^2$) are also favorable parameters for the entrance into the cell by small-molecule drugs. [67, 68] Though these values are not absolute, they provide insight into the therapeutic potential of a compound of interest. Additionally, this compound resembles the bromodomain inhibitors discussed earlier (Figure 2). The hit

compound has less substituents than the previously reported bromodomain inhibitors which may suggest that the hit compound is closer to the pharmacophore necessary for the BET protein compound interaction. The previously reported bromodomain inhibitors were not explored for their activity in any neuroblastoma cell lines. Therefore, the identified hit compound for this study is a novel tool that can be explored to better understand and identify differentiating agents in MYCN amplified NB cells.

j. Project aims

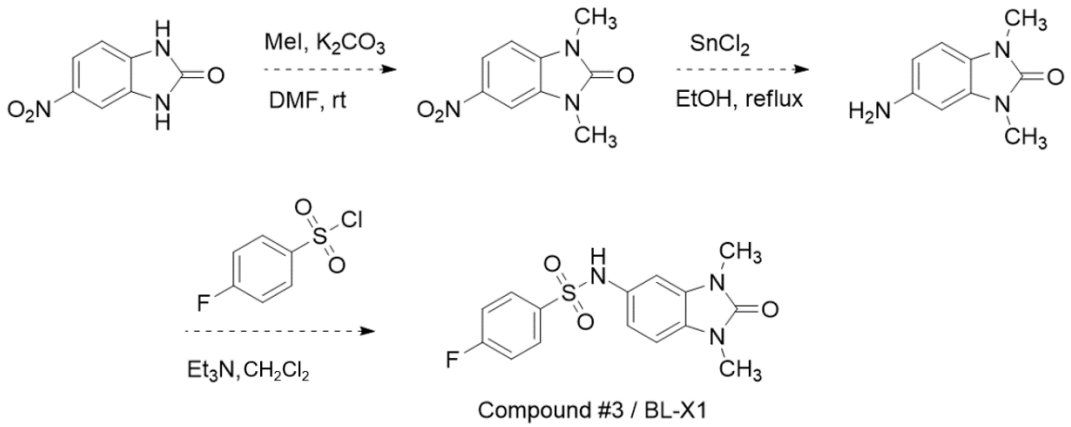

Scheme 1. Proposed synthetic method of BL-X1. Recoded from Compound #3

There are two aims of the proposed SAR study. The first aim is to synthesize Compound #3 in-house (Scheme 1). The success of the proposed synthetic method for Compound #3 is expected to substantiate the general synthetic method for producing analogues, as well. This aim will also eliminate the need to purchase the compound from a commercial source. The re-synthesized compound's structure will be confirmed by nuclear magnetic resonance (NMR) spectroscopy. The second aim of this project is to synthesize analogues of Compound #3 with the intent to increase the potency of neurite outgrowth and investigate structural moieties necessary for activity. Once the analogue's

structure is confirmed by NMR, *in vitro* assays will be performed to determine the analogues neurite differentiation potential and effect on cell viability. This SAR study was used to gain a better understanding of the chemical groups important for activity. Conclusively, this study has the potential to give rise to more efficacious treatments as well as offer a better understanding of biological targets involved in differentiation.

II. EXPERIMENTAL

a. Synthesis

All reagents, solvents, and catalysts were purchased from commercial sources and used without purification. All reactions were performed in oven-dried flasks open to the atmosphere or under nitrogen and monitored by thin layer chromatography (TLC) on TLC precoated (250 μm) silica gel XHL glass-backed plates (Sorbent Technologies.). Visualization was accomplished with UV light. Flash column chromatography was performed on silica gel (32−63 μm, 60 Å pore size). ^{1}H NMR spectra were recorded on a Bruker 400 or 500-megahertz (MHz) spectrometer. Chemical shifts (δ) are reported in ppm relative to the tetramethylsilane (TMS) internal standard. Abbreviations are as follows: s (singlet), d (doublet), t (triplet), q (quartet), m (multiplet).

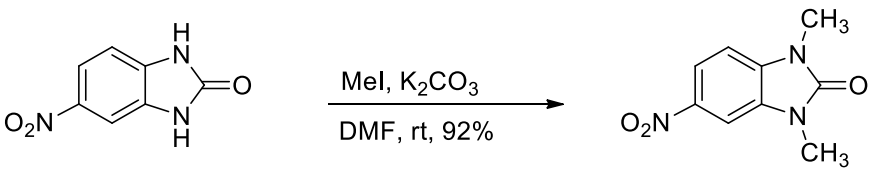

Scheme 2 BL-01

One gram of 5-nitro-2-benzimidazolinone (5.6 mmol) was added to ca. 15 mL of DMF in a round bottom flask. Potassium carbonate (K_2CO_3, 1.6 mg, 11.2 mmol) was added and the mixture was cooled to 0 ℃. 2.52 mL of iodomethane (14.0 mmol) was then added dropwise. The reaction was stirred at room temperature and then water (10 mL) was added. The resulting suspension was filtered, the solids were collected and washed with water (150 mL) and dried. Further purification was not required. This procedure afforded a 92% yield. The product was a yellow solid. ^{1}H NMR data was consistent with the literature data. [69]

^{1}H NMR (500 MHz, DMSO) δ 8.02 – 7.97 (m, 2H), 7.29 (d, *J* = 8.5 Hz, 1H), 3.38 (s, 3H), 3.36 (s, 3H).

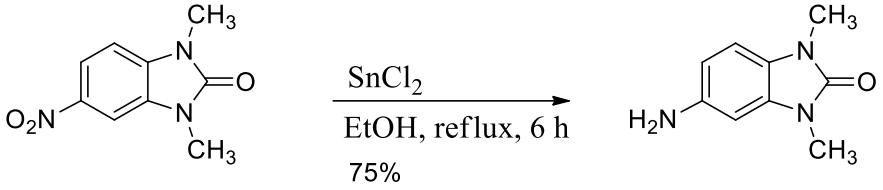

Scheme 3 BL-02

A mixture of 1,3-dimethyl-5-nitro-1,3-dihydrobenzimidazol-2-one (1.8 g, 8.5 mmol) and tin (II) chloride dihydrate ($SnCl_2 \cdot 2H_2O$, 9.6 g, 42.5 mmol) in ethanol was refluxed for 6 hours. After cooling, the reaction was concentrated under reduced pressure. The solid residue was suspended in saturated $NaHCO_3$ and extracted with ethyl acetate (3 x 50 mL). The organic phase was evaporated under reduced pressure and then purified by column chromatography to yield 75% of the compound as a yellow solid. ^{1}H NMR data were consistent with the literature data. [69]

^{1}H NMR (400 MHz, $CDCl_3$) δ 6.74 (d, *J* = 8.2 Hz, 1H), 6.45 (dd, *J* = 8.2, 2.1 Hz, 1H), 6.36 (d, *J* = 2.0 Hz, 1H), 3.36 (s, 3H), 3.35 (s, 3H).

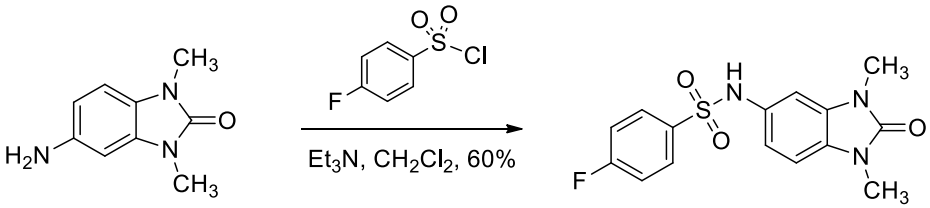

Scheme 4 BL-X1

A mixture of 5-amino-1,3-dimethyl-1,3-dihydrobenzimidazol2-one (40 mg, 0.22 mmol) and 64 µL of triethylamine (0.46 mmol) was dissolved in DCM then treated with 4-fluorobenzenesulfonyl chloride (48.7mg, 0.25 mmol) in a round bottom flask under nitrogen. The resulting mixture was stirred at room temperature for one hour and

monitored by TLC for completion. Upon product formation, the mixture was quenched with methanol, concentrated under reduced pressure and purified by column chromatography. A 60% yield of BL-X1 was achieved as a white solid.

^{1}H NMR (400 MHz, $CDCl_3$) δ 7.71 (dd, *J* = 8.9, 5.0 Hz, 2H), 7.10 (t, *J* = 8.6 Hz, 2H), 6.89 (d, *J* = 1.9 Hz, 1H), 6.77 (d, *J* = 8.2 Hz, 1H), 6.60 (dd, *J* = 8.2, 2.0 Hz, 1H), 6.50 (s, 1H), 3.38 (s, 6H). ^{13}C NMR (126 MHz, $CDCl_3$) δ 166.2, 164.2, 154.8, 135.0, 130.6, 130.1, 130.0, 129.7, 128.7, 117.3, 116.3, 116.1, 107.3, 104.6, 29.7, 27.3, 27.2. HRMS m/z calcd for $C_{15}H_{14}FN_3O_3S$ $(M+H^+)^+$ 336.0813, found 336.0808.

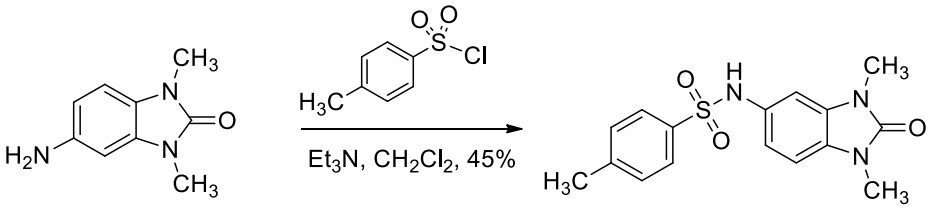

Scheme 5 BL-X2

A mixture of 5-amino-1,3-dimethyl-1,3-dihydrobenzimidazol2-one (8.4 mg, 0.047 mmol) and 13.4 µL of triethylamine (0.096 mmol) was dissolved in DCM then treated with 4-Methylbenzenesulfonyl chloride (13.8 mg, 0.072 mmol) in a round bottom flask under nitrogen. The resulting mixture was stirred at room temperature for one hour and monitored by TLC for completion. Upon product formation, the mixture was quenched with methanol, concentrated under reduced pressure and purified by TLC. A 45% yield of BL-X2 was achieved as a white solid.

^{1}H NMR (400 MHz, $CDCl_3$) δ 7.60 (d, *J* = 8.2 Hz, 2H), 7.21 (d, *J* = 8.2 Hz, 2H), 6.88 (d, *J* = 1.9 Hz, 1H), 6.76 (d, *J* = 8.2 Hz, 1H), 6.67 (s, 1H), 6.64 (dd, *J* = 8.2, 1.9 Hz, 1H), 3.37 (s, 3H), 3.36 (s, 3H), 2.38 (s, 3H). ^{13}C NMR (101 MHz, $CDCl_3$) δ 143.8, 136.0, 130.5, 130.2, 129.6, 128.4, 127.3, 117.0, 107.3, 104.2, 27.3, 27.2, 21.5. HRMS m/z calcd

for $C_{16}H_{17}N_3O_3S$ $(M+H^+)^+$ 332.1063, found 332.1056.

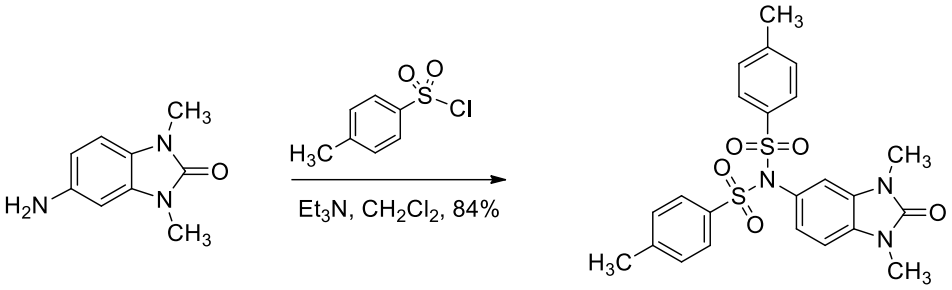

Scheme 6 BL-X3

A mixture of 5-amino-1,3-dimethyl-1,3-dihydrobenzimidazol2-one (41 mg, 0.23 mmol) and 80 µL of triethylamine (0.58 mmol) was dissolved in DCM then treated with 4-Methylbenzenesulfonyl chloride (87.6 mg, 0.46 mmol) in a round bottom flask under nitrogen. The resulting mixture was stirred at room temperature for one hour and monitored by TLC for completion. Upon product formation, the mixture was quenched with methanol, concentrated under reduced pressure and purified by column chromatography. An 84% yield of BL-X3 was achieved as a white solid.

^{1}H NMR (500 MHz, $CDCl_3$) δ 7.82 (d, *J* = 8.3 Hz, 4H), 7.33 (d, *J* = 8.3 Hz, 4H), 6.88 (d, *J* = 8.3 Hz, 1H), 6.74 – 6.70 (m, 1H), 6.62 (d, *J* = 1.9 Hz, 1H), 3.41 (s, 3H), 3.31 (s, 3H), 2.47 (s, 6H). ^{13}C NMR (126 MHz, $CDCl_3$) δ 154.7, 145.1, 136.6, 131.3, 130.2, 129.6, 128.7, 127.6, 125.1, 110.6, 107.2, 27.3, 21.7. HRMS m/z calcd for $C_{23}H_{23}N_3O_5S_2$ $(M+H^+)^+$ 486.1152, found 486.1145.

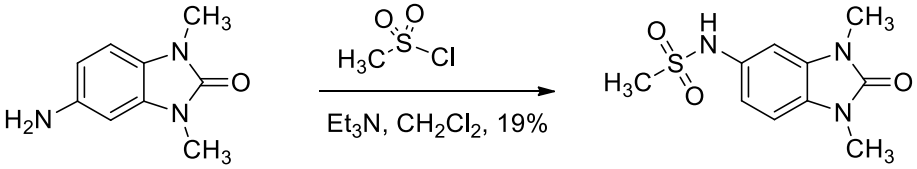

Scheme 7 BL-X4

A mixture of 5-amino-1,3-dimethyl-1,3-dihydrobenzimidazol2-one (13.6 mg,

0.08 mmol) and 16 µL of triethylamine (0.12 mmol) was dissolved in DCM then treated with 6.5 µL of methanesulfonyl chloride (mg, 0.08 mmol) in a round bottom flask under nitrogen. The resulting mixture was stirred at room temperature for three hours and monitored by TLC for completion. Upon product formation, the mixture was quenched with methanol, concentrated under reduced pressure and purified by TLC resulting in a 19% yield of BL-X4 as a white solid.

^{1}H NMR (400 MHz, $CDCl_3$) δ 7.11 (d, *J* = 8.2 Hz, 1H), 7.02 (d, *J* = 8.2 Hz, 1H), 6.95 (d, *J* = 2.0 Hz, 1H), 3.45 (s, 3H), 3.44 (s, 3H), 3.43 (s, 3H).

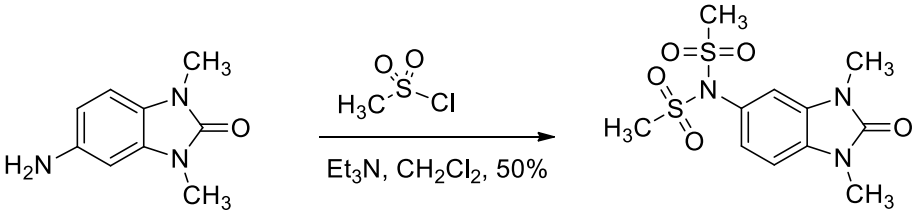

Scheme 8 B2-X4

A mixture of 5-amino-1,3-dimethyl-1,3-dihydrobenzimidazol2-one (52 mg, 0.29 mmol) and 81 µL of triethylamine (0.58 mmol) was dissolved in DCM then treated with 20.3 µL of methanesulfonyl chloride (0.26 mmol) in a round bottom flask under nitrogen. The resulting mixture was stirred at room temperature for one hour and monitored by TLC for completion. Upon product formation, the mixture was quenched with methanol, concentrated under reduced pressure and purified by column chromatography. A 50% yield of B2-X4 was achieved as a white solid.

^{1}H NMR (500 MHz, $CDCl_3$) δ 7.10 (d, *J* = 2.0 Hz, 1H), 7.00 (s, 1H), 6.92 (d, *J* = 2.0 Hz, 1H), 3.42 – 3.40 (m, 12H). ^{13}C NMR (101 MHz, $CDCl_3$) δ 154.7, 131.7, 130.8, 126.6, 123.9, 109.7, 107.6, 42.6, 27.5, 27.4. HRMS m/z calcd for $C_{11}H_{15}N_3O_5S_2$ $(M+H^+)^+$

334.0526, found 334.0518.

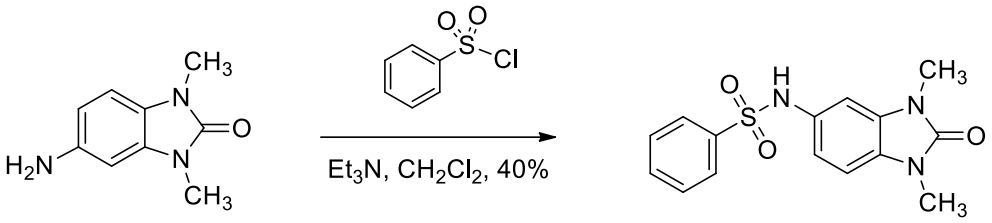

Scheme 9 BL-X5

A mixture of 5-amino-1,3-dimethyl-1,3-dihydrobenzimidazol2-one (16 mg, 0.09 mmol) and 9.3 µL of triethylamine (0.14 mmol) was dissolved in DCM then treated with 12.7 µL benzenesulfonyl chloride (0.10 mmol) in a round bottom flask under nitrogen. The resulting mixture was stirred at room temperature for one hour and monitored by TLC for completion. Upon product formation, the mixture was quenched with methanol, concentrated under reduced pressure and purified by TLC. A 40% yield of BL-X5 was achieved as a white solid.

^{1}H NMR (400 MHz, $CDCl_3$) δ 7.73 – 7.68 (m, 2H), 7.55 (s, 1H), 7.44 (d, *J* = 7.9 Hz, 2H), 6.86 (d, *J* = 1.8 Hz, 1H), 6.76 (d, *J* = 8.2 Hz, 1H), 6.61 (dd, *J* = 8.2, 1.9 Hz, 1H), 6.43 (s, 1H), 3.37 (s, 3H), 3.36 (s, 3H). HRMS m/z calcd for $C_{15}H_{15}N_3O_3S$ $(M+H^+)^+$ 318.0907, found 318.0909.

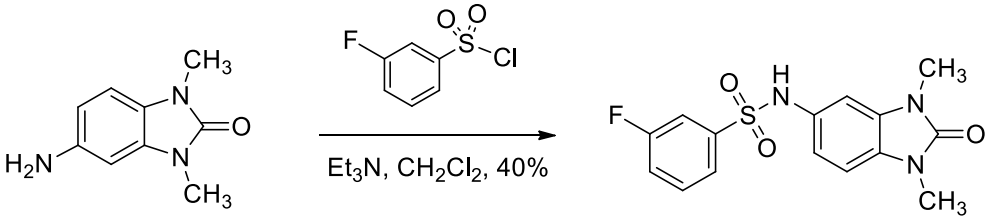

Scheme 10 BL-X6

A mixture of 5-amino-1,3-dimethyl-1,3-dihydrobenzimidazol2-one (29 mg, 0.16 mmol) and 44.6 µL of triethylamine (0.32 mmol) was dissolved in DCM then treated with 3-fluorobenzenesulfonyl chloride (34 mg, 0.18 mmol) in a round bottom flask under

nitrogen. The resulting mixture was stirred at room temperature for one hour and monitored by TLC for completion. Upon product formation, the mixture was quenched with methanol, concentrated under reduced pressure and purified by TLC. A 40% yield of BL-X6 was achieved as a white solid.

^{1}H NMR (500 MHz, $CDCl_3$) δ 7.51 – 7.47 (m, 1H), 7.44 – 7.39 (m, 2H), 7.25 – 7.22 (m, 1H), 6.88 (d, *J* = 1.9 Hz, 1H), 6.78 (d, J = 8.2 Hz, 1H), 6.64 (d, *J* = 2.0 Hz, 1H), 6.57 (s, 1H), 3.38 (s, 3H), 3.38 (s, 3H). ^{13}C NMR (101 MHz, DMSO) δ 163.3, 154.4, 141.9, 132.0, 131.1, 130.4, 127.8, 123.6, 120.5, 115.7, 114.3, 108.2, 103.1, 27.4. HRMS m/z calcd for $C_{15}H_{14}FN_3O_3S$ $(M+H^+)^+$ 336.0813, found 336.0813.

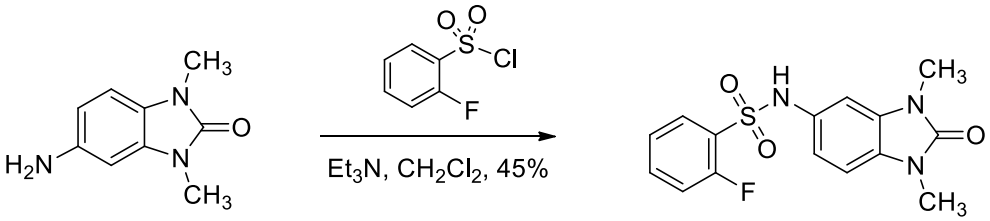

Scheme 11 BL-X7

A mixture of 5-amino-1,3-dimethyl-1,3-dihydrobenzimidazol2-one (40 mg, 0.23 mmol) and 62 µL of triethylamine (0.44 mmol) was dissolved in DCM then treated with 39 µL of 2-fluorobenzenesulfonyl chloride (0.30 mmol) in a round bottom flask under nitrogen. The resulting mixture was stirred at room temperature for one hour and monitored by TLC for completion. Upon product formation, the mixture was quenched with methanol, concentrated under reduced pressure and purified by column chromatography. A 45% yield of BL-X7 was achieved as a white solid.

^{1}H NMR (500 MHz, $CDCl_3$) δ 7.72 (td, *J* = 7.6, 1.8 Hz, 1H), 7.54 – 7.49 (m, 1H), 7.22 – 7.18 (m, 1H), 7.14 (dd, *J* = 7.7, 1.1 Hz, 1H), 6.87 (d, *J* = 1.8 Hz, 1H), 6.72 (s, 1H), 6.70 (d, *J* = 2.0 Hz, 1H), 3.33 (s, 3H), 3.31 (s, 3H). **^{13}C** NMR (126 MHz, $CDCl_3$) δ 135.4,

135.3, 131.0, 130.6, 129.4, 128.7, 124.6, 116.8, 116.6, 116.5, 107.3, 103.9, 27.3, 27.2. HRMS m/z calcd for $C_{15}H_{14}FN_3O_3S$ $(M+H^+)^+$ 336.0813, found 336.0818.

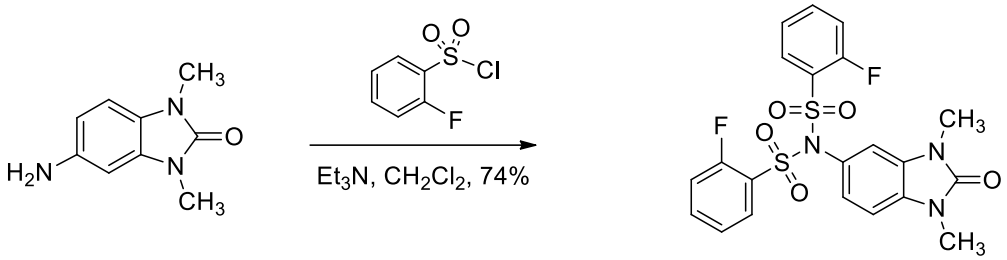

Scheme 12 BL-X8

A mixture of 5-amino-1,3-dimethyl-1,3-dihydrobenzimidazol2-one (40 mg, 0.23 mmol) and 47 µL of triethylamine (0.34 mmol) was dissolved in DCM then treated with 2-fluorobenzenesulfonyl chloride (88 mg, 0.45 mmol) in a round bottom flask under nitrogen. The resulting mixture was stirred at room temperature for one hour and monitored by TLC for completion. Upon product formation, the mixture was quenched with methanol, concentrated under reduced pressure and purified by column chromatography. A 74% yield of BL-X8 was achieved as a white solid. ^{1}H NMR (400 MHz, $CDCl_3$) δ 8.03 – 7.97 (m, 2H), 7.72 – 7.64 (m, 2H), 7.36 – 7.29 (m, 2H), 7.25 – 7.18 (m, 2H), 6.95 (d, *J* = 3.4 Hz, 2H), 6.91 (d, *J* = 8.2 Hz, 1H), 3.42 (s, 3H), 3.38 (s, 3H). ^{13}C NMR (126 MHz, $CDCl_3$) δ 160.1, 158.1, 154.7, 136.7, 132.3, 131.6, 130.3, 126.9, 125.8, 125.3, 124.5, 117.3, 111.0, 107.1, 27.4. HRMS m/z calcd for $C_{21}H_{17}F_2N_3O_5S_2$ $(M+H^+)^+$ 494.0650, found 494.0656.

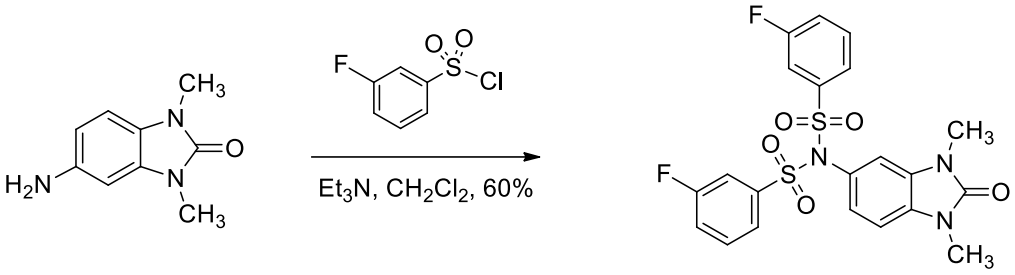

Scheme 13 BL-X10

A mixture of 5-amino-1,3-dimethyl-1,3-dihydrobenzimidazol2-one (40 mg, 0.23 mmol) and 47 µL of triethylamine (0.34 mmol) was dissolved in DCM then treated with 3-fluorobenzenesulfonyl chloride (88 mg, 0.45 mmol) in a round bottom flask under nitrogen. The resulting mixture was stirred at room temperature for two hours and monitored by TLC for completion. Upon product formation, the mixture was quenched with methanol, concentrated under reduced pressure and purified by column chromatography. A 60% yield of BL-X10 was achieved as a white solid.

^{1}H NMR (500 MHz, $CDCl_3$) δ 7.80 – 7.75 (m, 2H), 7.68 (d, *J* = 7.9 Hz, 2H), 7.57 (d, *J* = 5.2 Hz, 2H), 7.42 (d, *J* = 1.7 Hz, 2H), 6.93 (d, *J* = 8.3 Hz, 1H), 6.74 (s, 1H), 6.63 (d, *J* = 2.0 Hz, 1H), 3.44 (s, 3H), 3.35 (s, 3H). ^{13}C NMR (126 MHz, $CDCl_3$) δ 163.2, 161.2, 154.7, 141.0, 131.7, 130.8, 130.5, 126.8, 124.9, 124.5, 121.6, 121.4, 116.2, 116.0, 110.2, 107.4, 100.0, 27.4. HRMS m/z calcd for $C_{21}H_{17}F_2N_3O_5S_2$ $(M+H^+)^+$ 494.0650, found 494.0641.

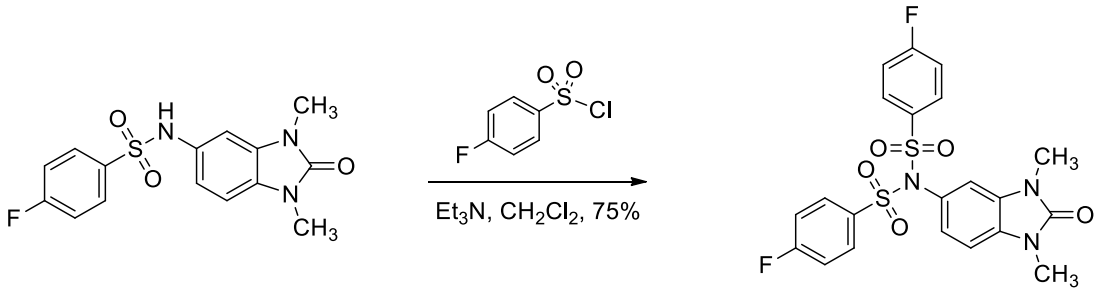

Scheme 14 BL-X11

A mixture of BL-X1 (35 mg, 0.10 mmol) and 22 µL of triethylamine (0.16 mmol) was dissolved in DCM then treated with 4-fluorobenzenesulfonyl chloride (22 mg, 0.11 mmol) in a round bottom flask under nitrogen. The resulting mixture was stirred at room temperature for one hour and monitored by TLC for completion. Upon product formation, the mixture was quenched with methanol, concentrated under reduced pressure and purified by column chromatography. A 75% yield of BL-X11 was achieved as a white solid.

^{1}H NMR (400 MHz, $CDCl_3$) δ 8.00 – 7.91 (m, 4H), 7.27 – 7.17 (m, 4H), 6.90 (s, 1H), 6.69 (d, *J* = 8.3 Hz, 1H), 6.61 (s, 1H), 3.43 (s, 3H), 3.34 (s, 3H). ^{13}C NMR (101 MHz, $CDCl_3$) δ 167.3, 164.7, 154.6, 135.3, 135.2, 131.7, 131.6, 130.5, 127.0, 124.9, 116.5, 116.3, 110.3, 107.3, 27.4. HRMS m/z calcd for $C_{21}H_{17}F_2N_3O_5S_2$ $(M+H^+)^+$ 494.0650, found 494.0659.

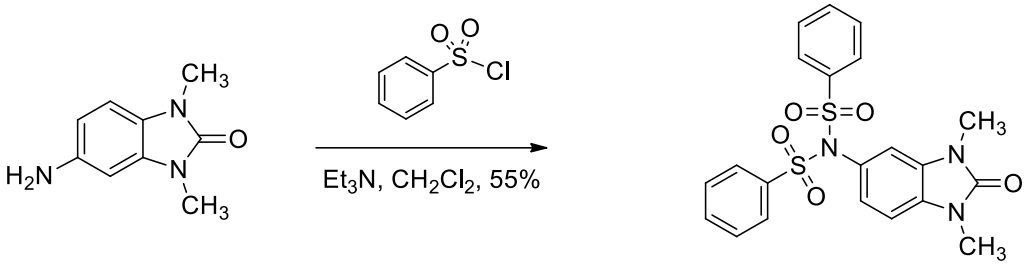

Scheme 15 BL-X12

A mixture of 5-amino-1,3-dimethyl-1,3-dihydrobenzimidazol2-one (20 mg, 0.11 mmol) and 24 µL of triethylamine (0.17 mmol) was dissolved in DCM then treated with benzenesulfonyl chloride (40 mg, 0.23 mmol) in a round bottom flask under nitrogen. The resulting mixture was stirred at room temperature for one hour and monitored by TLC for completion. Upon product formation, the mixture was quenched with methanol, concentrated under reduced pressure and purified by column chromatography. A 55%

yield of BL-X12 was achieved as a white solid.

^{1}H NMR (400 MHz, $CDCl_3$) δ 7.98 – 7.93 (m, 4H), 7.69 (t, *J* = 7.7 Hz, 2H), 7.56 (t, *J* = 7.7 Hz, 4H), 6.89 (d, *J* = 8.3 Hz, 1H), 6.73 (dd, *J* = 8.3, 1.9 Hz, 1H), 6.59 (d, *J* = 1.9 Hz, 1H), 3.42 (s, 3H), 3.31 (s, 3H). ^{13}C NMR (126 MHz, $CDCl_3$) δ 154.7, 139.4, 134.0, 131.4, 130.3, 129.0, 128.7, 127.3, 125.0, 110.5, 107.2, 27.3. HRMS m/z calcd for $C_{21}H_{19}N_3O_5S_2$ $(M+H^+)^+$ 494.0839, found 494.0846.

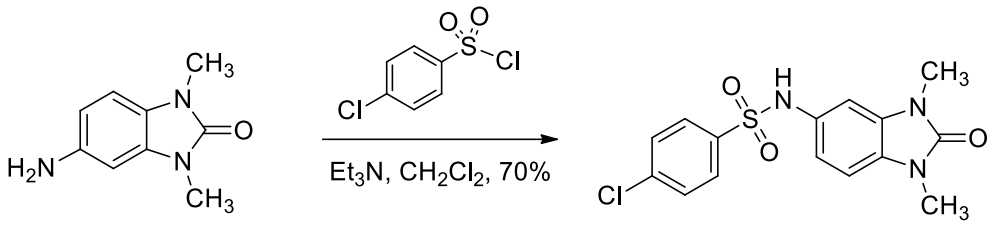

Scheme 16 BL-X13

A mixture of 5-amino-1,3-dimethyl-1,3-dihydrobenzimidazol2-one (2.5 g, 14.0 mmol) and 1.9 mL of triethylamine (13.8 mmol) was dissolved in DCM then treated with 4-chlorobenzenesulfonyl chloride (2.06 g, 9.6 mmol) in a round bottom flask under nitrogen. The resulting mixture was stirred at room temperature for one hour and monitored by TLC for completion. Upon product formation, the mixture was quenched with methanol, concentrated under reduced pressure and purified by column chromatography. A 70% yield of BL-X13 was achieved.

^{1}H NMR (500 MHz, $CDCl_3$) δ 7.67 – 7.61 (m, 2H), 7.40 (dd, *J* = 6.7, 1.9 Hz, 2H), 6.89 (d, *J* = 1.9 Hz, 1H), 6.78 (d, *J* = 8.3 Hz, 2H), 6.63 (d, *J* = 2.0 Hz, 1H), 3.38 (s, 6H). ^{13}C NMR (126 MHz, $CDCl_3$) δ 154.8, 139.5, 137.4, 130.6, 129.6, 129.3, 128.8, 128.7, 117.3, 107.4, 107.4, 104.5, 100.0, 27.4. HRMS m/z calcd for $C_{15}H_{14}ClN_3O_3S$ $(M+H^+)^+$ 352.0517, found 352.0513.

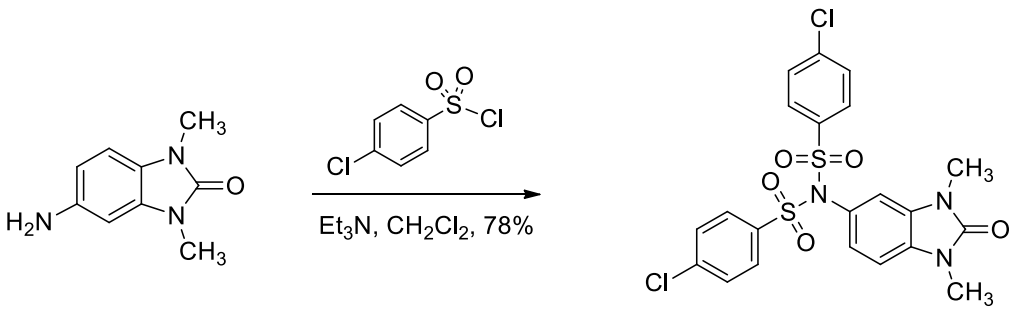

Scheme 17 BL-X14

A mixture of 5-amino-1,3-dimethyl-1,3-dihydrobenzimidazol2-one (760 mg, 4.3 mmol) and 0.90 mL of triethylamine (6.4 mmol) was dissolved in DCM then treated with 4-chlorobenzenesulfonyl chloride (1.8 g, 8.6 mmol) in a round bottom flask under nitrogen. The resulting mixture was stirred at room temperature for one hour and monitored by TLC for completion. Upon product formation, the mixture was quenched with methanol, concentrated under reduced pressure and purified by column chromatography. A 78% yield of BL-X14 was achieved.

^{1}H NMR (400 MHz, $CDCl_3$) δ 7.89 (d, *J* = 8.7 Hz, 4H), 7.89 (d, *J* = 8.7 Hz, 1H), 7.54 (d, *J* = 8.7 Hz, 4H), 6.91 (d, *J* = 8.3 Hz, 1H), 6.69 (dd, *J* = 8.3, 2.0 Hz, 1H), 6.62 (d, *J* = 1.9 Hz, 1H), 3.43 (s, 3H), 3.35 (s, 3H). ^{13}C NMR (101 MHz, $CDCl_3$) δ 154.6, 141.0, 137.7, 131.6, 130.5, 130.1, 129.4, 126.9, 124.9, 110.2, 107.3, 27.4, 27.4. HRMS m/z calcd for $C_{21}H_{17}ClN_3O_5S_2$ $(M+H^+)^+$ 526.0059, found 526.0058.

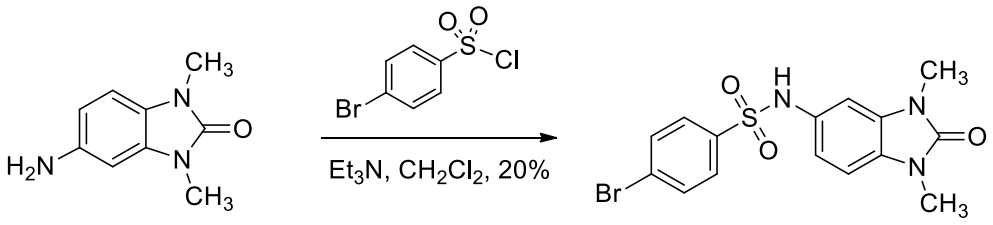

Scheme 18 BL-X15

A mixture of 5-amino-1,3-dimethyl-1,3-dihydrobenzimidazol2-one (59 mg, 0.33 mmol) and 35 µL of triethylamine (0.35 mmol) was dissolved in DCM then treated with 4-bromobenzenesulfonyl chloride (65 mg, 0.25 mmol) in a round bottom flask under nitrogen. The resulting mixture was stirred at room temperature for one hour and monitored by TLC for completion. Upon product formation, the mixture was quenched with methanol, concentrated under reduced pressure and purified by column chromatography. A 20% yield of BL-X15 was achieved.

^{1}H NMR (500 MHz, $CDCl_3$) δ 7.56 (s, 4H), 6.89 (d, *J* = 1.9 Hz, 1H), 6.78 (d, *J* = 8.2 Hz, 1H), 6.64 – 6.60 (m, 2H), 3.38 (s, 3H), 3.38 (s, 3H). ^{13}C NMR (101 MHz, $CDCl_3$) δ 154.8, 138.0, 132.3, 129.5, 129.0, 128.0, 117.3, 107.4, 104.5, 27.4, 27.3. HRMS m/z calcd for $C_{15}H_{14}BrN_3O_3S$ $(M+H^+)^+$ 396.0012, found 396.0001.

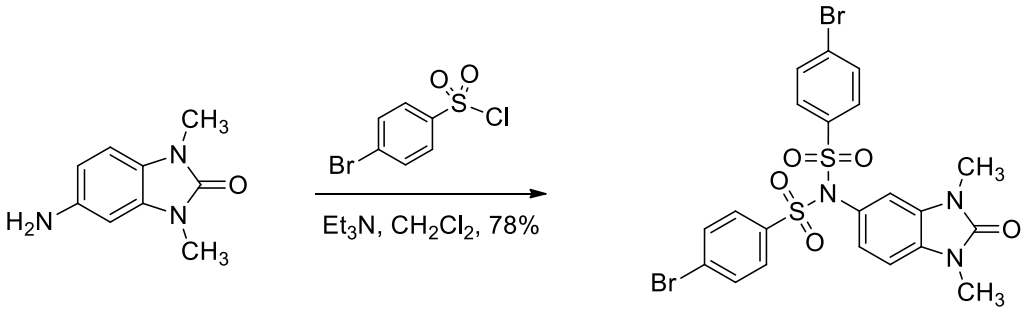

Scheme 19 BL-X16

A mixture of 5-amino-1,3-dimethyl-1,3-dihydrobenzimidazol2-one (40 mg, 0.23 mmol) and 47 µL of triethylamine (0.34 mmol) was dissolved in DCM then treated with 4-bromobenzenesulfonyl chloride (115 mg, 0.45 mmol) in a round bottom flask under nitrogen. The resulting mixture was stirred at room temperature for one hour and monitored by TLC for completion. Upon product formation, the mixture was quenched with methanol, concentrated under reduced pressure and purified by column

chromatography. A 78% yield of BL-X16 was achieved as a white solid.

^{1}H NMR (500 MHz, $CDCl_3$) δ 7.80 (d, *J* = 8.7 Hz, 4H), 7.70 (d, *J* = 8.7 Hz, 4H), 6.90 (d, *J* = 8.3 Hz, 1H), 6.69 (dd, *J* = 8.2, 2.0 Hz, 1H), 6.61 (d, *J* = 1.9 Hz, 1H), 3.42 (s, 3H), 3.34 (s, 3H). ^{13}C NMR (101 MHz, $CDCl_3$) δ 154.6, 138.2, 132.4, 130.1, 129.6, 126.9, 124.9, 107.3, 53.4, 27.4, 27.3. HRMS m/z calcd for $C_{21}H_{17}BrN_3O_5S_2$ $(M+H^+)^+$ 613.9049, found 613.9032.

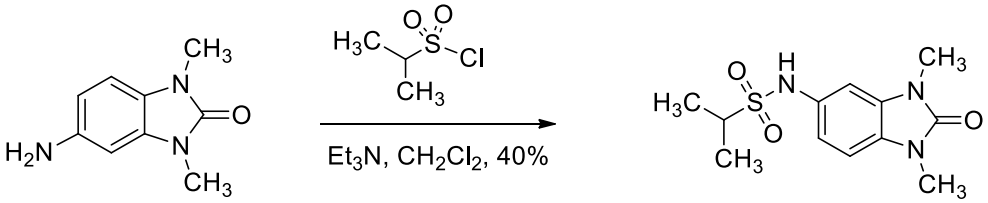

Scheme 20 BL-X17

A mixture of 5-amino-1,3-dimethyl-1,3-dihydrobenzimidazol2-one (30 mg, 0.17 mmol) and 28 µL of triethylamine (0.2 mmol) was dissolved in DCM then treated with 2-propanesulfonyl chloride (27 mg, 0.19 mmol) in a round bottom flask under nitrogen. The resulting mixture was stirred at room temperature for one hour and monitored by TLC for completion. Upon product formation, the mixture was quenched with methanol, concentrated under reduced pressure and purified by column chromatography. A 40% yield of BL-X17 was achieved.

^{1}H NMR (400 MHz, $CDCl_3$) δ 7.06 (d, *J* = 1.8 Hz, 1H), 6.94 (dd, *J* = 8.2, 2.0 Hz, 1H), 6.90 (d, *J* = 8.2 Hz, 1H), 6.66 (s, 1H), 3.43 (s, 3H), 3.42 (s, 3H), 1.43 (s, 3H), 1.41 (s, 3H). ^{13}C NMR (101 MHz, $CDCl_3$) δ ^{13}C NMR (101 MHz, $CDCl_3$) δ 154.8, 131.1, 130.8, 127.9, 115.4, 107.6, 102.7, 52.1, 27.4, 27.3, 16.6. HRMS m/z calcd for $C_{12}H_{17}N_3O_3S$ $(M+H^+)^+$ 284.1063, found 284.1055.

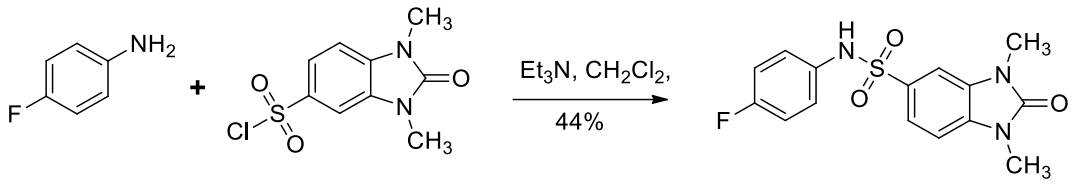

Scheme 21 BL-X30

A mixture of 4-fluoroaniline (24 mg, 0.22 mmol) and 30 µL of triethylamine (0.22 mmol) was dissolved in DCM then treated with 2,3-Dihydro-1,3-dimethyl-2-oxo-1H-benzimidazole-5-sulfonyl chloride (50 mg, 0.20 mmol) in a round bottom flask under nitrogen. The resulting mixture was stirred at room temperature for four hours and monitored by TLC for completion. Upon product formation, the mixture was quenched with methanol, concentrated under reduced pressure and purified by column chromatography. A 44% yield of BL-X30 was achieved as a white solid.

^{1}H NMR (500 MHz, $CDCl_3$) δ 7.49 (d, *J* = 8.2 Hz, 1H), 7.32 (s, 1H), 7.03 (dd, *J* = 8.7, 4.6 Hz, 2H), 6.94 (d, *J* = 8.0 Hz, 2H), 6.59 (s, 1H), 3.43 (s, 3H), 3.39 (s, 3H). ^{13}C NMR (126 MHz, $CDCl_3$) δ 154.6, 133.7, 132.3, 131.4, 130.1, 125.0, 125.0, 121.5, 116.3, 116.1, 106.9, 106.3, 27.5, 27.4. HRMS m/z calcd for $C_{15}H_{14}FN_3O_3S$ $(M+H^+)^+$ 336.0813, found 336.0806.

b. Biological methods

To detect and quantify the neurite outgrowth induced by the compounds, BE(2)-C cells were plated and treated with the specific compound at 25 µM in triplicate in 96-well plates for 4 days. Cell images were taken under 20X microscopic magnification ZOOM IncuCyte Imaging System (Essen Bioscience). The neurite lengths associated with each treatment were calculated using the neurite definition defined by NeuroTrack system. [27]

Cell viability was measured by the MTT (2-(4,5—Dimethylthiazol-2-yl)-2,5-Diphenyltetrazolium Bromide) assay. Briefly, cells were plated in 96-well plates and treated as specified. By the end of compound treatment, MTT (15 µl at 2.5 mg/ml in 1 X PBS) was then added and incubated for 1 hour at 37ºC. Precipitates were spun down and dissolved in DMSO. The absorbance at 570 nm and 630 nm were measured and the difference in the two absorbance values was calculated to determine relative cell viability.

III. RESULTS AND DISCUSSION

a. Synthesis

The purpose of the current study was to optimize a hit compound from an HCS through the investigation of its pharmacophore by use of a SAR study. The first aim of this study was to produce the hit compound purchased from ChemBridge in-house. This would make the compound readily available and substantiate the general synthesis for making analogues. The synthesis was successful as verified by NMR and HRMS. To confirm that the compound was biologically active, BE(2)-C cells were treated with the in-house synthesized compound, named BL-X1 and the commercially purchased compound, named compound 3 (Fig 7). There was no significant difference between the two compounds in terms of neurite outgrowth or cell viability.

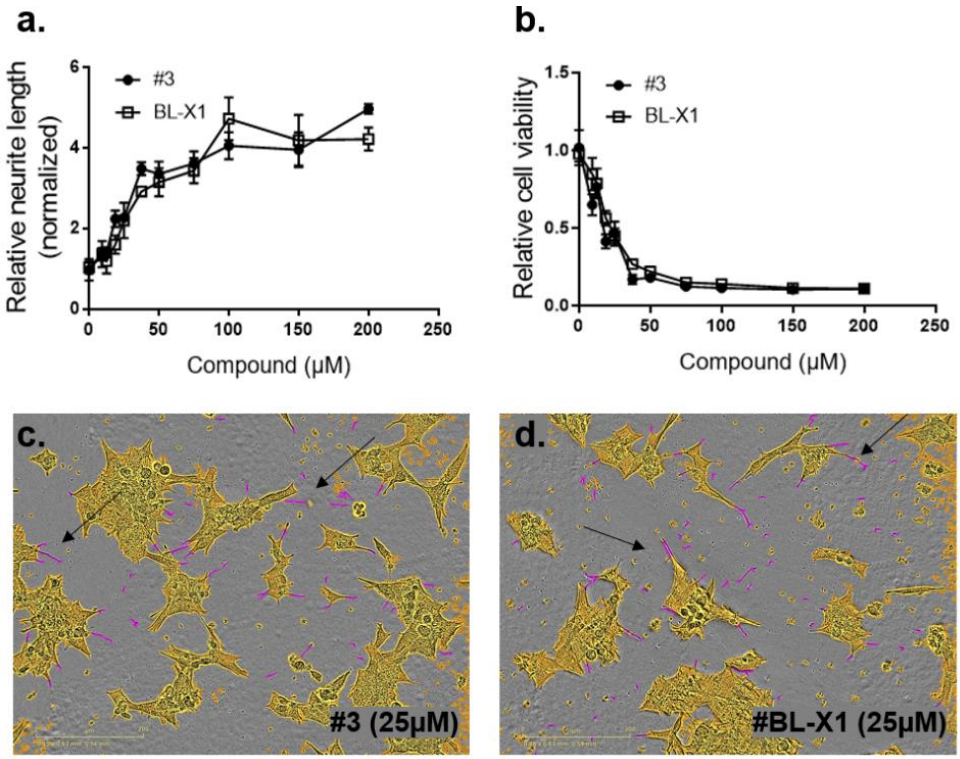

Figure 7. Biological activity of BL-X1 and compound #3. **a. & b.** serial concentrations of #3 and BL-X1 to obtain relative neurite outgrowth and cell viability. **c.** neurite image of cells treated with compound #3 at 25μM for four days. **d.** neurite image of cells treated with BL-X1 at 25μM for 4 days. Arrows indicate neurite outgrowth.

The second aim of this study was to synthesize analogues of the compound 3 to further understand the pharmacophore involved in the induction of differentiation in NB cells. To optimize time and synthetic effort, an assessment of the ChemBridge library was performed to determine which analogues of compound 3 were already available for purchase and which needed to be synthesized for this study. Analogues that varied only slightly from the original hit were selected for biological testing.

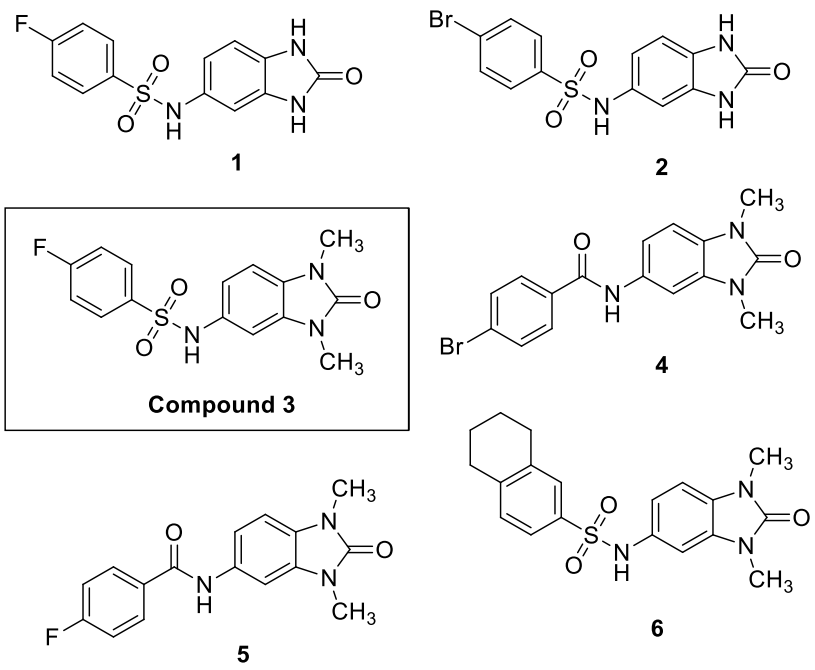

Figure 8. ChemBridge compounds. Selected due to their structural similarity to compound 3.

Compound **1** was selected for testing because it has almost the exact structure as the original hit; however, its urea moiety does not have the methyl substituents (Figure 8). Compound **2** was also selected because it resembles the structure of the original hit and only deviates by an unmethylated urea moiety and bromine in the para position rather than fluorine. Neither **1** nor **2** was found to induce neurite outgrowth which suggests that the dimethylated urea moiety plays a role in the biological activity of the hit compound. The methyl substituents may increase the compounds lipophilicity, decrease its polar surface area and aqueous solubility making it more likely to pass through the lipid bilayer of a cell, as mentioned in the introduction.

Compound **4** and **5** were selected for biological testing to investigate the role of the sulfonamide moiety of compound 3; the sulfonamide moiety is replaced with an amide in these compounds (Figure 8). Additionally compound **5** also contains a bromine

in the para position of the benzene moiety rather than fluorine. Neither of the amide containing compounds was found to be active. Sulfur containing compounds are found throughout the pharmaceutical industry and display a wide range of biological activities. Sulfonamide drugs were the first commercial antibiotics and were used for both Gram-negative and Gram-positive bacteria [70]. Since their discovery, the sulfonamide containing scaffolds have been applied to a wide range of indications and more recently, sulfonamide-containing compounds have been identified to have anticancer properties [70, 71]. Though more work is needed to be completed to gain a better understanding of the mechanism of action (MOA) of these drugs, our discovery supports the privileged nature of the sulfonamide scaffold.

Compound **6** was selected because it has a tetralin moiety in place of compound 3's 4-fluorobenzene moiety. This compound did display differentiating effects in the treated cells which prompted this study to further investigate the 4-fluorobenzene moiety of the hit compound. Analogues of compound 3 were synthesized that varied in the 4-fluorobenzene but had the same 1,3-dimethylbenzimidazolone moiety.

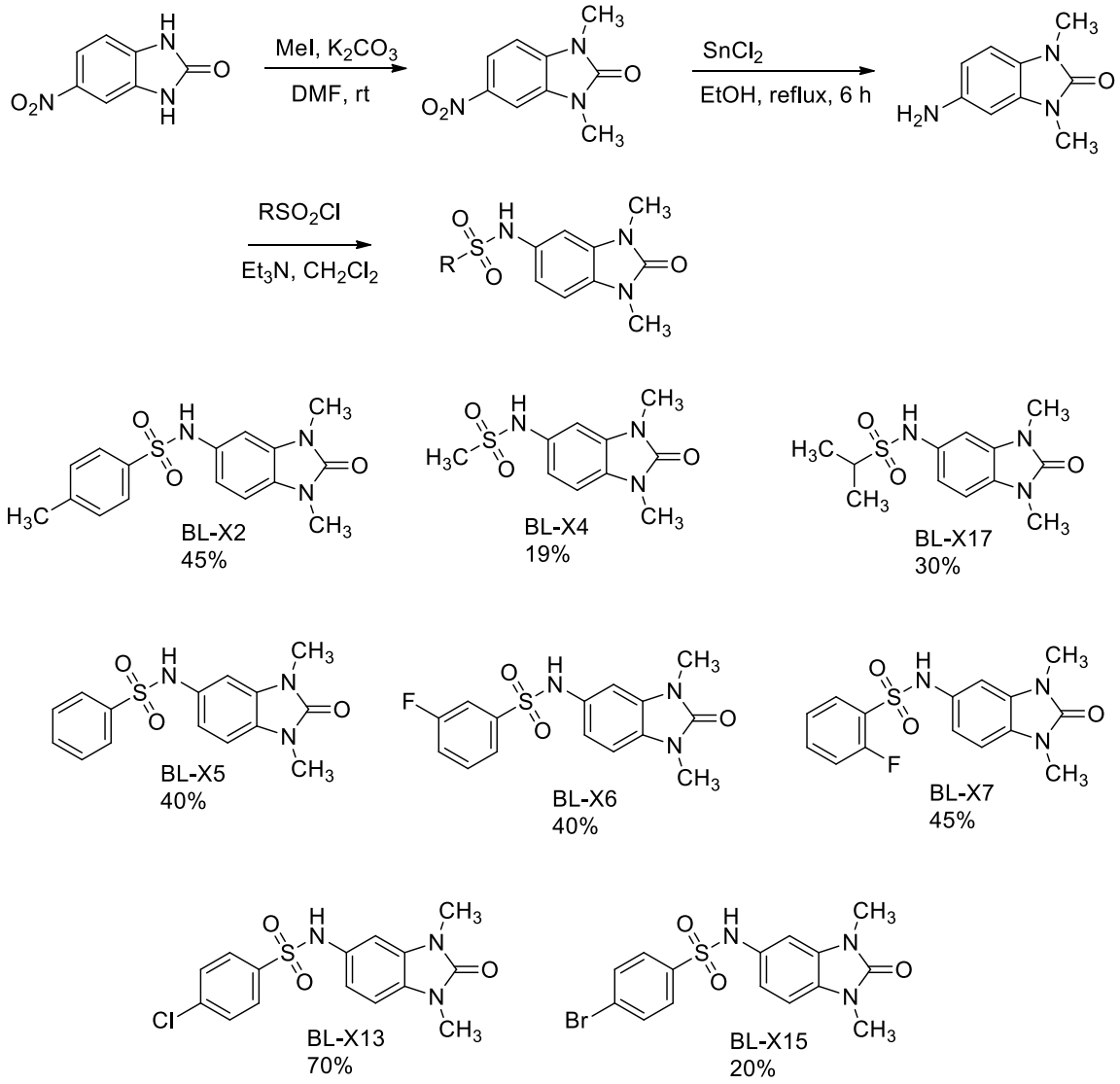

Figure 9. Synthesis of sulfonamides.

The synthetic procedure shown in Figure 9 was conducted to get the desired sulfonamides in yields varying from 19-70%. BL-X4 and BL-X17 were synthesized using methanesulfonyl chloride and 2-propanesulfonyl chloride, respectively. These sulfonyl chlorides possess acidic α-hydrogens that commonly get deprotonated by a base to form sulfenes which are highly unstable. The sulfene formation may explain the low yields of 19-30%. Other analogues were found to form more readily; however, even the

use of 0.9 equivalents of sulfonyl chloride relative to the 5-amino-1,3-dimethyl-1,3-dihydrobenzimidazol-2-one resulted in the formation of significant amounts of dimer forms of each analogue, which brought down the yields of the mono-substituted sulfonyl compounds further (Figure 10). These analogues were also resynthesized from BL-02 with two equivalents of the corresponding sulfonyl chloride.

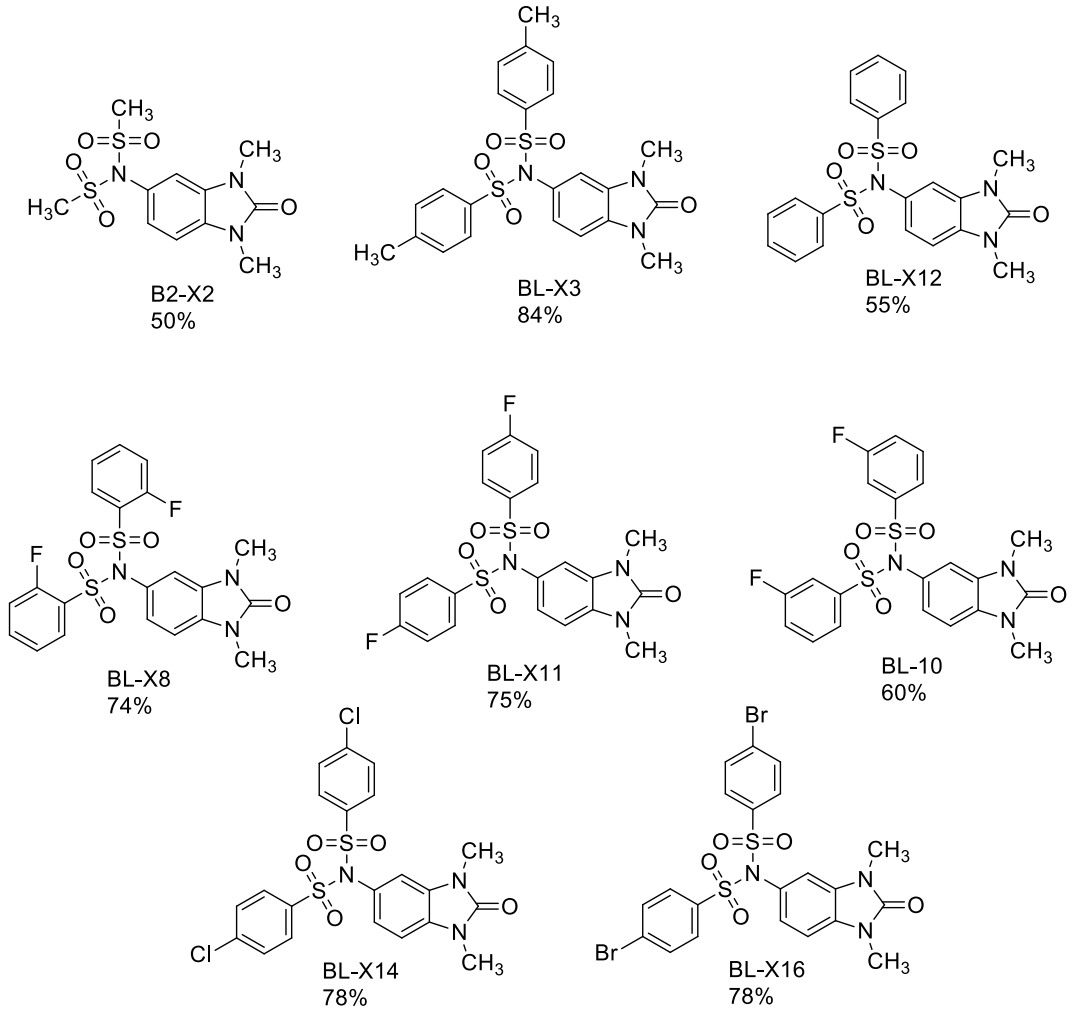

Figure 10. Disulfonyl analogues.

b. Biological evaluation and SAR analysis

Analogues were synthesized to gain a better understanding of the 4-fluorobenzene moiety of the original hit compound (Figure 9, 10). Altering the position of the fluorine on the benzene ring yielded active compounds that differentiated the cells (BL-X6, BL-X7, Figure 11). Additionally, the substitution of fluorine in the para position by chlorine or bromine also resulted in a retention of activity. BL-X5 which had no substituent on the benzene ring was also found to be active against the cell line; however, its potency was less than the analogues with halogenated rings. Replacing the halogen with a methyl group in BL-X2 also resulted in a retention of differentiating activity. Removing the ring entirely with only a methyl or isopropyl group resulted in no activity. Changing the orientation of the sulfonamide moiety in BL-X30 resulted in a loss of differentiating activity. Interestingly, parallels were seen in regard to the activity in the disulfonyl analogues though all were less potent than their monosulfonyl analogues.

None of the novel analogues were found to be more potent than the original hit; however, the most potent analogue, BL-X13, induces neurite outgrowth and reduces cell viability at a promising molar concentration (Figure 11, 12). Chlorine engages in halogen bonding [72]. Chlorine engages in this form of bonding due to its possession of an electron deficient region, known as a sigma hole which attracts nucleophiles [73]. Fluorine, on the other hand, has been well documented to be a weak hydrogen bond acceptor with nitrogen and oxygen in a C-F bond but likely does not have a positive sigma hole in BL-X1 due to not being bonded to a strong electron-withdrawing group [72, 74]. These differences in bonding may result in variations between BL-X1 or BL-X13-target interactions. Chlorine is also larger which could alter binding due to steric effects. These

differences in the halobenzene moiety between compound 3 and BL-X13 may indicate that a different interaction is occurring at the para position on these molecules. Additional studies should be conducted to further investigate the target-molecule interactions.

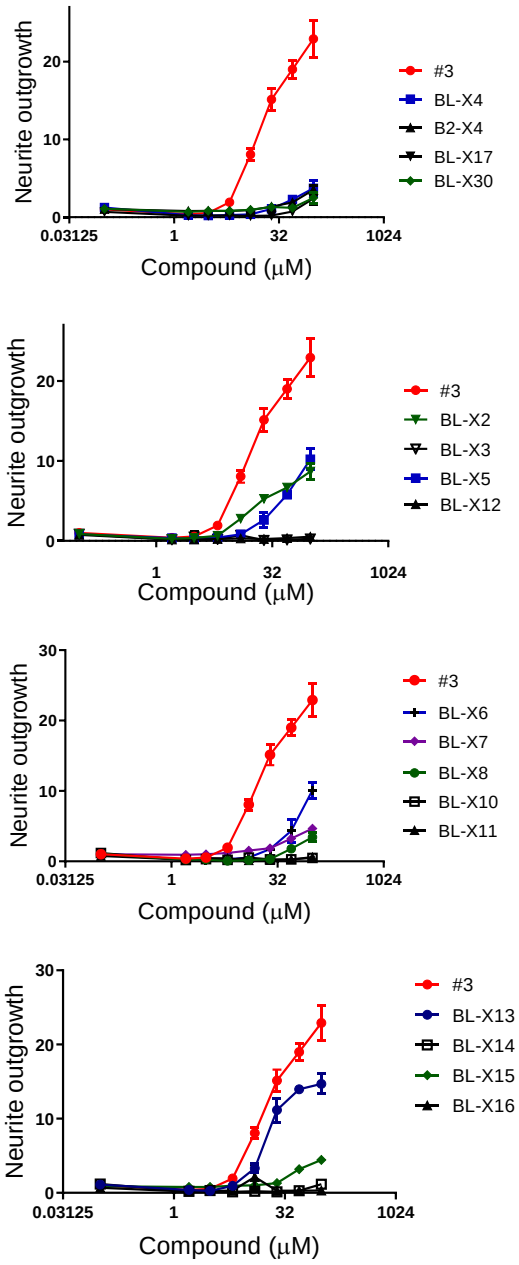

Figure 11. Dose-dependent neurite outgrowth curve of BL-X compounds. BE(2)-C cells were treated with indicated compounds at varying concentrations and the neurite outgrowth was measured after 4 days.#3 is the original hit compound.

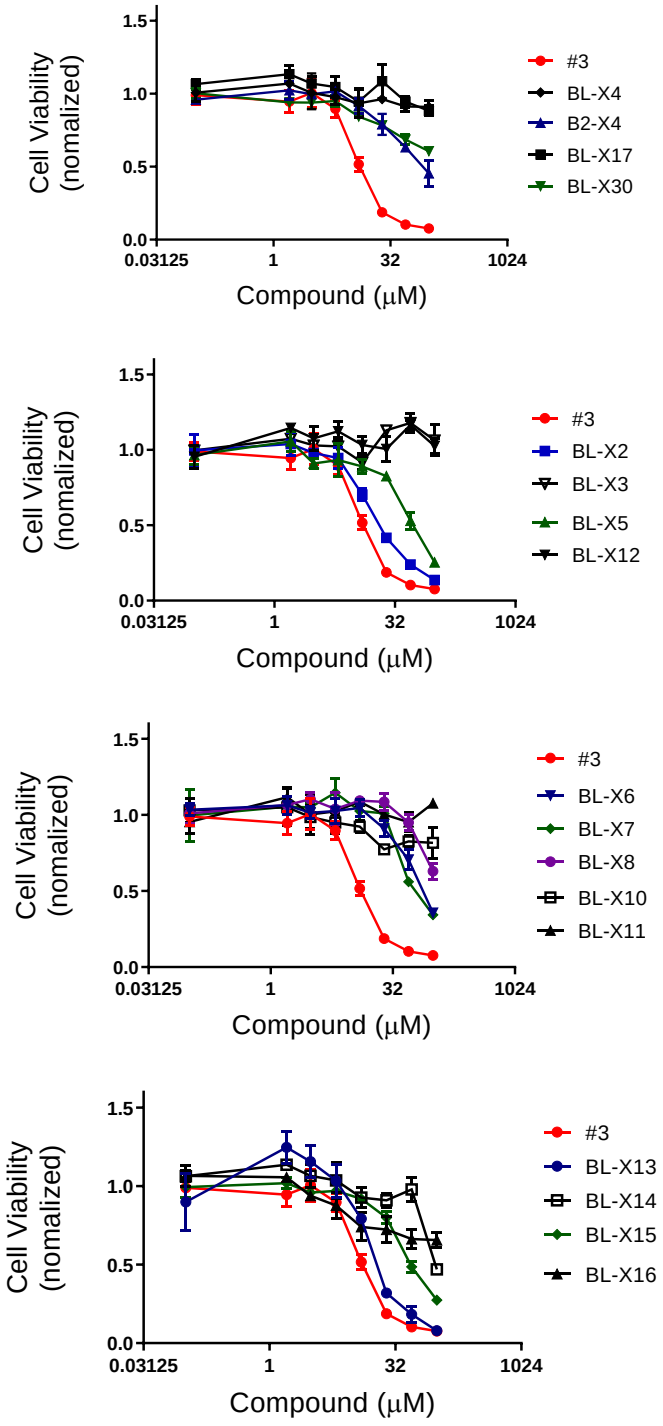

Figure 12. Dose-dependent cell viability curve of BL-X compounds. BE(2)-C cells were treated with indicated compounds at varying concentrations and the neurite outgrowth was measured after 4 days. #3 is the original hit compound.

IV. CONCLUSION AND FUTURE DIRECTIONS

Analogues were synthesized based on a hit compound from an HCS screening found to induce differentiation in BE(2)-C neuroblastoma cells. Each analogue contributed to the understanding of the SAR in this series of compounds. Specifically, the inactivity of compound **1** and **2** suggests that the dimethylated urea moiety plays a role in the biological activity of the hit compound. The sulfonamide moiety was determined to be significant for activity, as suggested by the inactivity of compound **4** and **5**. Changing the 4-fluorobenzene moiety to a tetralin in compound **6** retained activity. Replacing the 4-fluorobenzene moiety with a methyl group in BL-X4, or isopropyl group in BL-X17, resulted in a loss of differentiating but having a benzenesulfonamide (BL-X5) retained activity suggesting the importance of the benzene moiety. Varying the position of the fluorine on the benzene resulted in a retention of activity; however, these alterations reduced the compounds potency. Switching the orientation of the sulfonamide also reduced the activity in BL-X30. Halogen substitution to bromine resulted in a decrease in potency but retained the greatest activity when substituted to chlorine in BL-X13.

BL-X13, along with the original hit compound have been selected to be further investigated in animal studies. Mice, carrying human tumor xenografts, will be the *in vivo* model for evaluating the compounds therapeutic potential. Animal studies is the next step in the long process of drug discovery. If the compounds reduce the size of tumors in *in vivo* models without substantial toxic side effects, they may continue along the path and may be candidates for human trials.

Due to the predicted ideal parameters, such as log P and molecular weight, and the structural similarity to other molecules that have been identified to play a major role in the cell cycle, these novel compounds may be promising to apply to treat other forms

of cancer. MYC targeting has been an ongoing challenge in medicinal chemistry aimed at the treatment of cancer as this pathway is dysregulated in many different types of cancer [32, 75]. Previous studies have shown that molecules that inhibit one member of the MYC family also affects another such as c-Myc and MYCN [33, 76]. These novel analogues may have therapeutic properties that may go beyond the neuroblastoma cell line of the current study. Additional research should be conducted to get a better understanding of the novel compounds' role on the cell cycle as well as their direct target (s).

APPENDIX SECTION

^{1}H NMR BL-01

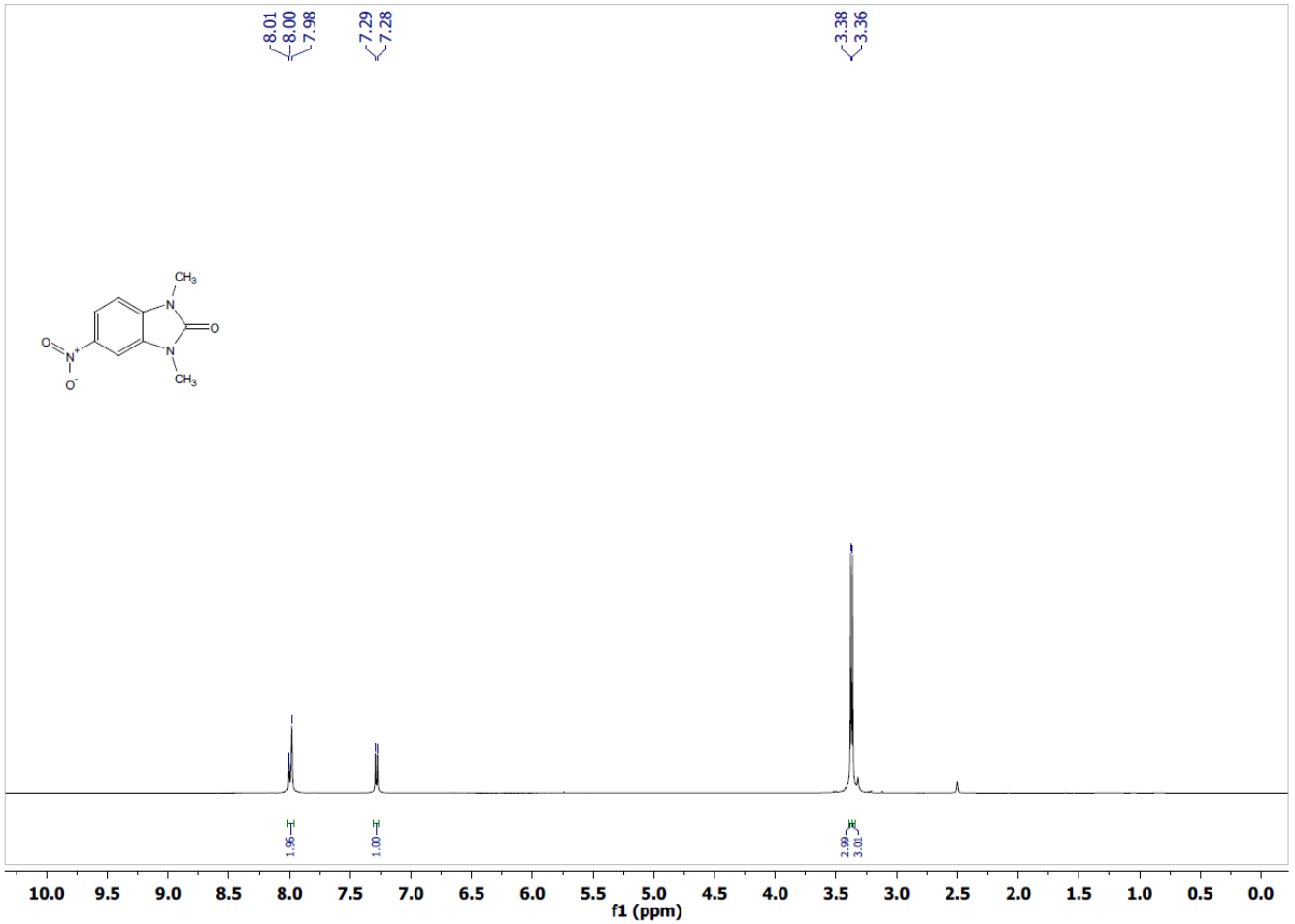

^{1}H NMR BL-02

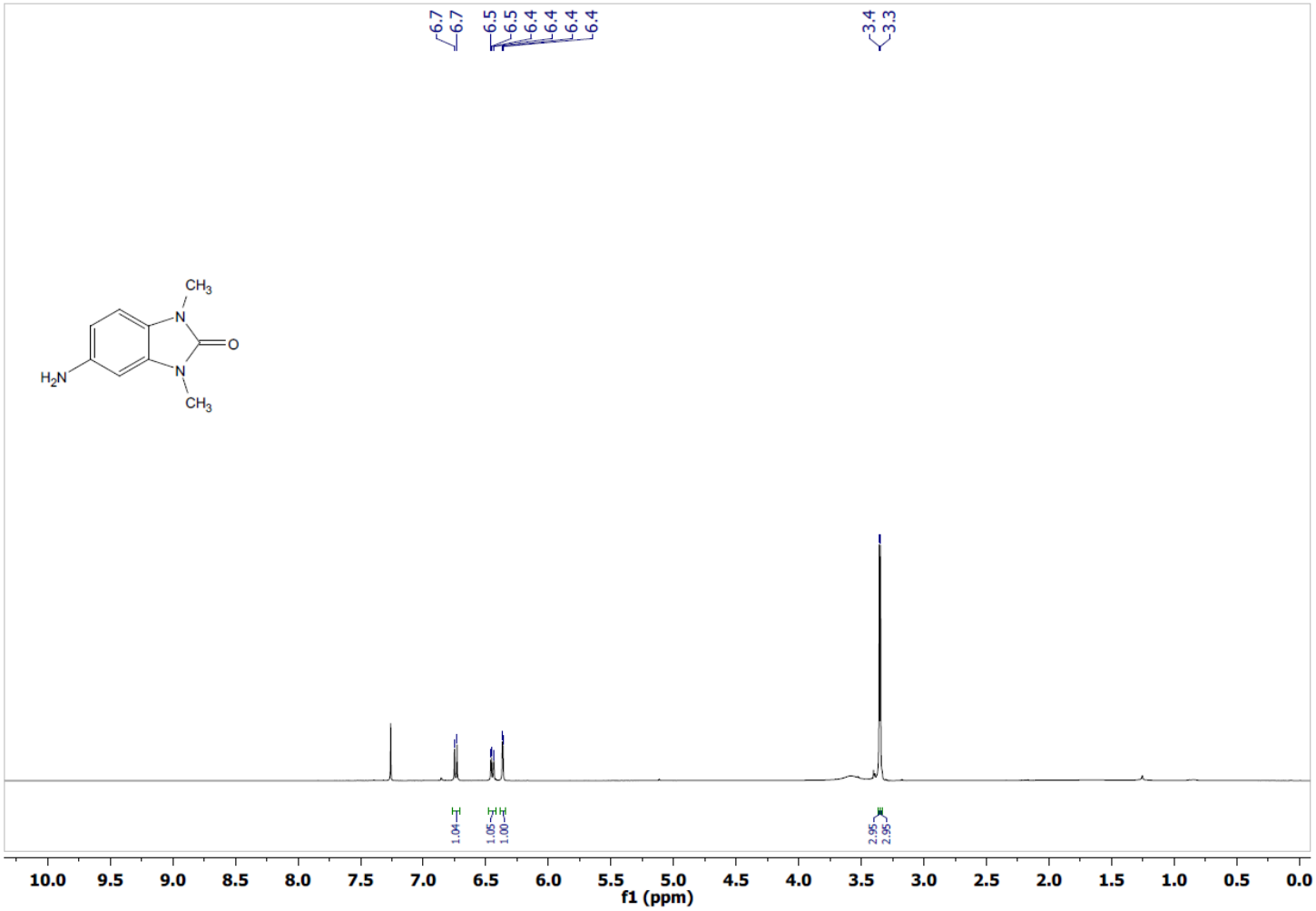
6.7
6.7
6.5
6.5
6.4
6.4
6.4
6.4
3.4
3.3
CH3
N
O
H2N
N
CH3
1.04
1.05
1.00
2.95
2.95
10.0 9.5 9.0 8.5 8.0 7.5 7.0 6.5 6.0 5.5 5.0 4.5 4.0 3.5 3.0 2.5 2.0 1.5 1.0 0.5 0.0
f1 (ppm)

^{1}H NMR BL-X1

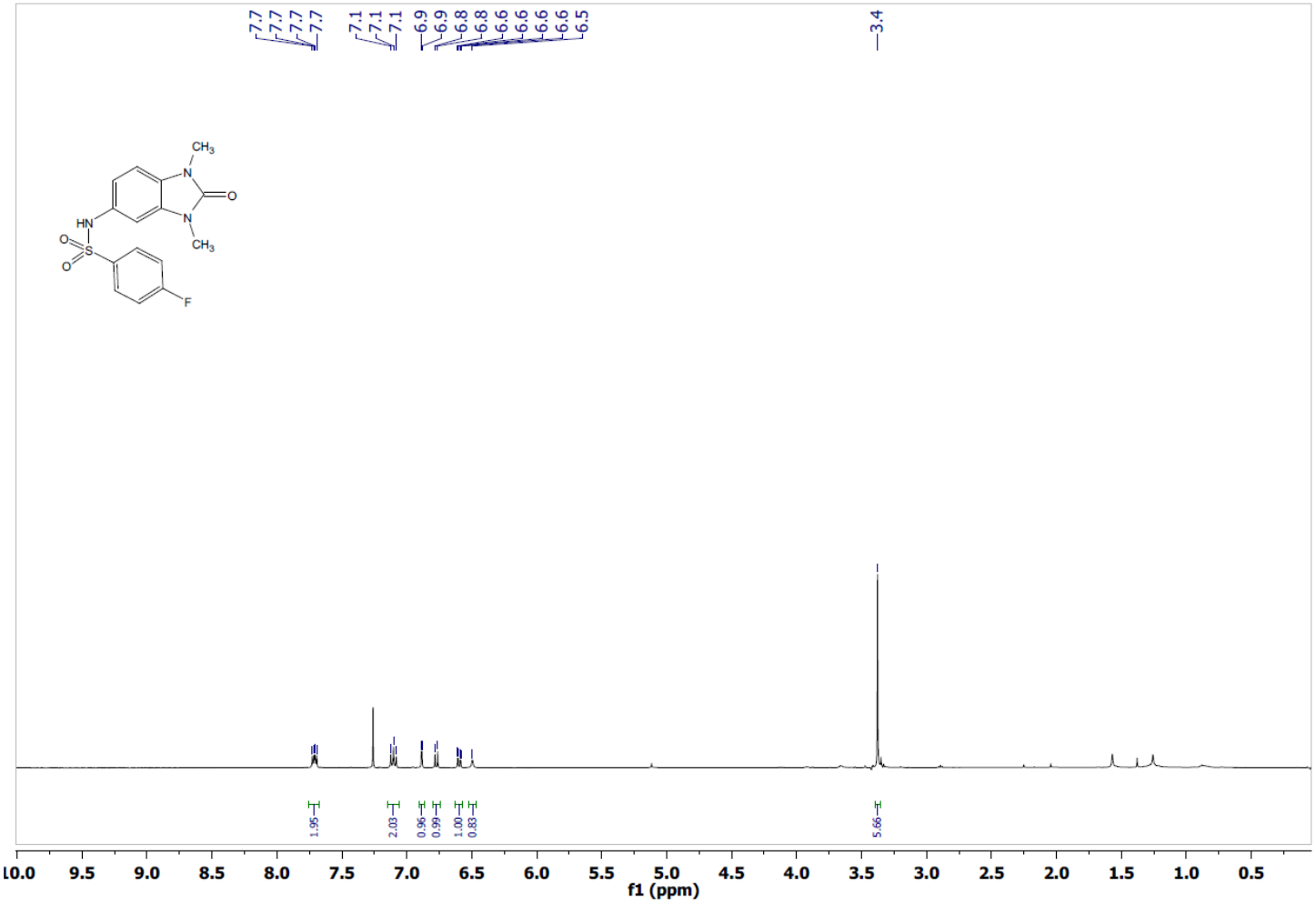
7.7
7.7
7.7
7.7
7.1
7.1
7.1
6.9
6.9
6.8
6.8
6.6
6.6
6.6
6.6
6.5
3.4
CH3
N
O
HN
O
S
O
N
CH3
F
1.95
2.03
0.96
0.99
1.00
0.83
5.66
10.0
9.5
9.0
8.5
8.0
7.5
7.0
6.5
6.0
5.5
5.0
4.5
4.0
3.5
3.0
2.5
2.0
1.5
1.0
0.5
f1 (ppm)

^{13}C NMR BL-X1

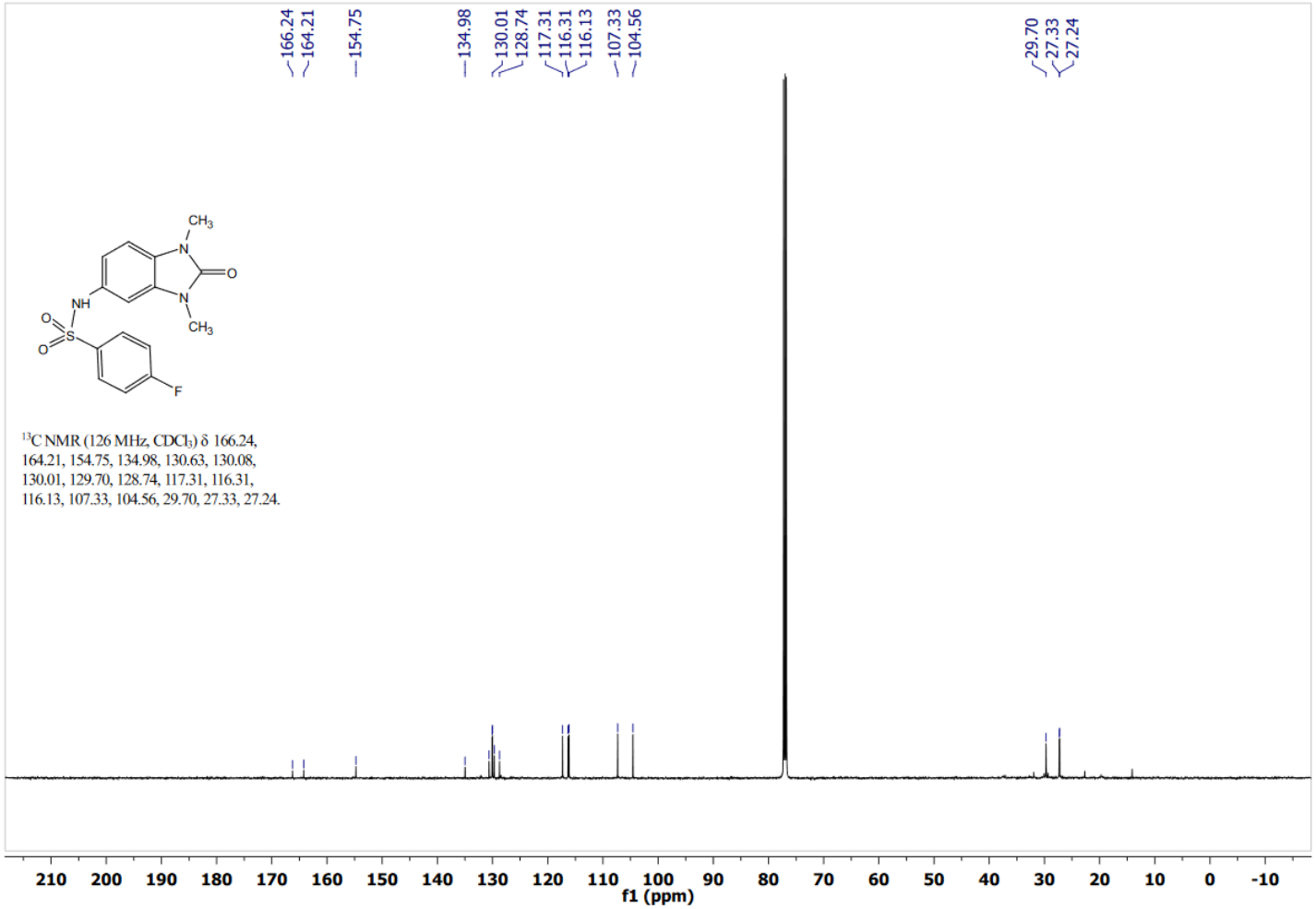
166.24
164.21
154.75
134.98
130.01
128.74
117.31
116.31
116.13
107.33
104.56
29.70
27.33
27.24
CH3
N
O
NH
O
S
O
N
CH3
F
13C NMR (126 MHz, CDCl3) δ 166.24, 164.21, 154.75, 134.98, 130.63, 130.08, 130.01, 129.70, 128.74, 117.31, 116.31, 116.13, 107.33, 104.56, 29.70, 27.33, 27.24.
210 200 190 180 170 160 150 140 130 120 110 100 90 80 70 60 50 40 30 20 10 0 -10
f1 (ppm)

^{1}H NMR BL-X2

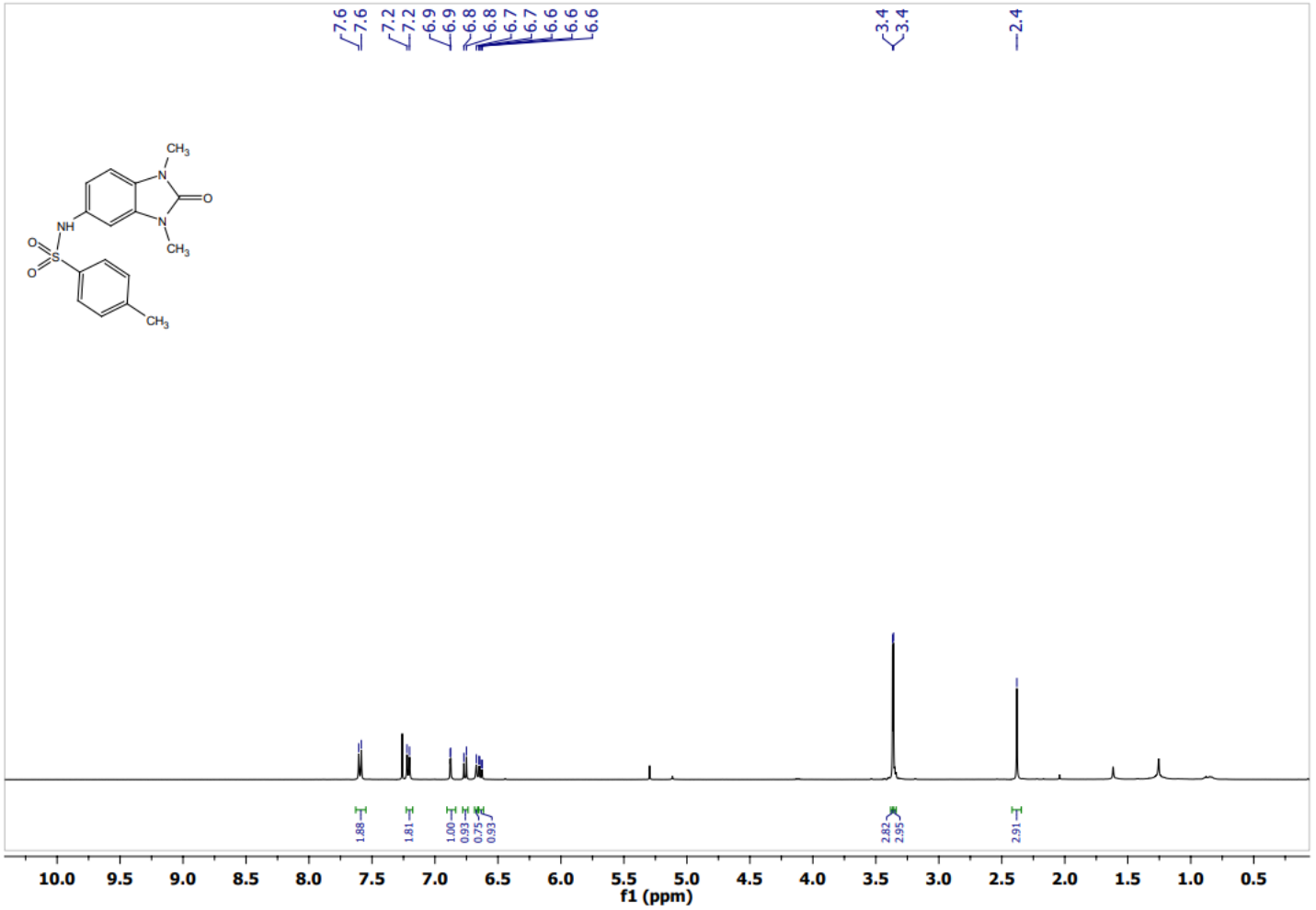
7.6
7.6
7.2
7.2
6.9
6.9
6.8
6.8
6.7
6.7
6.6
6.6
6.6
3.4
3.4
2.4
CH3
N
O
NH
S
O
O
N
CH3
CH3
1.88
1.81
1.00
0.93
0.75
0.93
2.82
2.95
2.91
10.0
9.5
9.0
8.5
8.0
7.5
7.0
6.5
6.0
5.5
5.0
4.5
4.0
3.5
3.0
2.5
2.0
1.5
1.0
0.5
f1 (ppm)

^{13}C NMR BL-X2

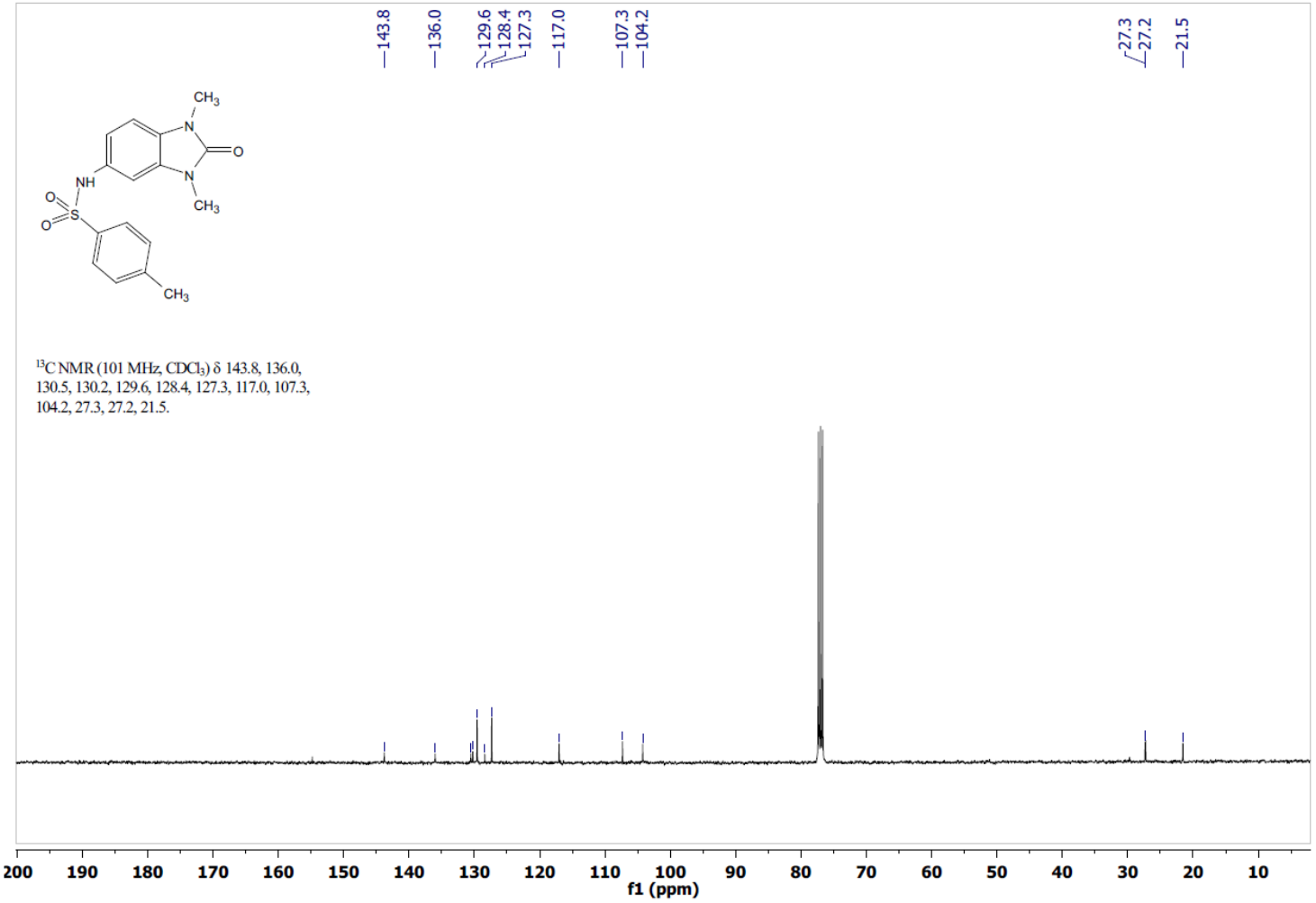
143.8
136.0
129.6
128.4
127.3
117.0
107.3
104.2
27.3
27.2
21.5
CH3
N
O
NH
S
CH3
CH3
13C NMR (101 MHz, CDCl3) δ 143.8, 136.0, 130.5, 130.2, 129.6, 128.4, 127.3, 117.0, 107.3, 104.2, 27.3, 27.2, 21.5.
200 190 180 170 160 150 140 130 120 110 100 90 80 70 60 50 40 30 20 10
f1 (ppm)

^{1}H NMR BL-X3

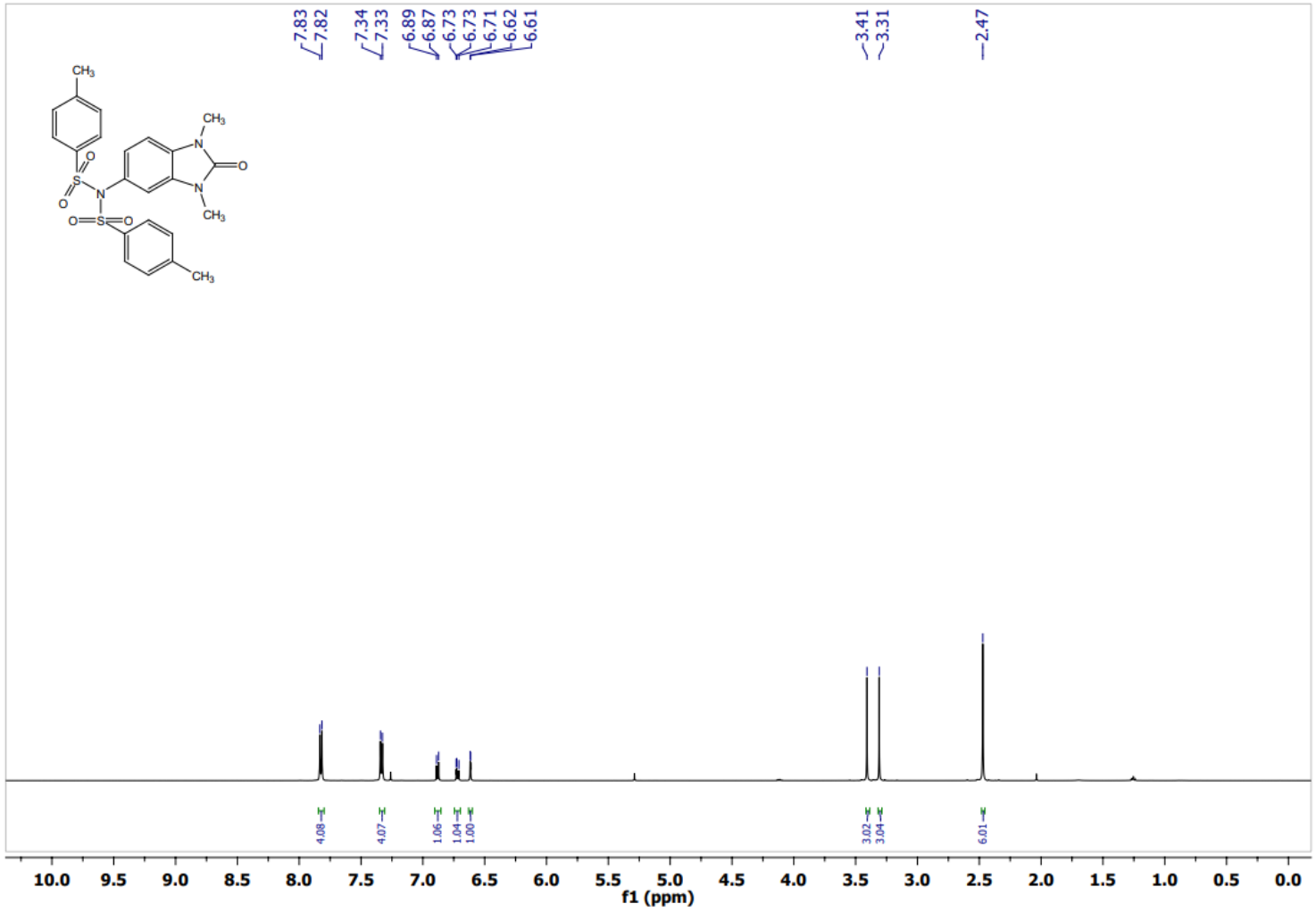
7.83
7.82
7.34
7.33
6.89
6.87
6.73
6.73
6.71
6.62
6.61
3.41
3.31
2.47
4.08
4.07
1.06
1.04
1.00
3.02
3.04
6.01
10.0 9.5 9.0 8.5 8.0 7.5 7.0 6.5 6.0 5.5 5.0 4.5 4.0 3.5 3.0 2.5 2.0 1.5 1.0 0.5 0.0
f1 (ppm)

^{13}C NMR BL-X3

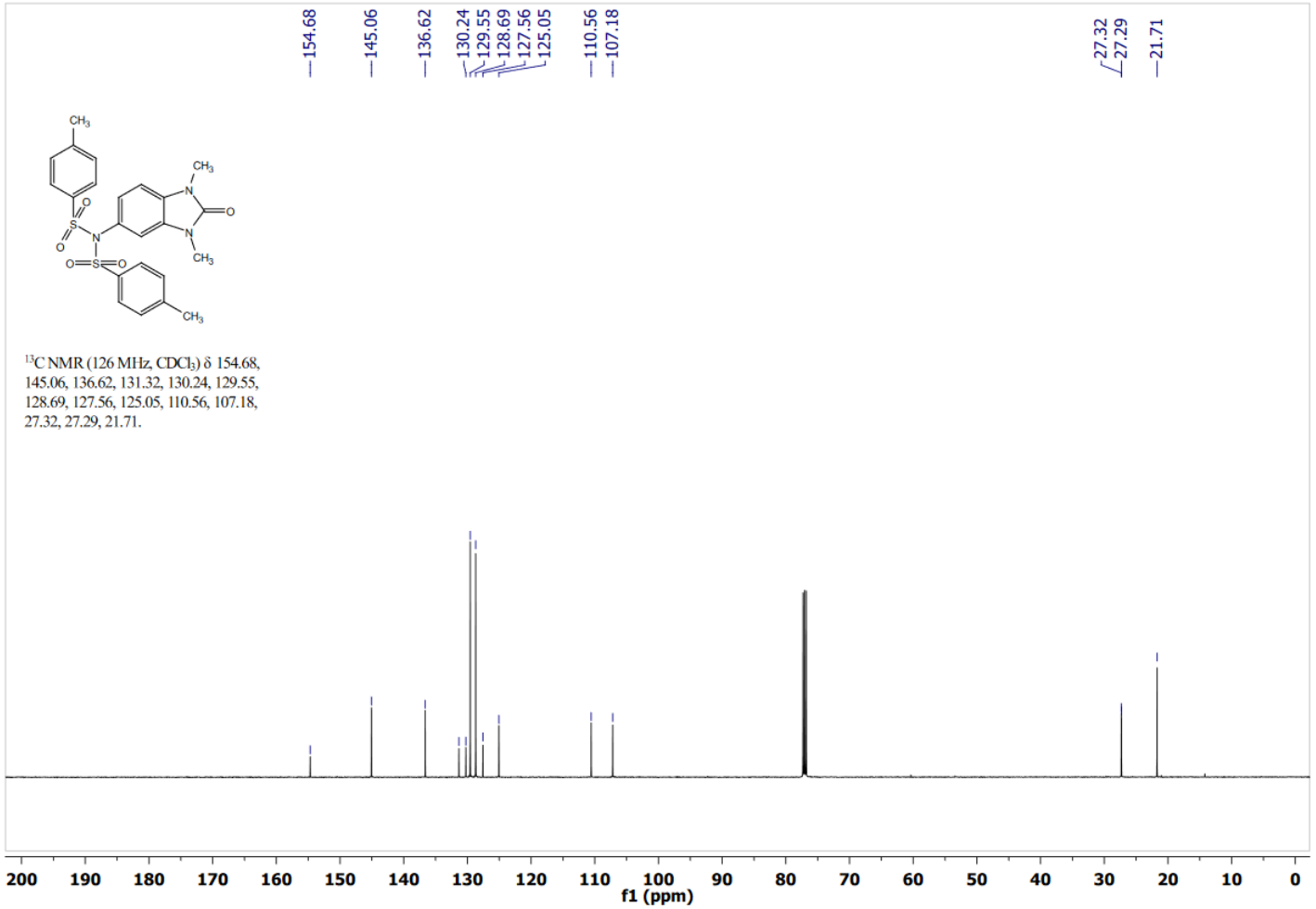
154.68
145.06
136.62
130.24
129.55
128.69
127.56
125.05
110.56
107.18
27.32
27.29
21.71
13C NMR (126 MHz, CDCl3) δ 154.68, 145.06, 136.62, 131.32, 130.24, 129.55, 128.69, 127.56, 125.05, 110.56, 107.18, 27.32, 27.29, 21.71.
200 190 180 170 160 150 140 130 120 110 100 90 80 70 60 50 40 30 20 10 0
f1 (ppm)

^{1}H NMR BL-X4

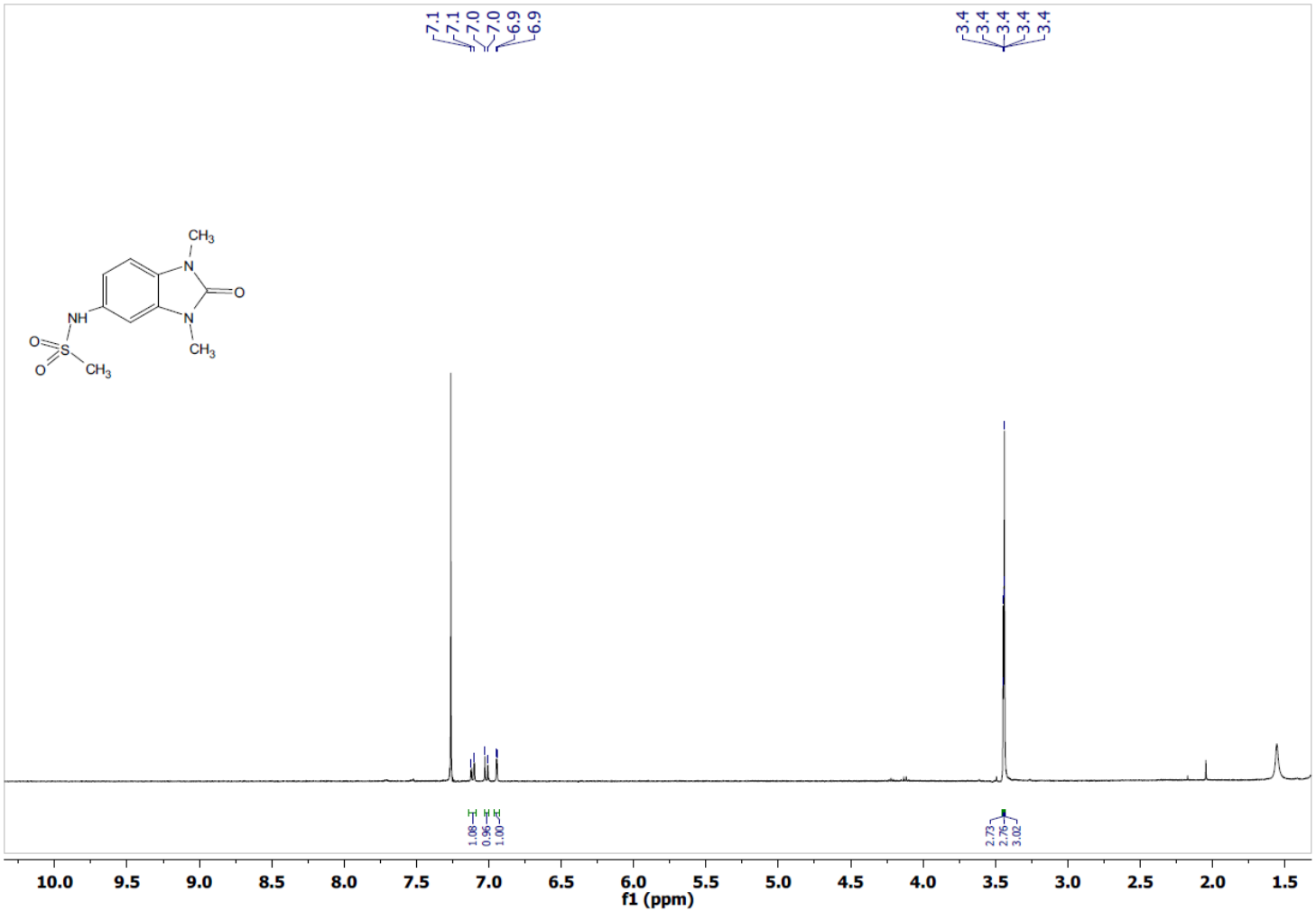
7.1
7.1
7.0
7.0
6.9
6.9
3.4
3.4
3.4
3.4
3.4
CH3
N
O
NH
N
CH3
O
S
O
CH3
1.08
0.96
1.00
2.73
2.76
3.02
10.0
9.5
9.0
8.5
8.0
7.5
7.0
6.5
6.0
5.5
5.0
4.5
4.0
3.5
3.0
2.5
2.0
1.5
f1 (ppm)

^{1}H NMR B2-X4

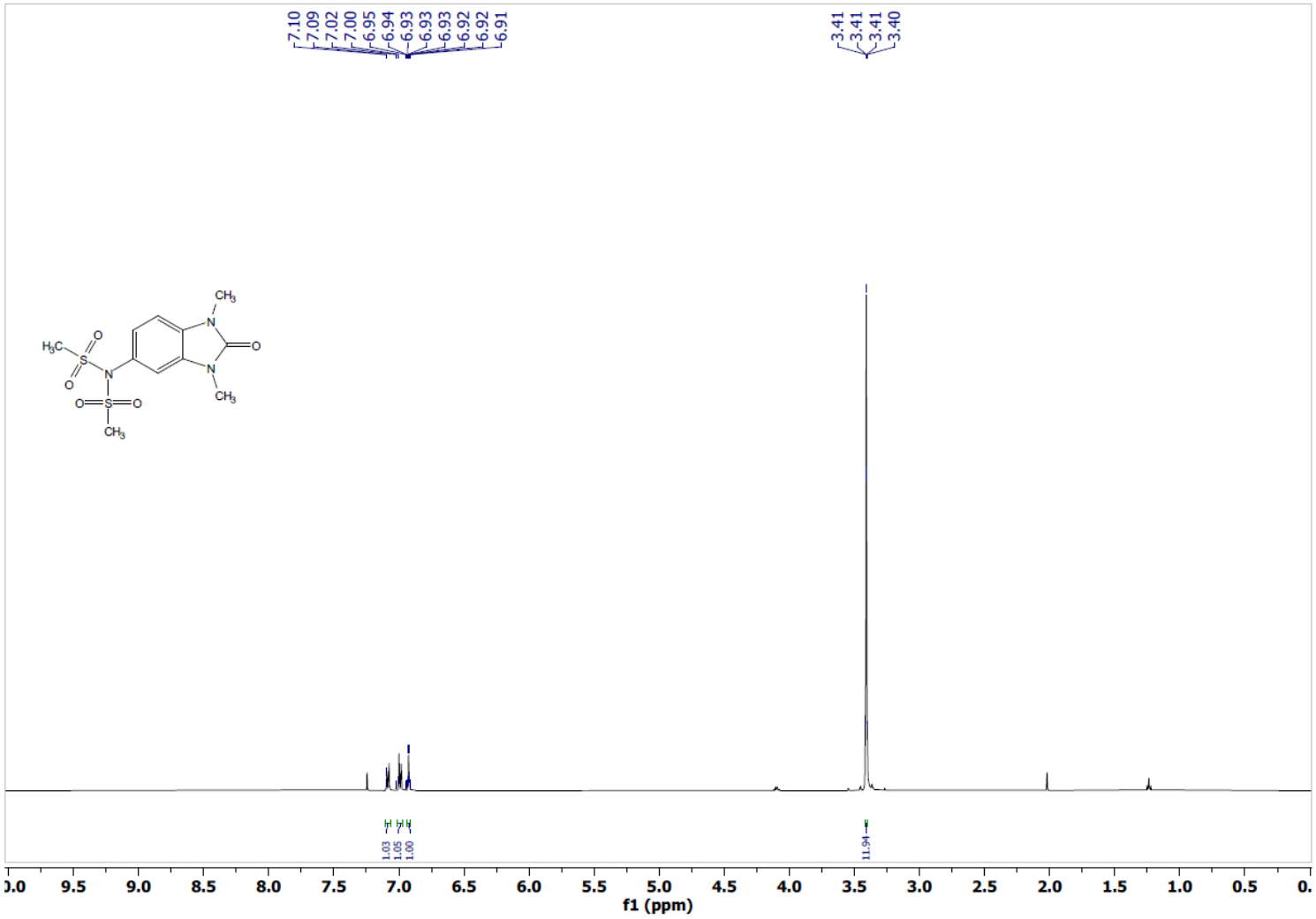
7.10
7.09
7.02
7.00
6.95
6.94
6.93
6.93
6.93
6.92
6.92
6.91
3.41
3.41
3.41
3.40
1.03
1.05
1.00
11.94
f1 (ppm)

^{13}C NMR B2-X4

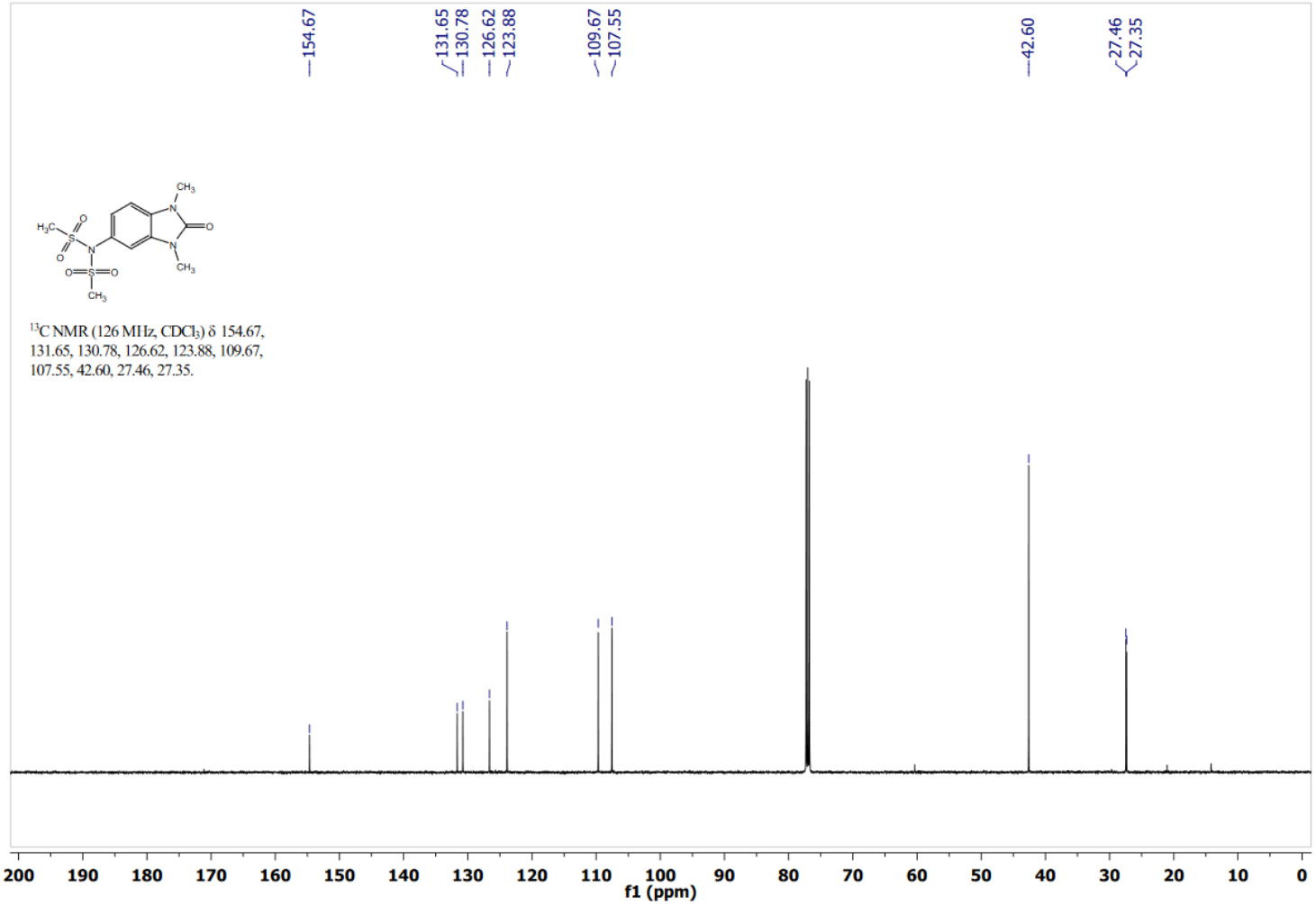
154.67
131.65
130.78
126.62
123.88
109.67
107.55
42.60
27.46
27.35
13C NMR (126 MHz, CDCl3) δ 154.67, 131.65, 130.78, 126.62, 123.88, 109.67, 107.55, 42.60, 27.46, 27.35.
200 190 180 170 160 150 140 130 120 110 100 90 80 70 60 50 40 30 20 10 0
f1 (ppm)

^{1}H NMR BL-X5

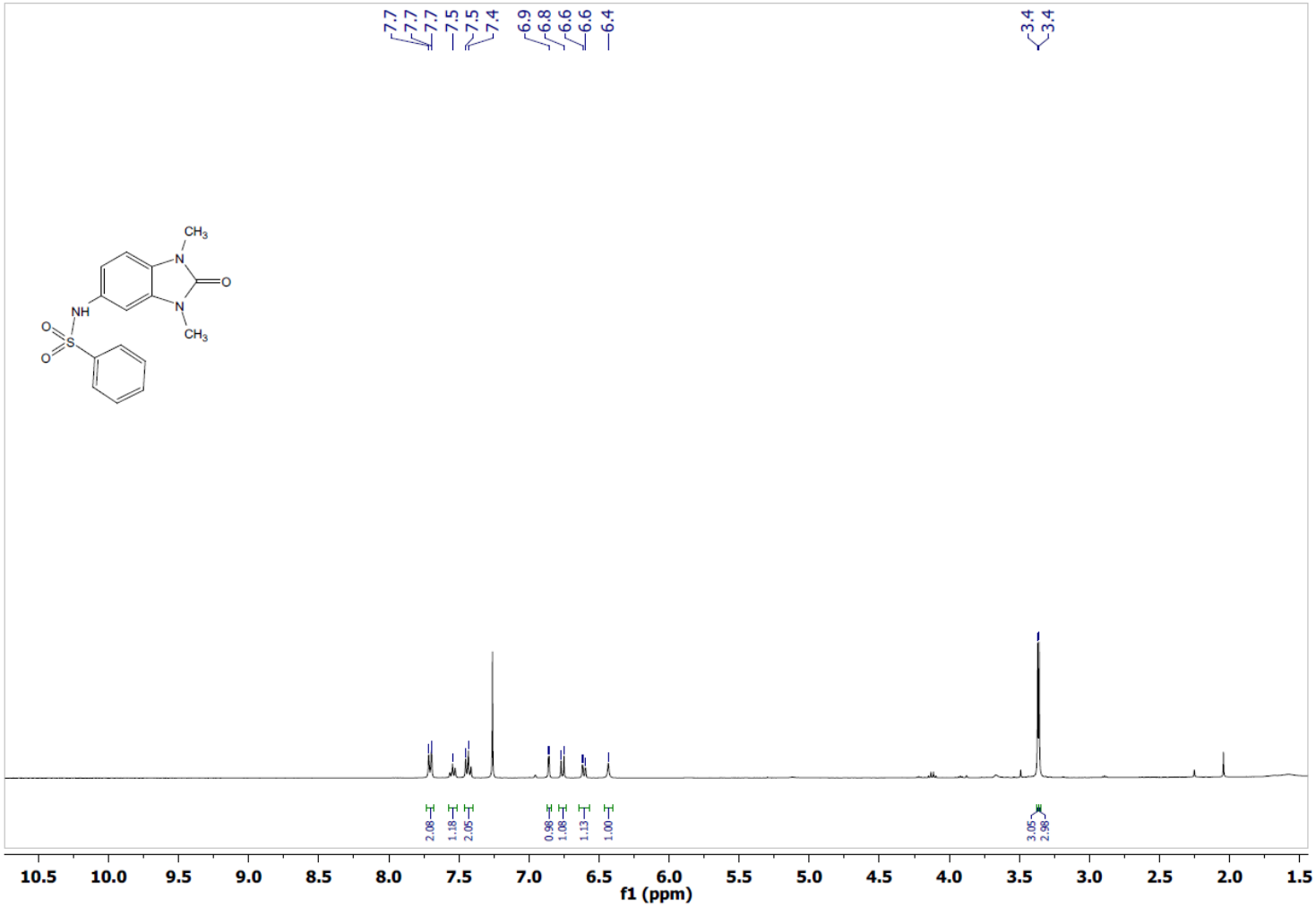
7.7
7.7
7.7
7.5
7.5
7.4
6.9
6.8
6.6
6.6
6.4
3.4
3.4
CH3
N
O
NH
O
S
O
N
CH3
2.08
1.18
2.05
0.98
1.08
1.13
1.00
3.05
2.98
10.5
10.0
9.5
9.0
8.5
8.0
7.5
7.0
6.5
6.0
5.5
5.0
4.5
4.0
3.5
3.0
2.5
2.0
1.5
f1 (ppm)

^{1}H NMR BL-X6

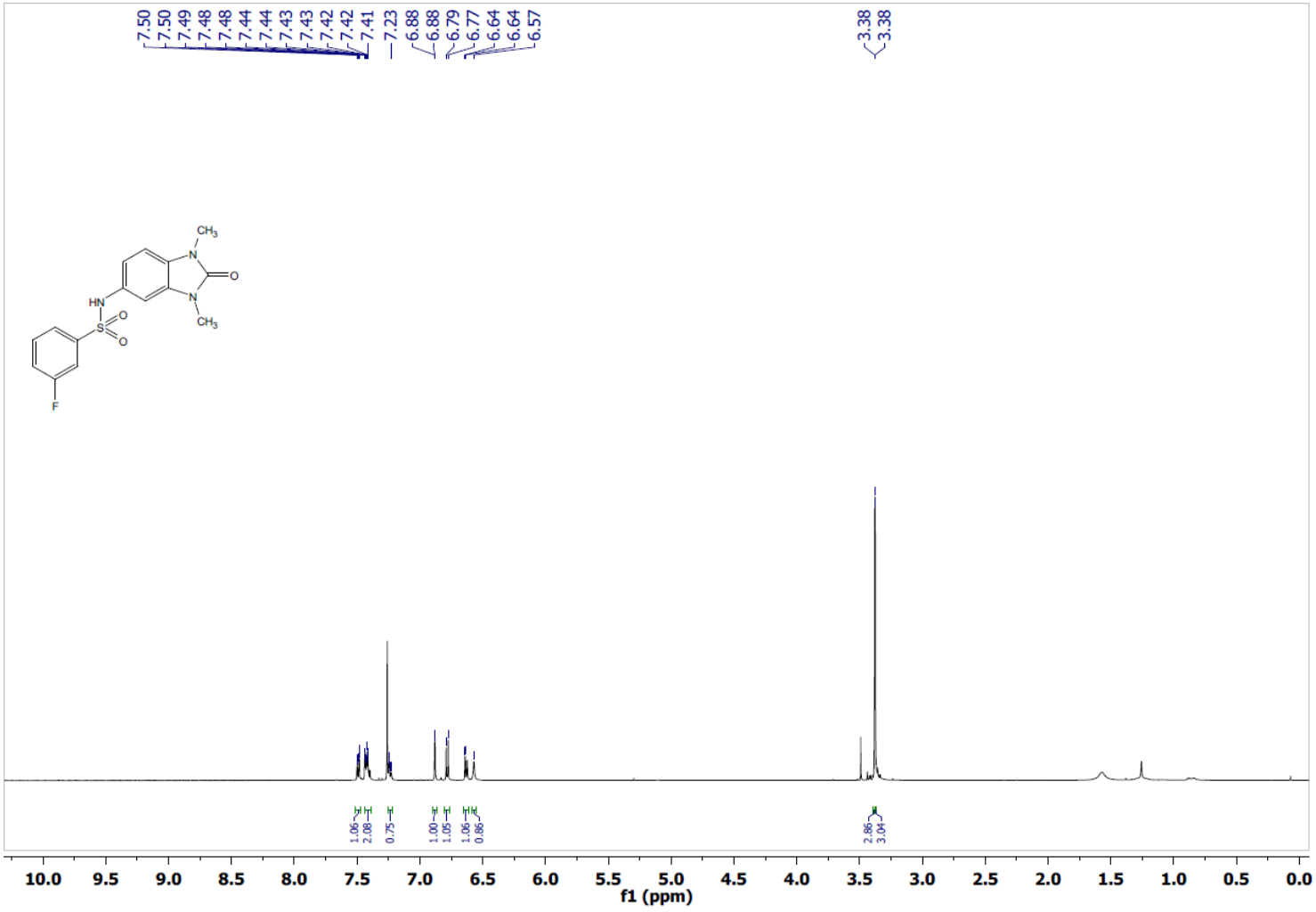
7.50
7.50
7.49
7.48
7.48
7.44
7.44
7.43
7.43
7.42
7.42
7.41
7.23
6.88
6.88
6.79
6.77
6.64
6.64
6.57
3.38
3.38
CH3
N
O
HN
S
O
O
N
CH3
F
1.06
2.08
0.75
1.00
1.05
1.06
0.86
2.86
3.04
10.0
9.5
9.0
8.5
8.0
7.5
7.0
6.5
6.0
5.5
5.0
4.5
4.0
3.5
3.0
2.5
2.0
1.5
1.0
0.5
0.0
f1 (ppm)

^{13}C NMR BL-X6

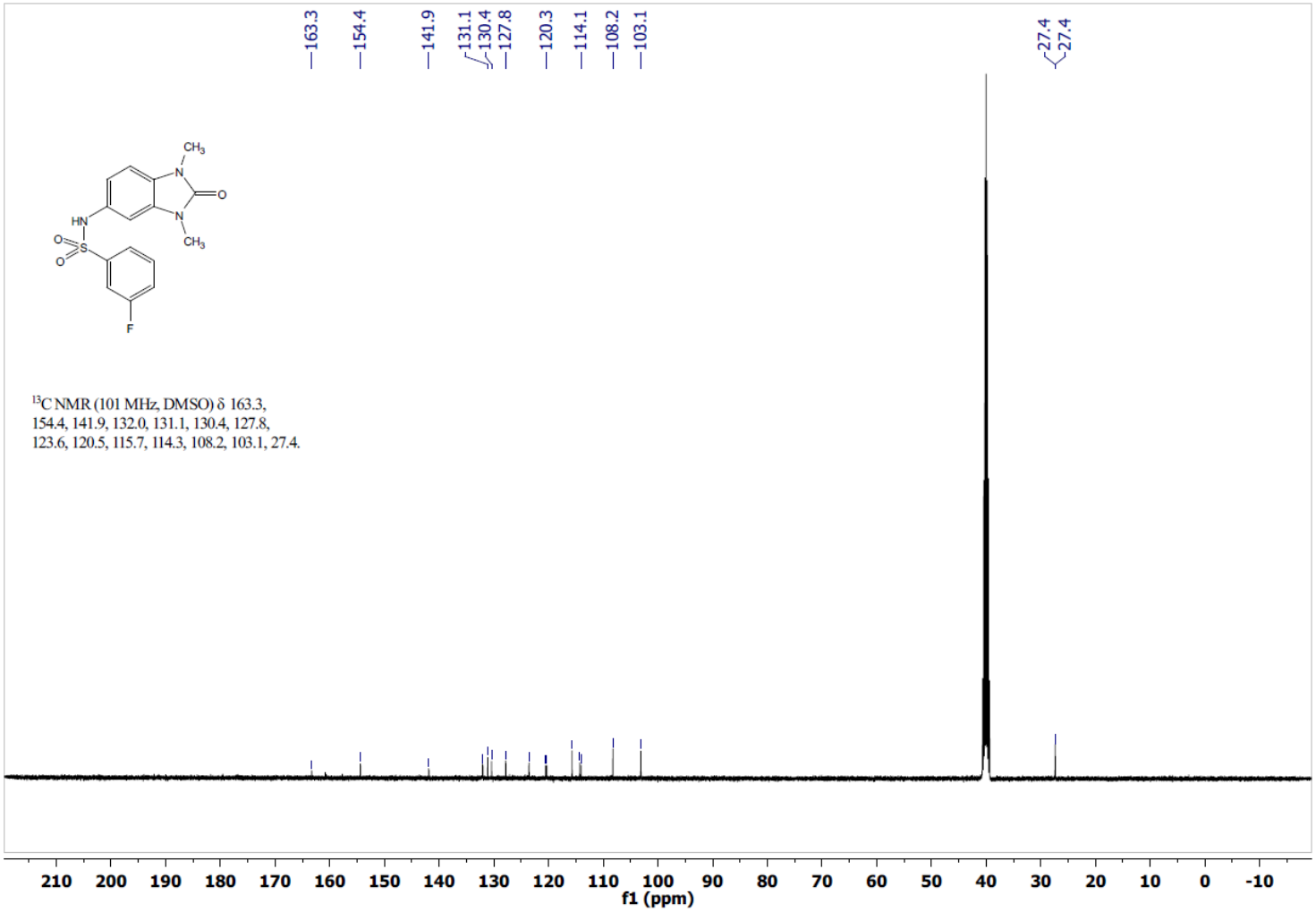
163.3
154.4
141.9
131.1
130.4
127.8
120.3
114.1
108.2
103.1
27.4
27.4
CH3
N
O
HN
O
S
O
N
CH3
F
13C NMR (101 MHz, DMSO) δ 163.3,
154.4, 141.9, 132.0, 131.1, 130.4, 127.8,
123.6, 120.5, 115.7, 114.3, 108.2, 103.1, 27.4.
210 200 190 180 170 160 150 140 130 120 110 100 90 80 70 60 50 40 30 20 10 0 -10
f1 (ppm)

^{1}H NMR BL-X7

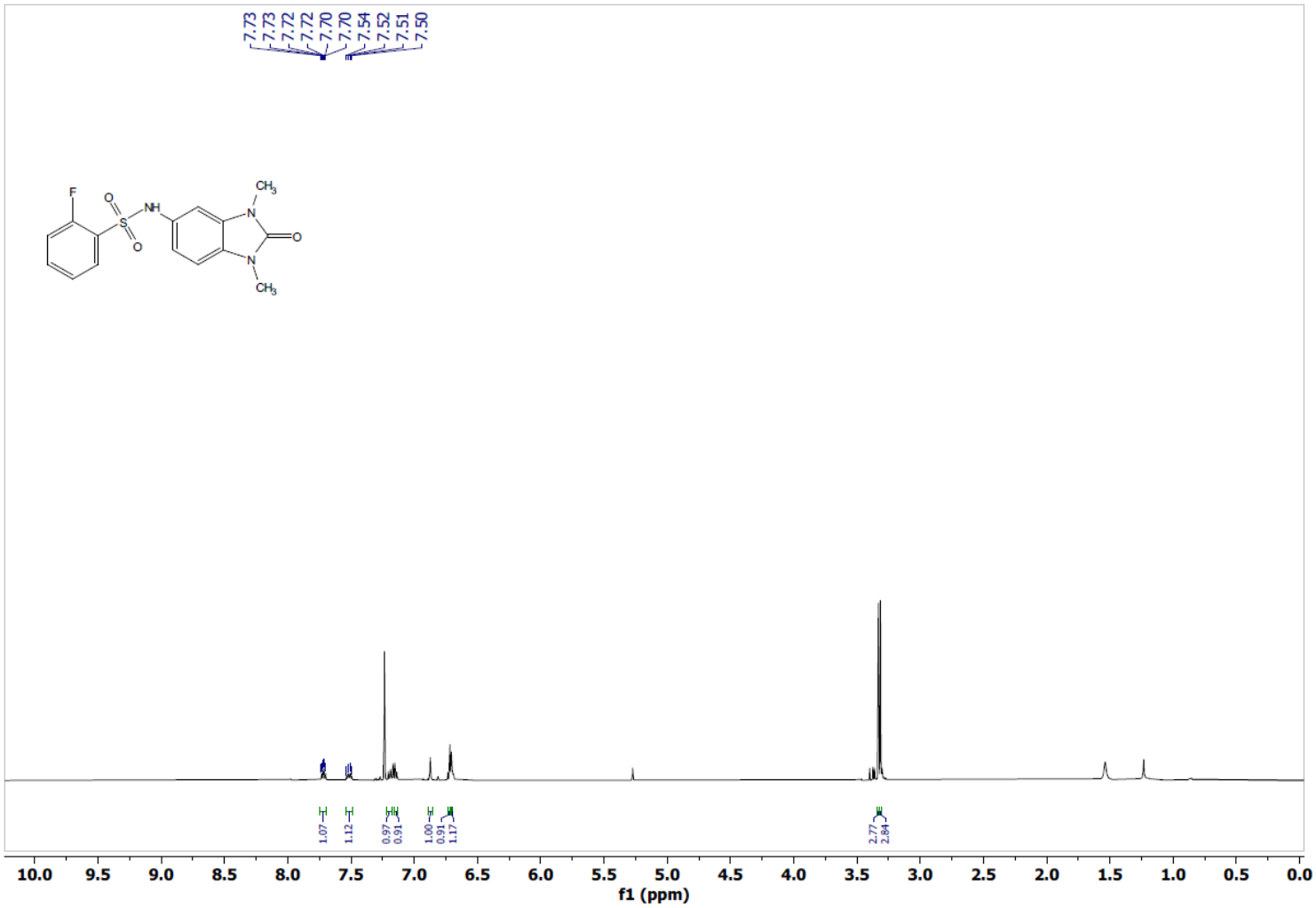
7.73
7.73
7.72
7.72
7.70
7.70
7.54
7.52
7.51
7.50
F
O
S
O
NH
CH3
N
O
N
CH3
1.07
1.12
0.97
0.91
1.00
0.91
1.17
2.77
2.84
10.0
9.5
9.0
8.5
8.0
7.5
7.0
6.5
6.0
5.5
5.0
4.5
4.0
3.5
3.0
2.5
2.0
1.5
1.0
0.5
0.0
f1 (ppm)

^{13}C NMR BL-X7

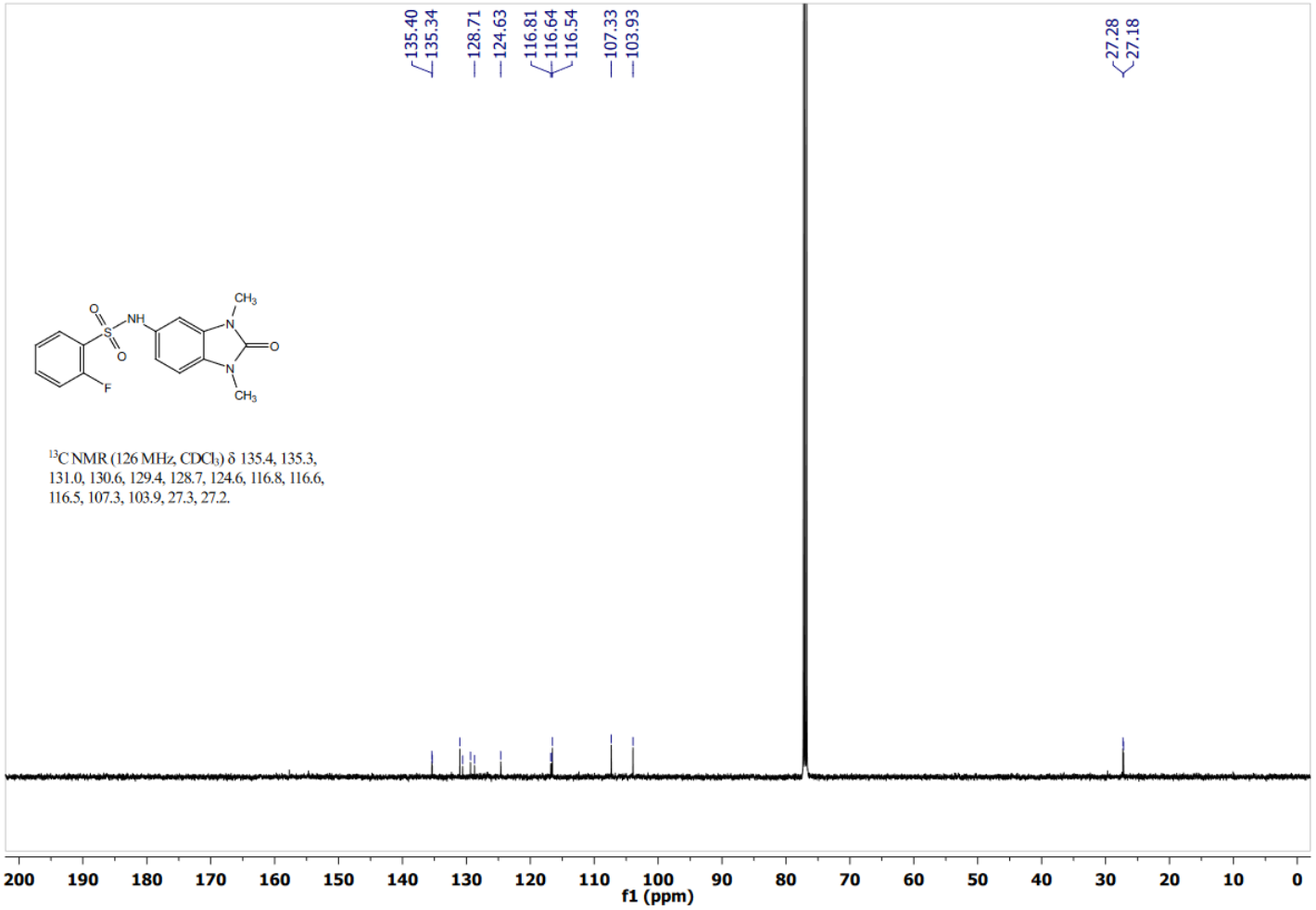
135.40
135.34
128.71
124.63
116.81
116.64
116.54
107.33
103.93
27.28
27.18
O
S
O
NH
F
CH3
N
O
N
CH3
13C NMR (126 MHz, CDCl3) δ 135.4, 135.3, 131.0, 130.6, 129.4, 128.7, 124.6, 116.8, 116.6, 116.5, 107.3, 103.9, 27.3, 27.2.
200 190 180 170 160 150 140 130 120 110 100 90 80 70 60 50 40 30 20 10 0
f1 (ppm)

^{1}H NMR BL-X8

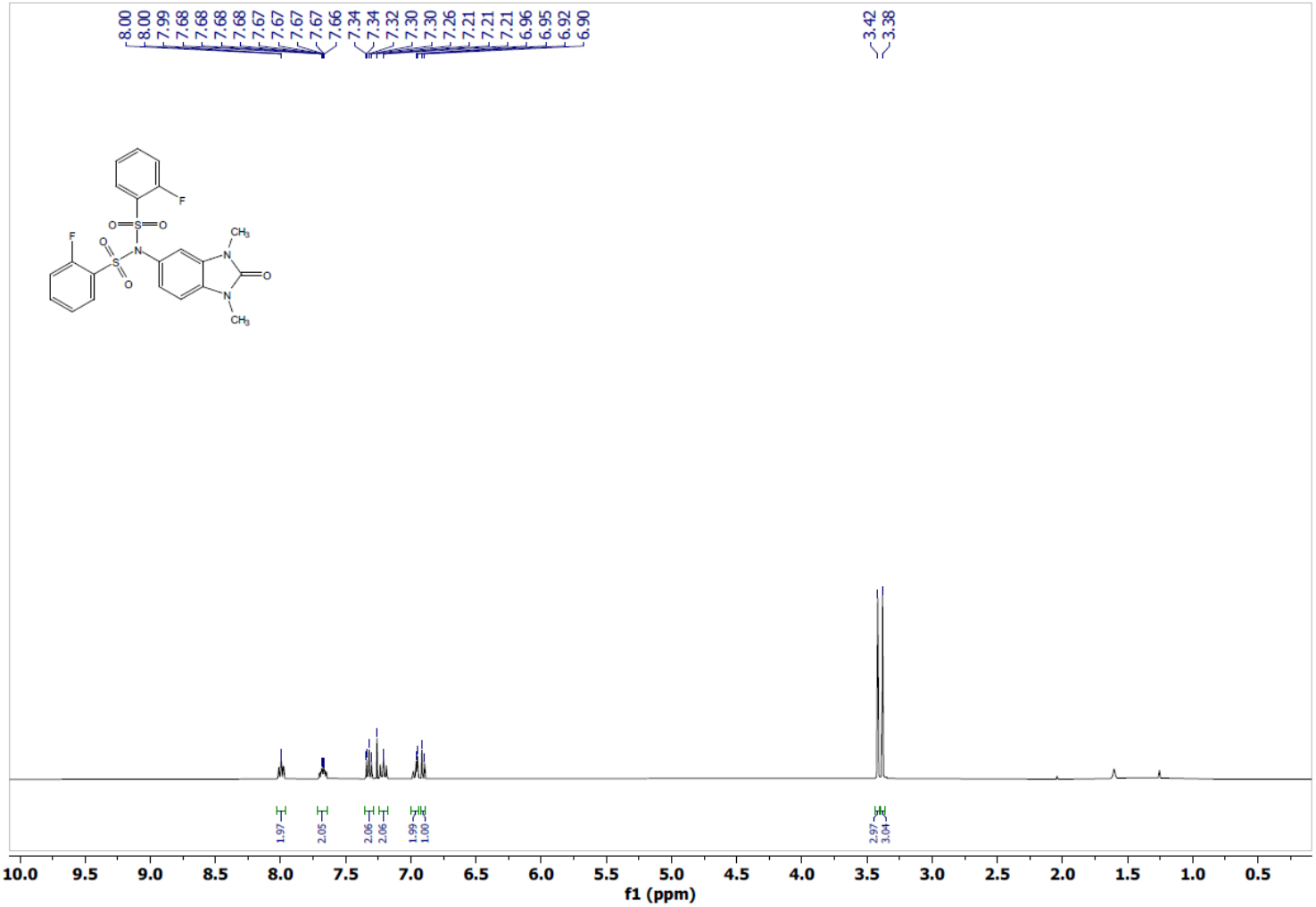
8.00
8.00
7.99
7.68
7.68
7.68
7.68
7.67
7.67
7.67
7.67
7.66
7.34
7.34
7.32
7.30
7.30
7.26
7.21
7.21
7.21
6.96
6.95
6.92
6.90
3.42
3.38
F
F
O=S=O
O
S
O
N
CH3
N
O
N
CH3
1.97
2.05
2.06
2.06
1.99
1.00
2.97
3.04
10.0
9.5
9.0
8.5
8.0
7.5
7.0
6.5
6.0
5.5
5.0
4.5
4.0
3.5
3.0
2.5
2.0
1.5
1.0
0.5
f1 (ppm)

^{13}C NMR BL-X8

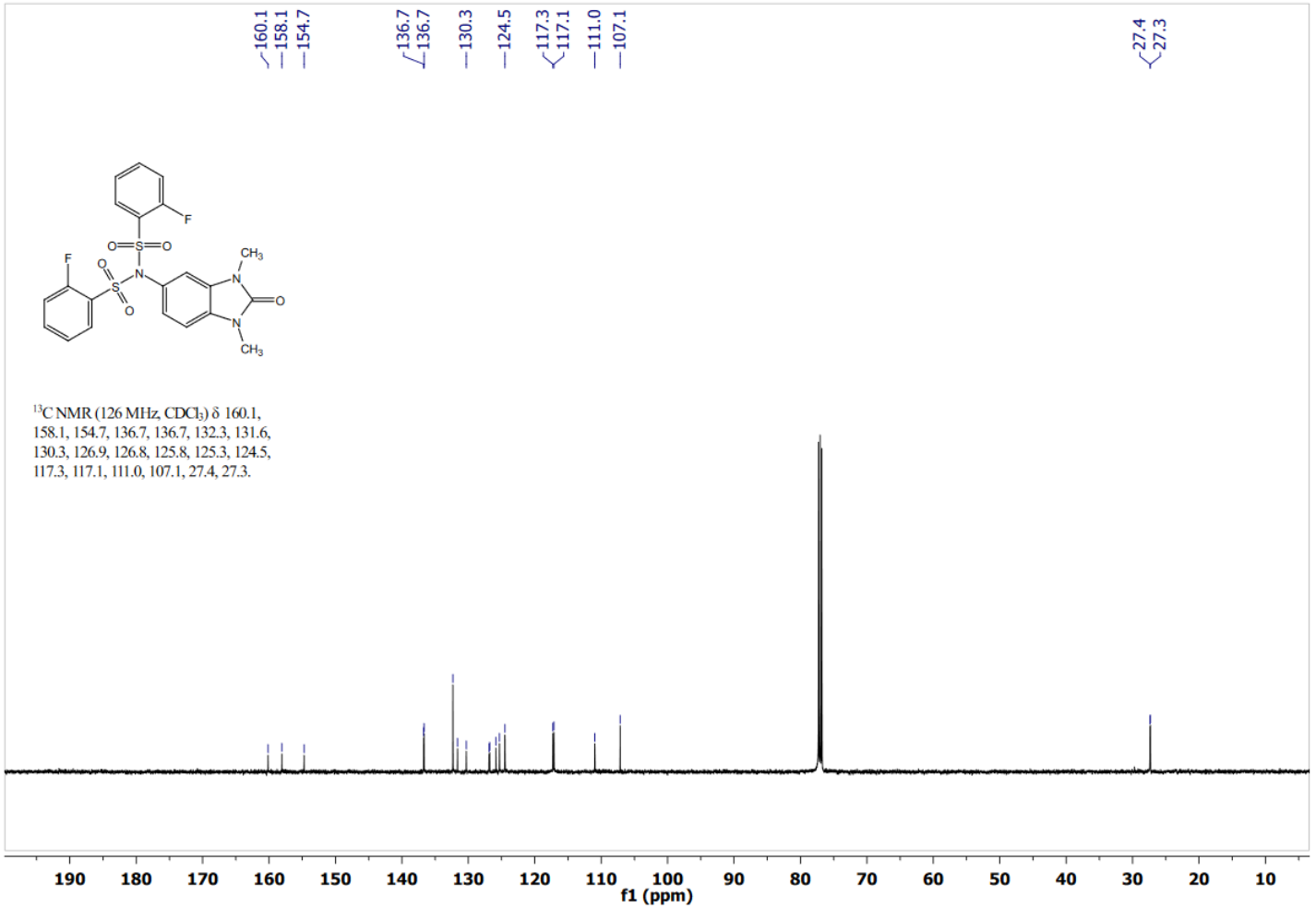
160.1
158.1
154.7
136.7
136.7
130.3
124.5
117.3
117.1
111.0
107.1
27.4
27.3
F
F
O
S
O
O
S
O
O
N
CH3
N
O
N
CH3
13C NMR (126 MHz, CDCl3) δ 160.1, 158.1, 154.7, 136.7, 136.7, 132.3, 131.6, 130.3, 126.9, 126.8, 125.8, 125.3, 124.5, 117.3, 117.1, 111.0, 107.1, 27.4, 27.3.
190
180
170
160
150
140
130
120
110
100
90
80
70
60
50
40
30
20
10
f1 (ppm)

^{1}H NMR BL-X10

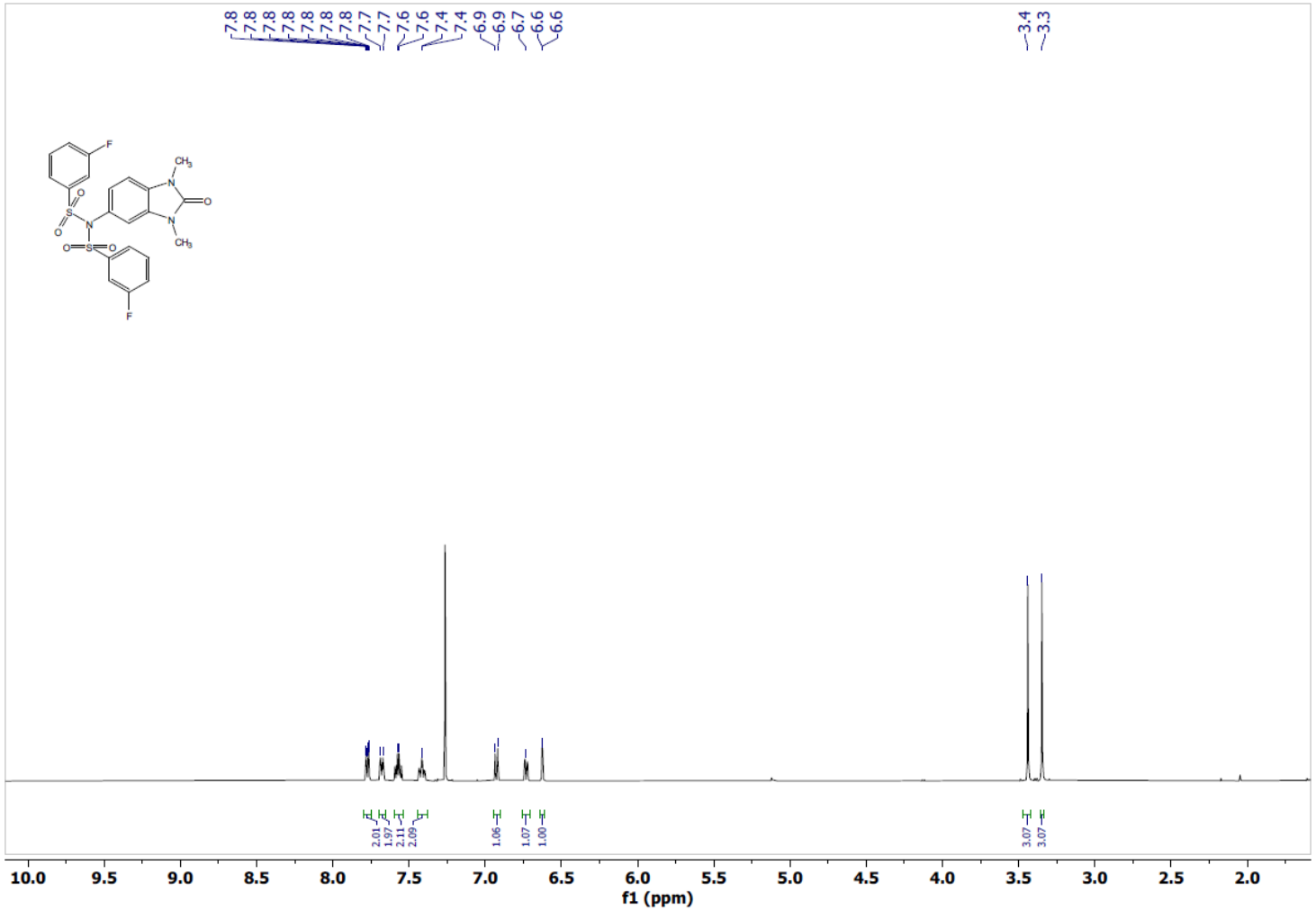
7.8
7.8
7.8
7.8
7.8
7.8
7.8
7.7
7.7
7.6
7.6
7.4
7.4
6.9
6.9
6.7
6.6
6.6
3.4
3.3
2.01
1.97
2.11
2.09
1.06
1.07
1.00
3.07
3.07
10.0
9.5
9.0
8.5
8.0
7.5
7.0
6.5
6.0
5.5
5.0
4.5
4.0
3.5
3.0
2.5
2.0
f1 (ppm)

^{13}C NMR BL-X10

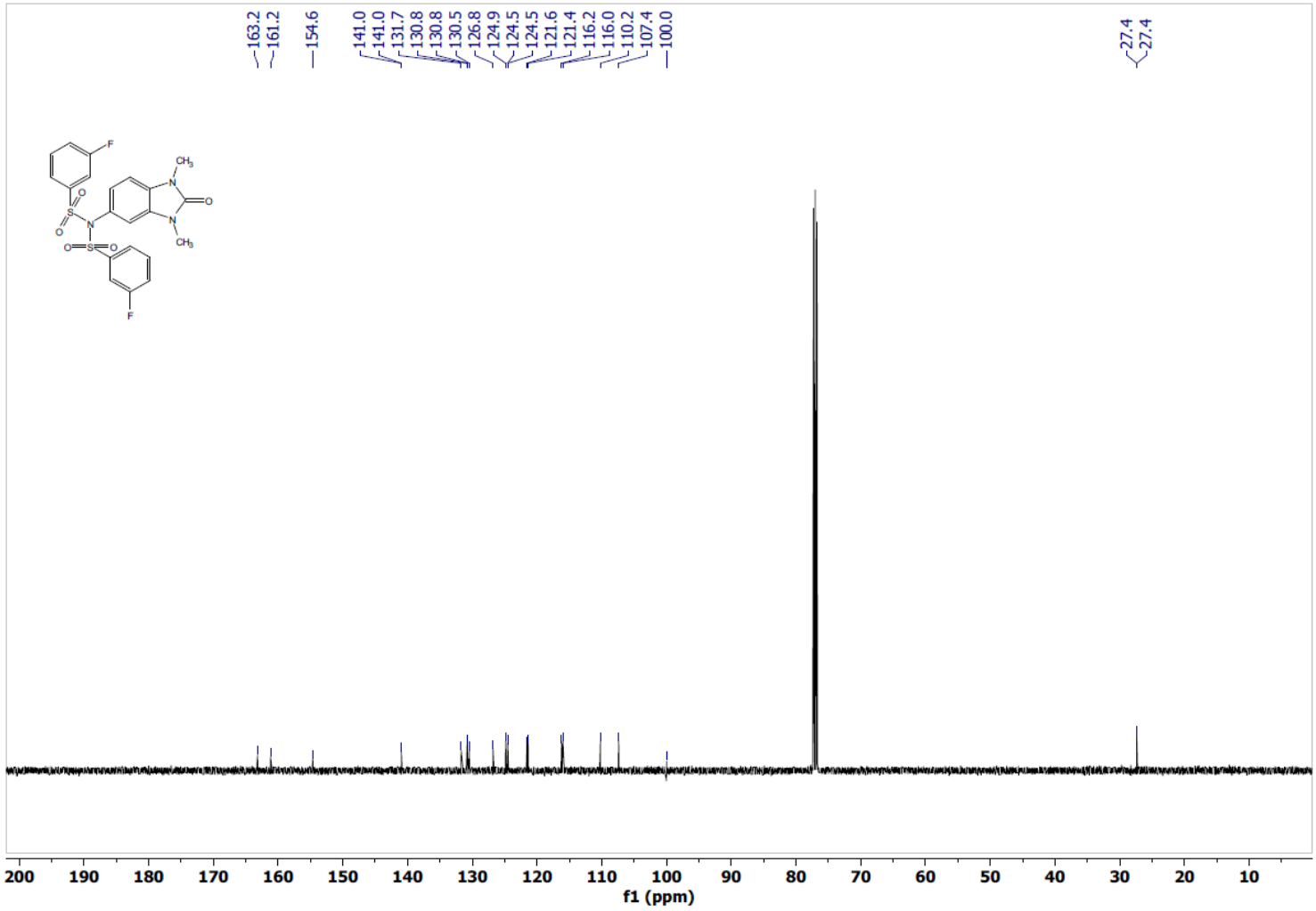

^{1}H NMR BL-X11

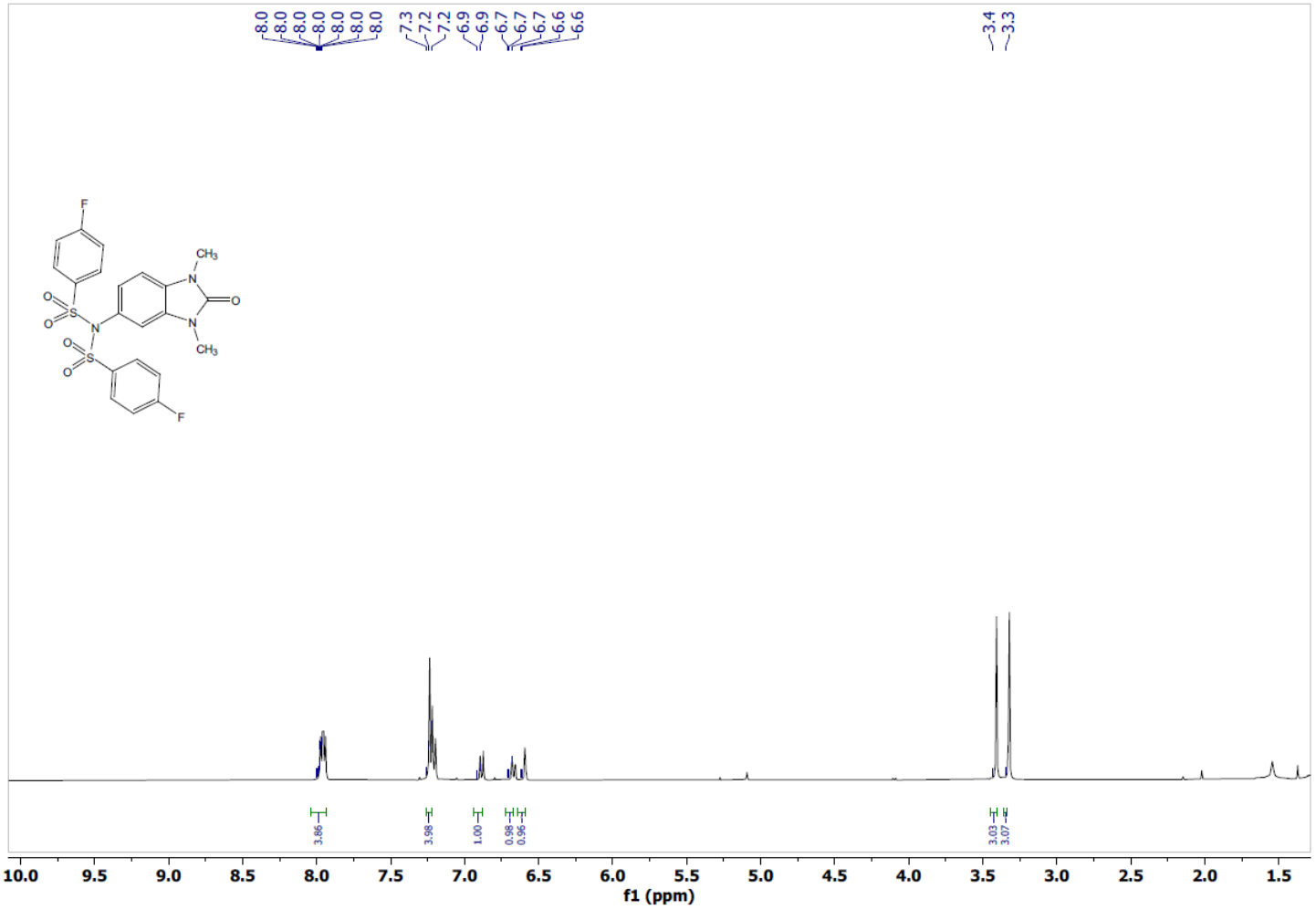
8.0
8.0
8.0
8.0
8.0
8.0
8.0
7.3
7.2
7.2
6.9
6.9
6.7
6.7
6.7
6.6
6.6
3.4
3.3
F
CH3
N
O
S
O
O
N
O
S
O
O
N
CH3
F
3.86
3.98
1.00
0.98
0.96
3.03
3.07
10.0
9.5
9.0
8.5
8.0
7.5
7.0
6.5
6.0
5.5
5.0
4.5
4.0
3.5
3.0
2.5
2.0
1.5
f1 (ppm)

^{13}C NMR BL-X11

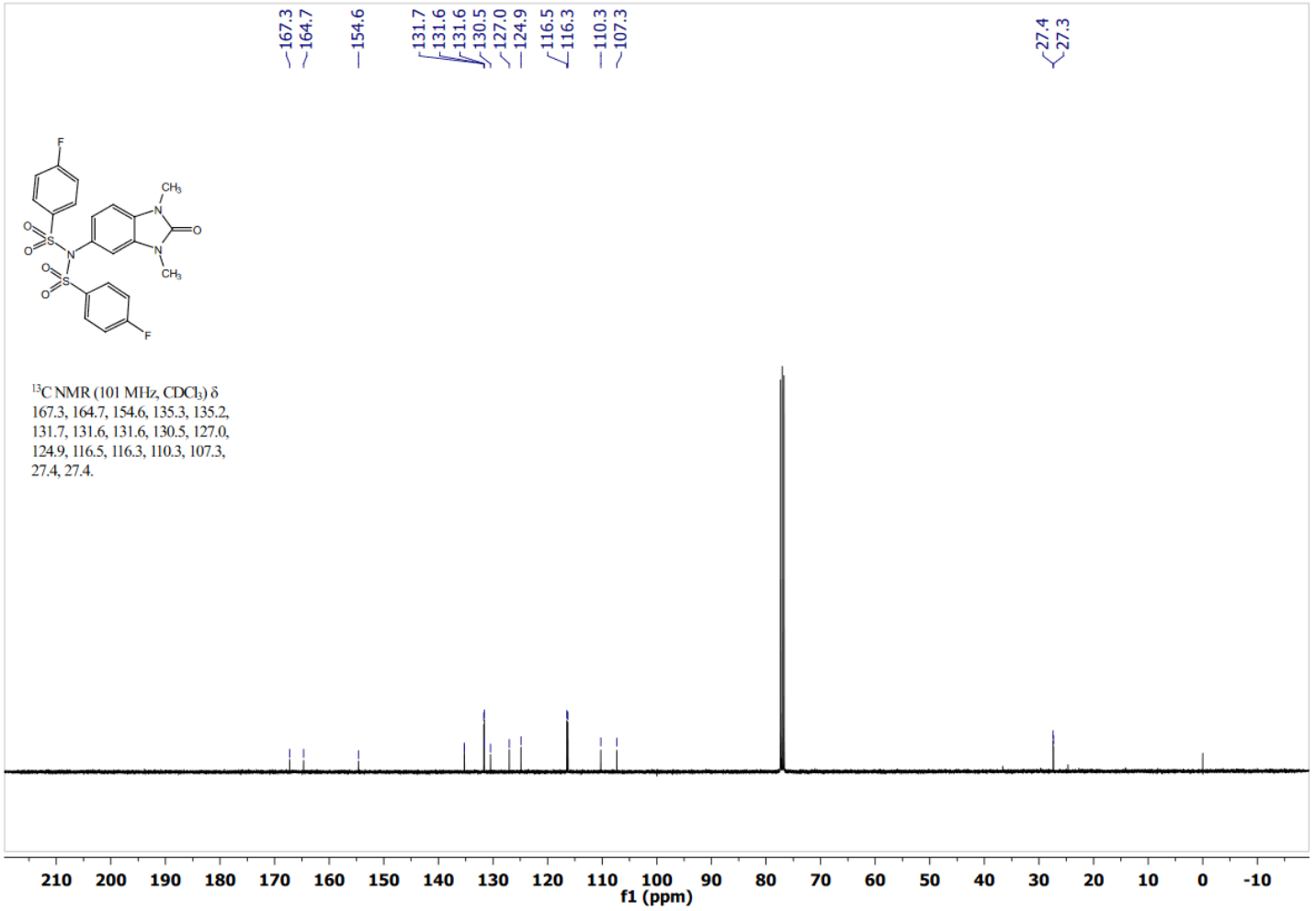

^{1}H NMR BL-X12

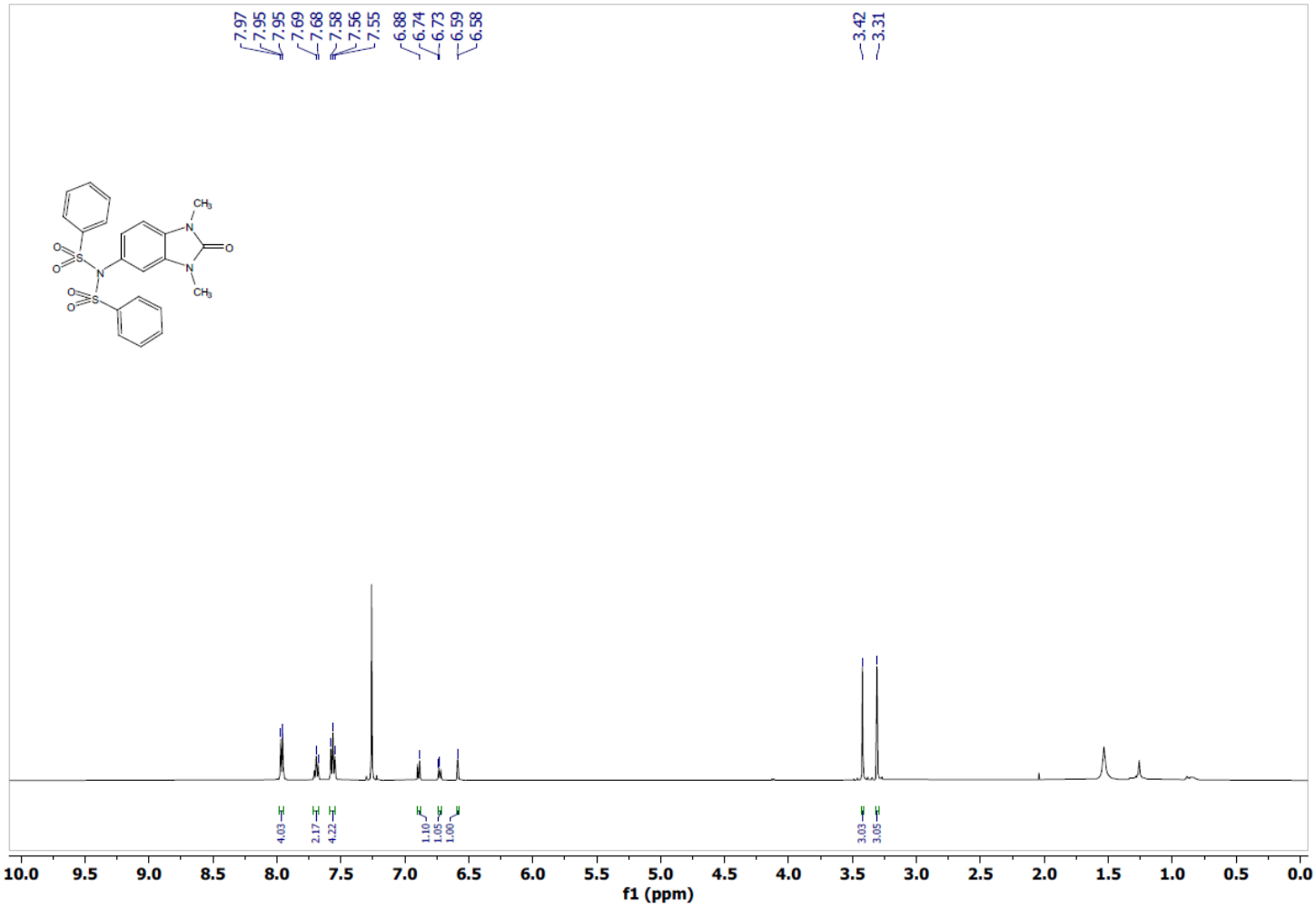
7.97
7.95
7.95
7.69
7.68
7.58
7.56
7.55
6.88
6.74
6.73
6.59
6.58
3.42
3.31
4.03
2.17
4.22
1.10
1.05
1.00
3.03
3.05
10.0 9.5 9.0 8.5 8.0 7.5 7.0 6.5 6.0 5.5 5.0 4.5 4.0 3.5 3.0 2.5 2.0 1.5 1.0 0.5 0.0
f1 (ppm)

^{13}C NMR BL-X12

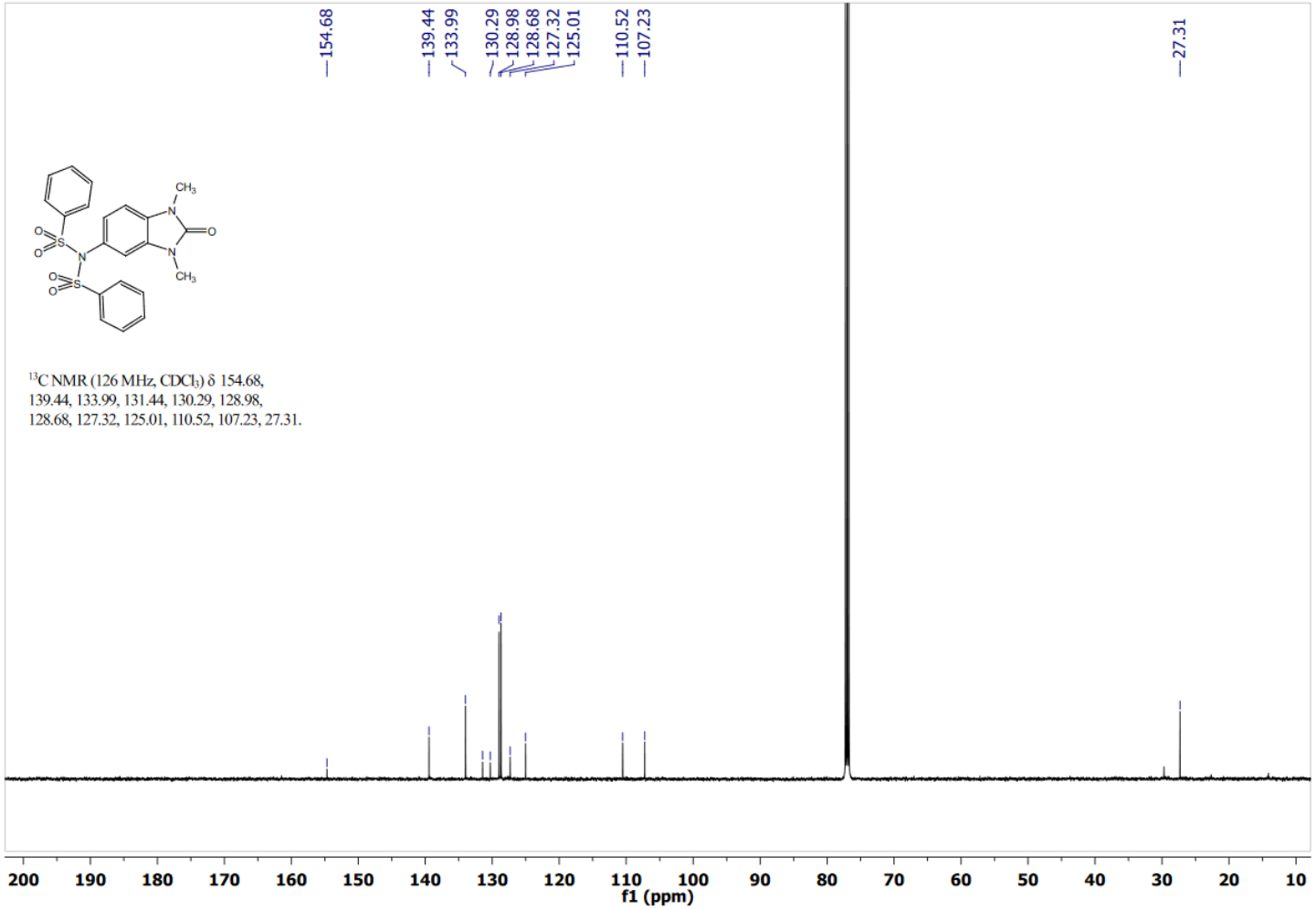

^{1}H NMR BL-X13

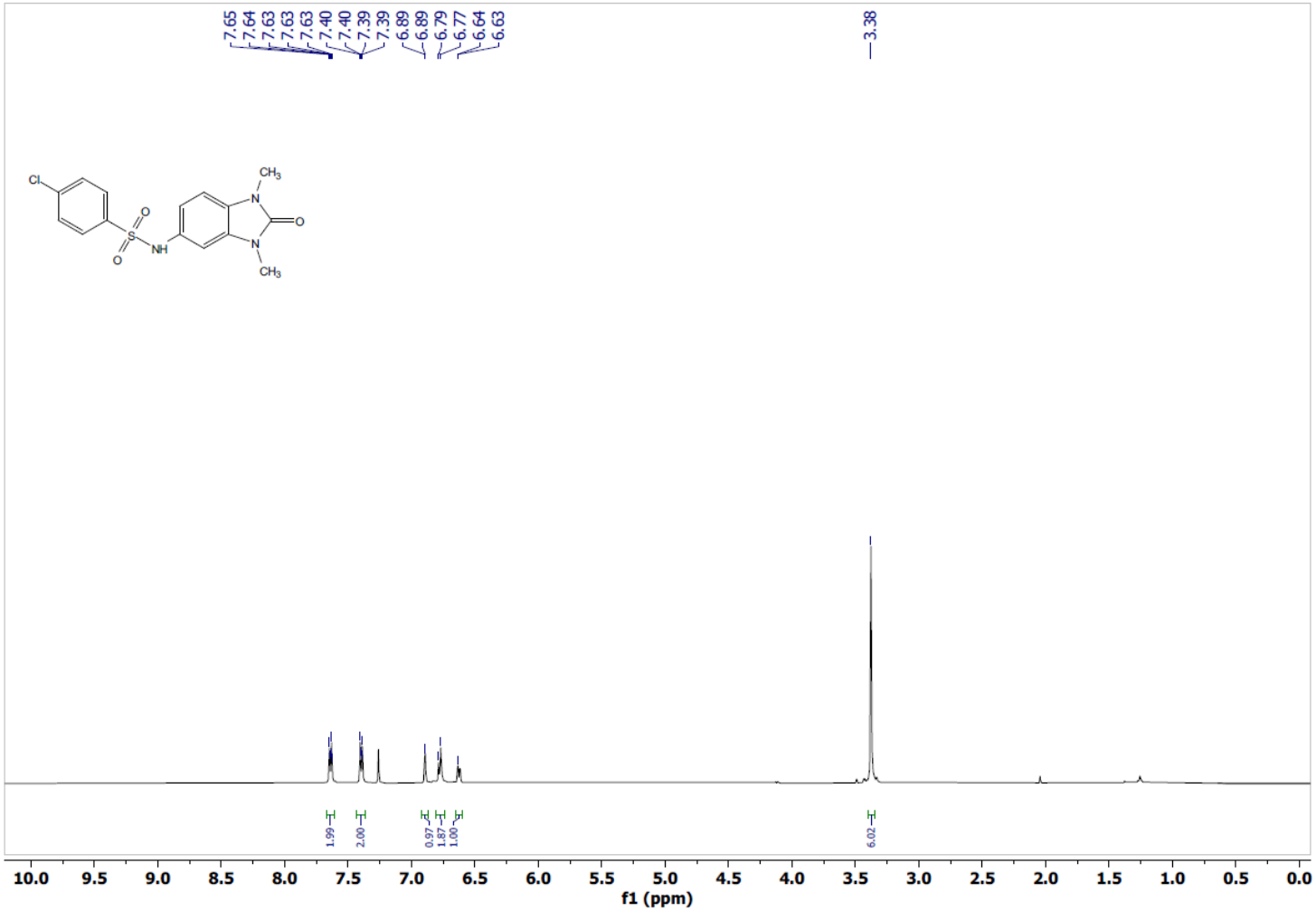
7.65
7.64
7.63
7.63
7.63
7.63
7.40
7.40
7.39
7.39
6.89
6.89
6.79
6.77
6.64
6.63
3.38
Cl
O
S
O
NH
N
CH3
O
N
CH3
1.99
2.00
0.97
1.87
1.00
6.02
10.0
9.5
9.0
8.5
8.0
7.5
7.0
6.5
6.0
5.5
5.0
4.5
4.0
3.5
3.0
2.5
2.0
1.5
1.0
0.5
0.0
f1 (ppm)

^{13}C NMR BL-X13

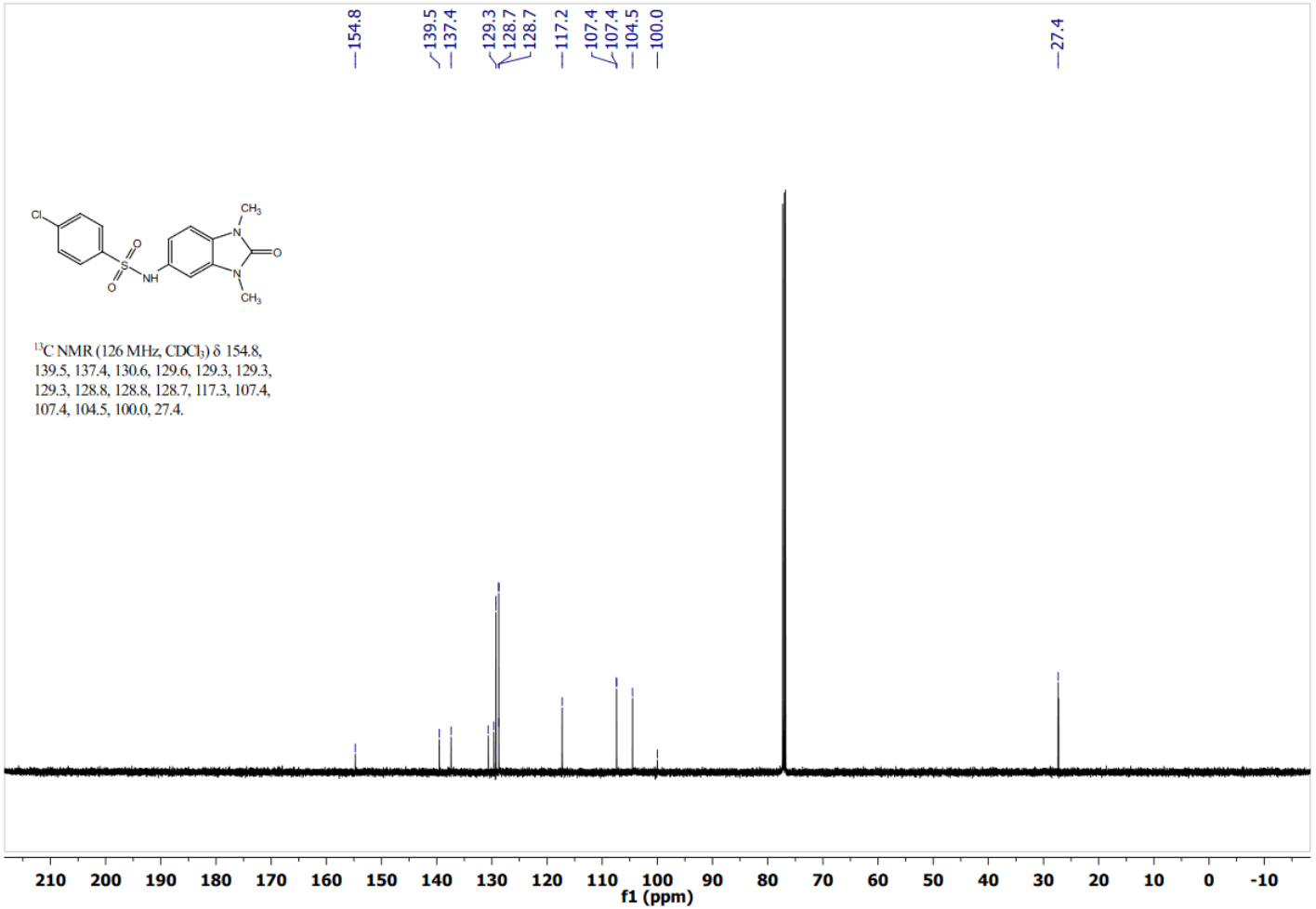

^{1}H NMR BL-X14

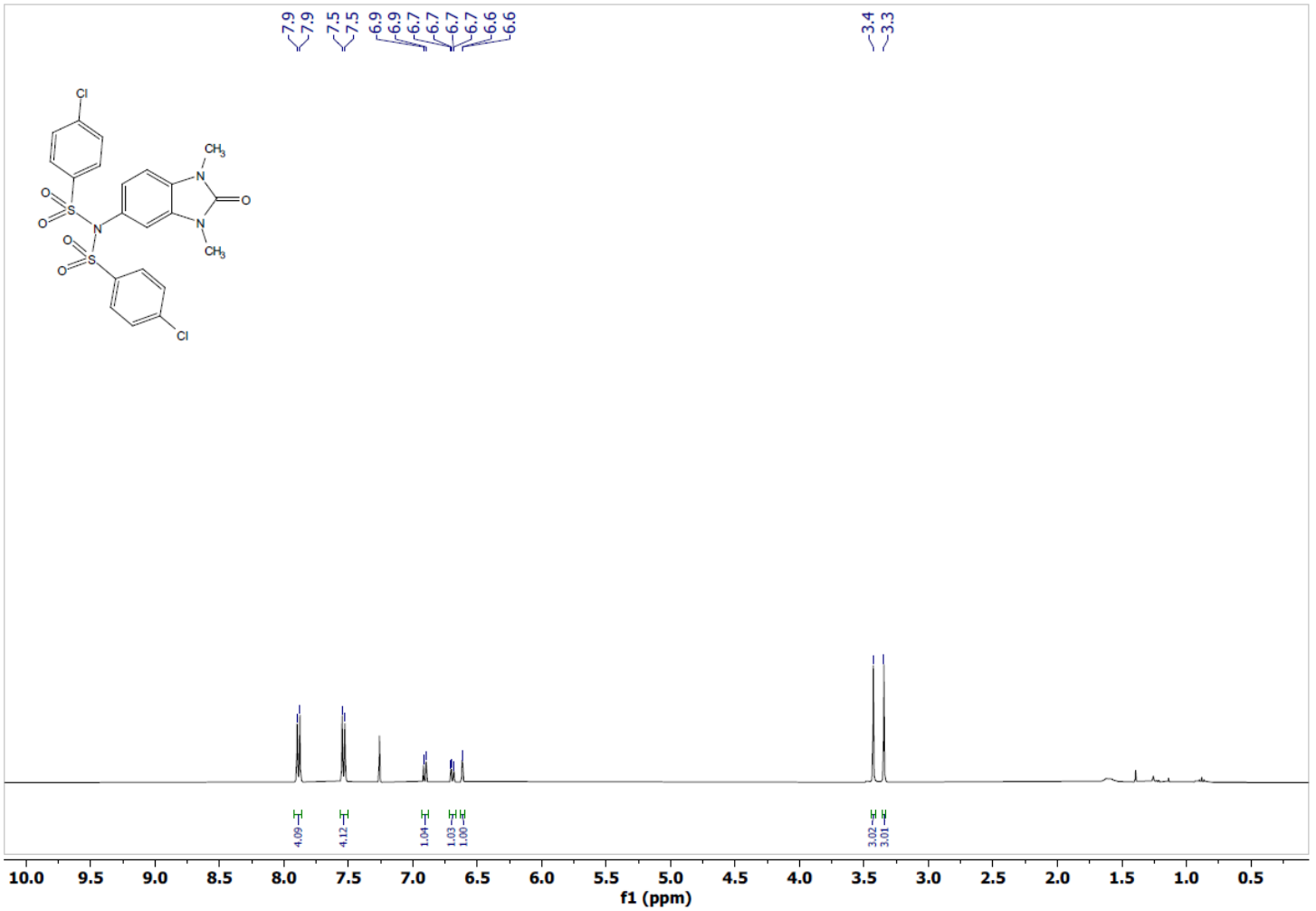
7.9
7.9
7.5
7.5
6.9
6.9
6.7
6.7
6.7
6.7
6.6
6.6
3.4
3.3
Cl
CH3
N
O
S
O
O
N
O
S
O
O
N
CH3
Cl
4.09
4.12
1.04
1.03
1.00
3.02
3.01
10.0
9.5
9.0
8.5
8.0
7.5
7.0
6.5
6.0
5.5
5.0
4.5
4.0
3.5
3.0
2.5
2.0
1.5
1.0
0.5
f1 (ppm)

^{13}C NMR BL-X14

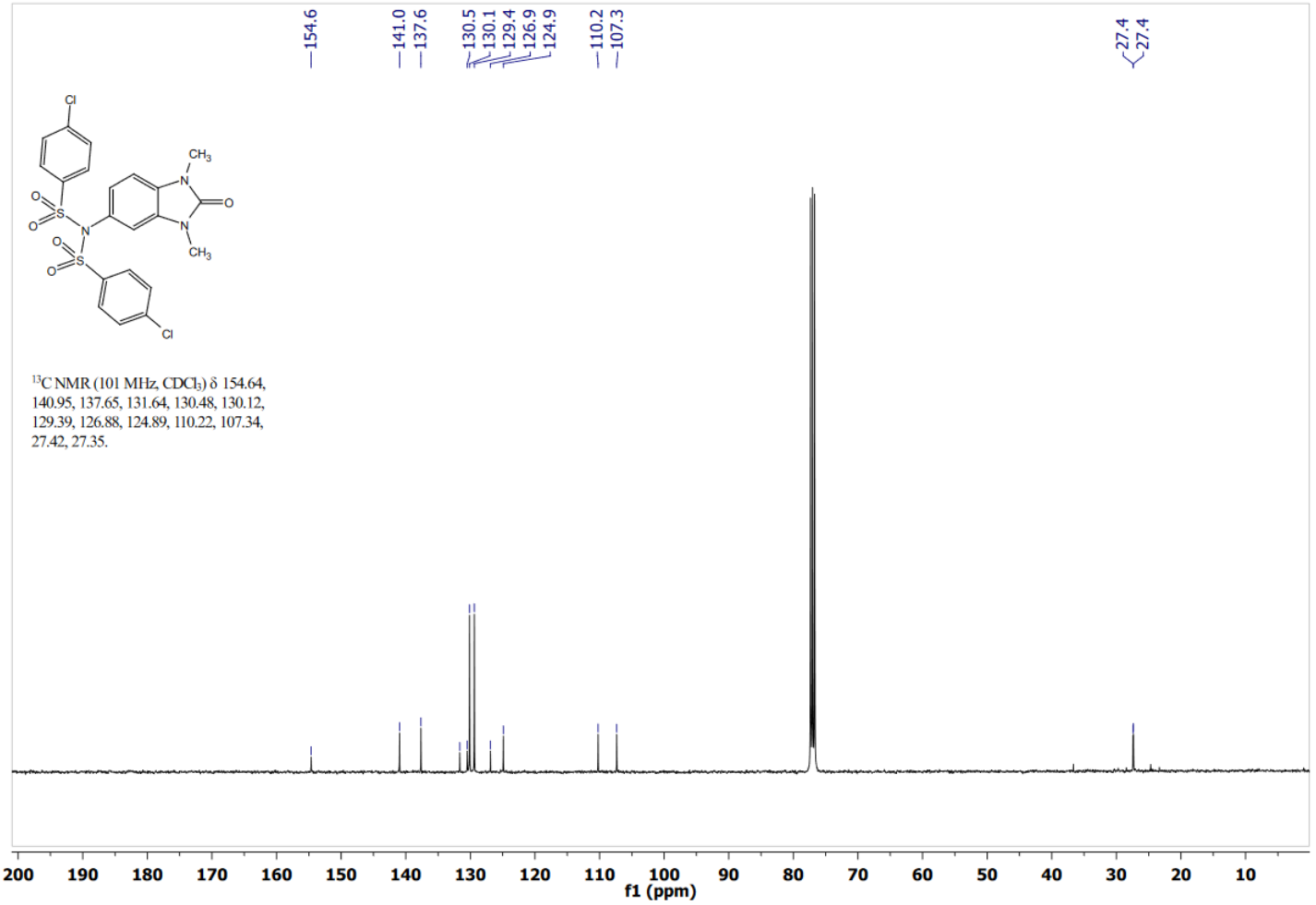

^{1}H NMR BL-X15

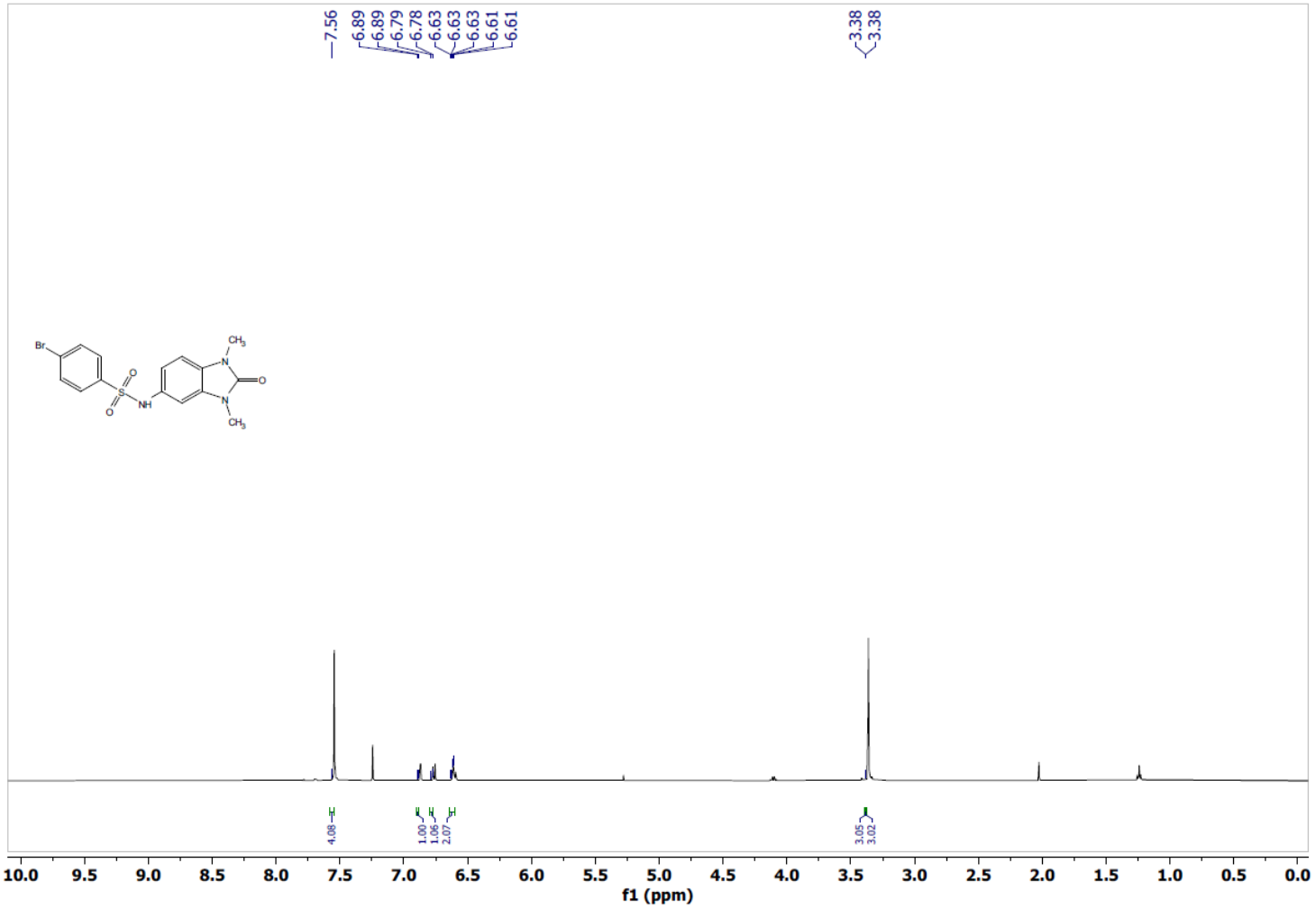
7.56
6.89
6.89
6.79
6.78
6.63
6.63
6.63
6.61
6.61
3.38
3.38
Br
S
O
O
NH
N
CH3
O
N
CH3
4.08
1.00
1.06
2.07
3.05
3.02
10.0
9.5
9.0
8.5
8.0
7.5
7.0
6.5
6.0
5.5
5.0
4.5
4.0
3.5
3.0
2.5
2.0
1.5
1.0
0.5
0.0
f1 (ppm)

^{13}C NMR BL-X15

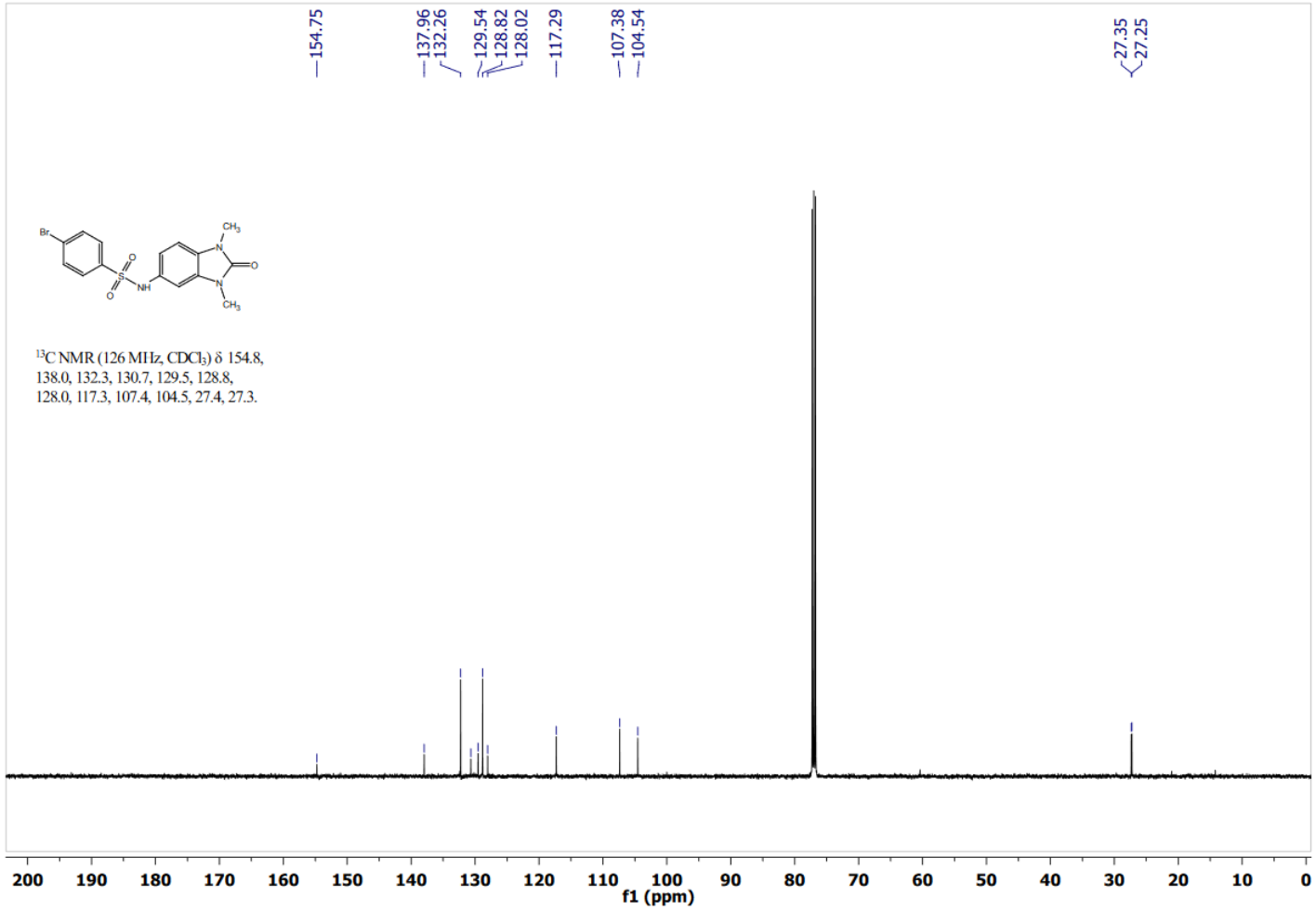

^{1}H NMR BL-X16

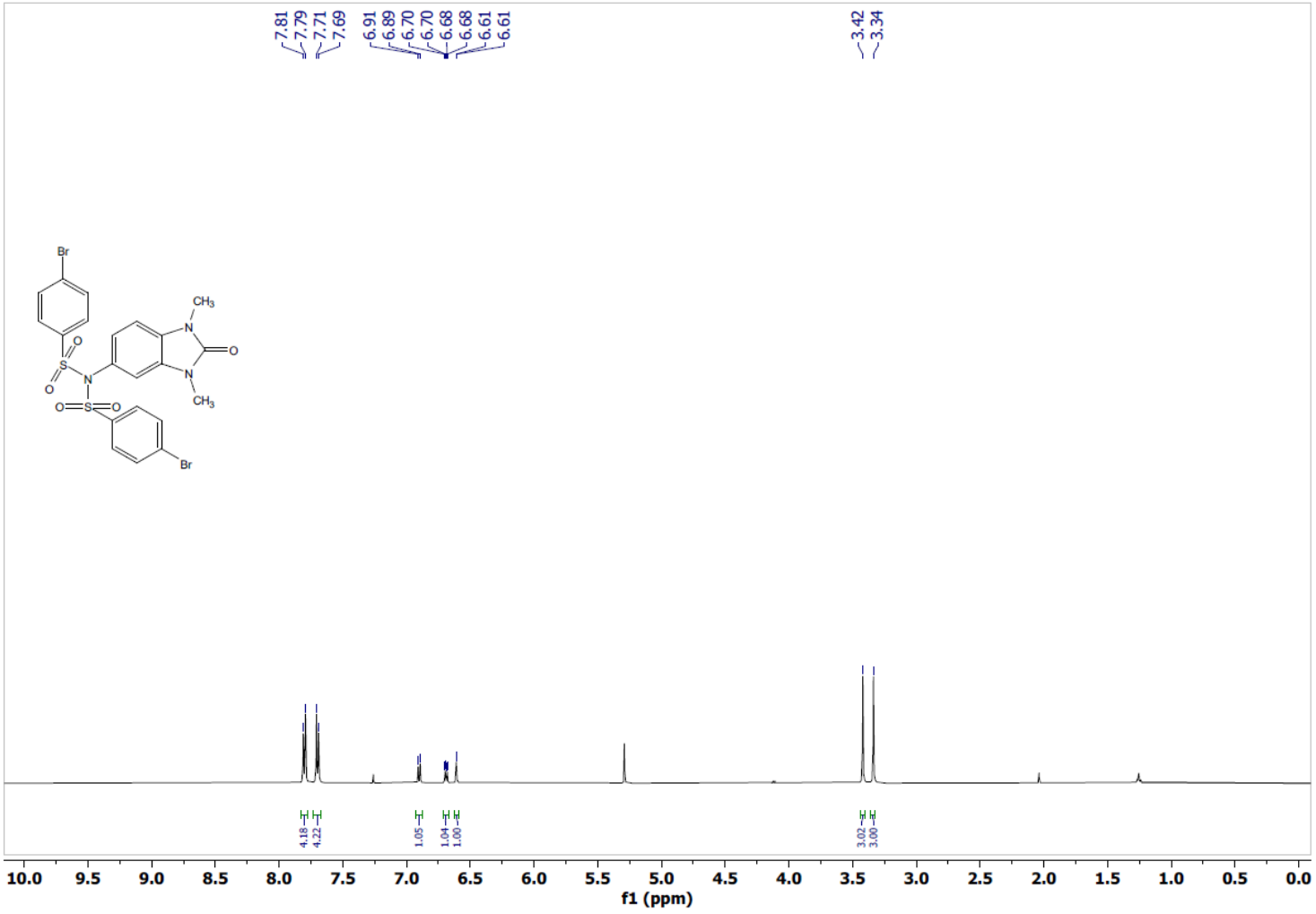
7.81
7.79
7.71
7.69
6.91
6.89
6.70
6.70
6.68
6.68
6.61
6.61
3.42
3.34
Br
CH3
N
O
S
O
N
O
S
O
CH3
Br
4.18
4.22
1.05
1.04
1.00
3.02
3.00
10.0
9.5
9.0
8.5
8.0
7.5
7.0
6.5
6.0
5.5
5.0
4.5
4.0
3.5
3.0
2.5
2.0
1.5
1.0
0.5
0.0
f1 (ppm)

^{13}C NMR BL-X16

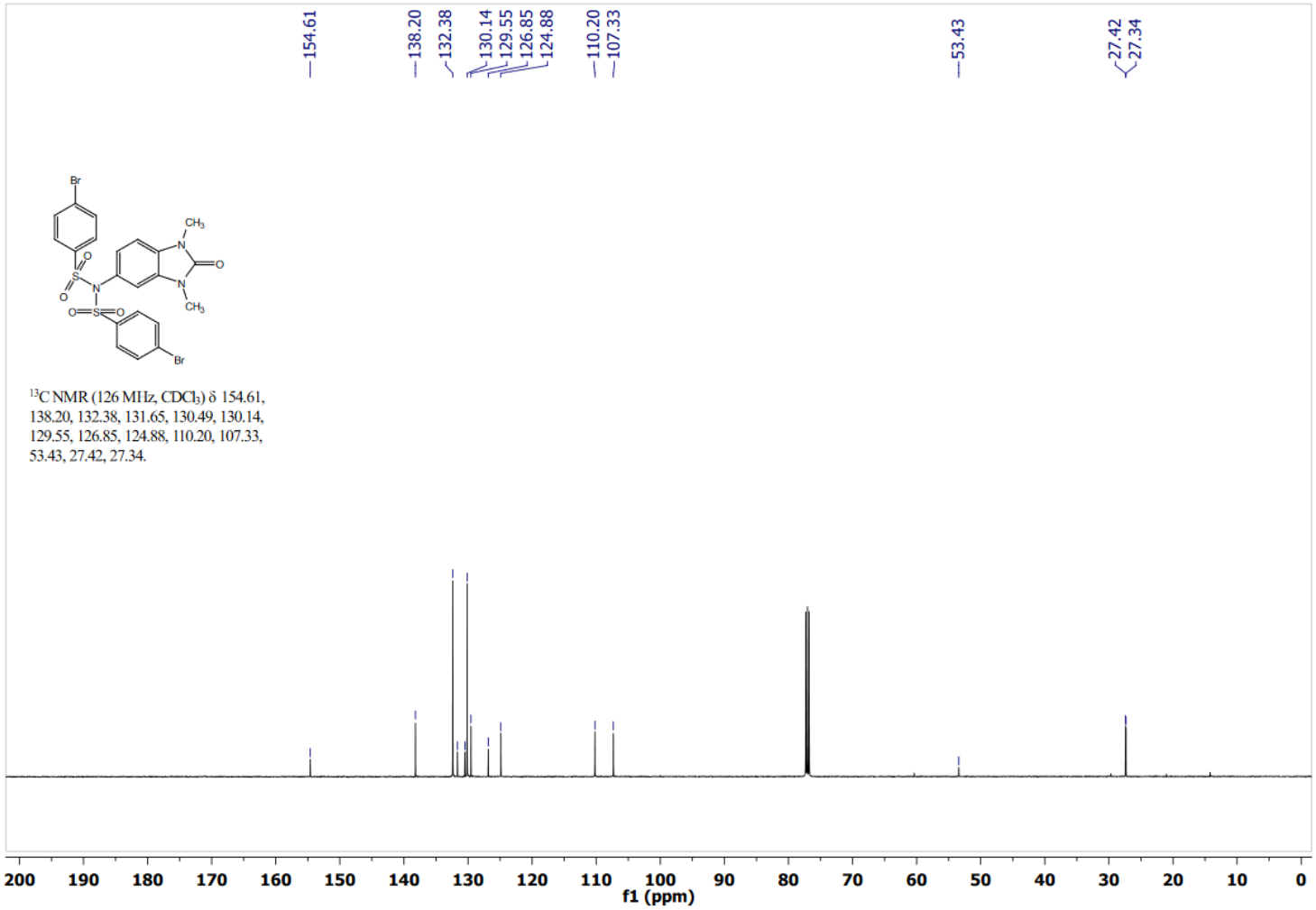

^{1}H NMR BL-X17

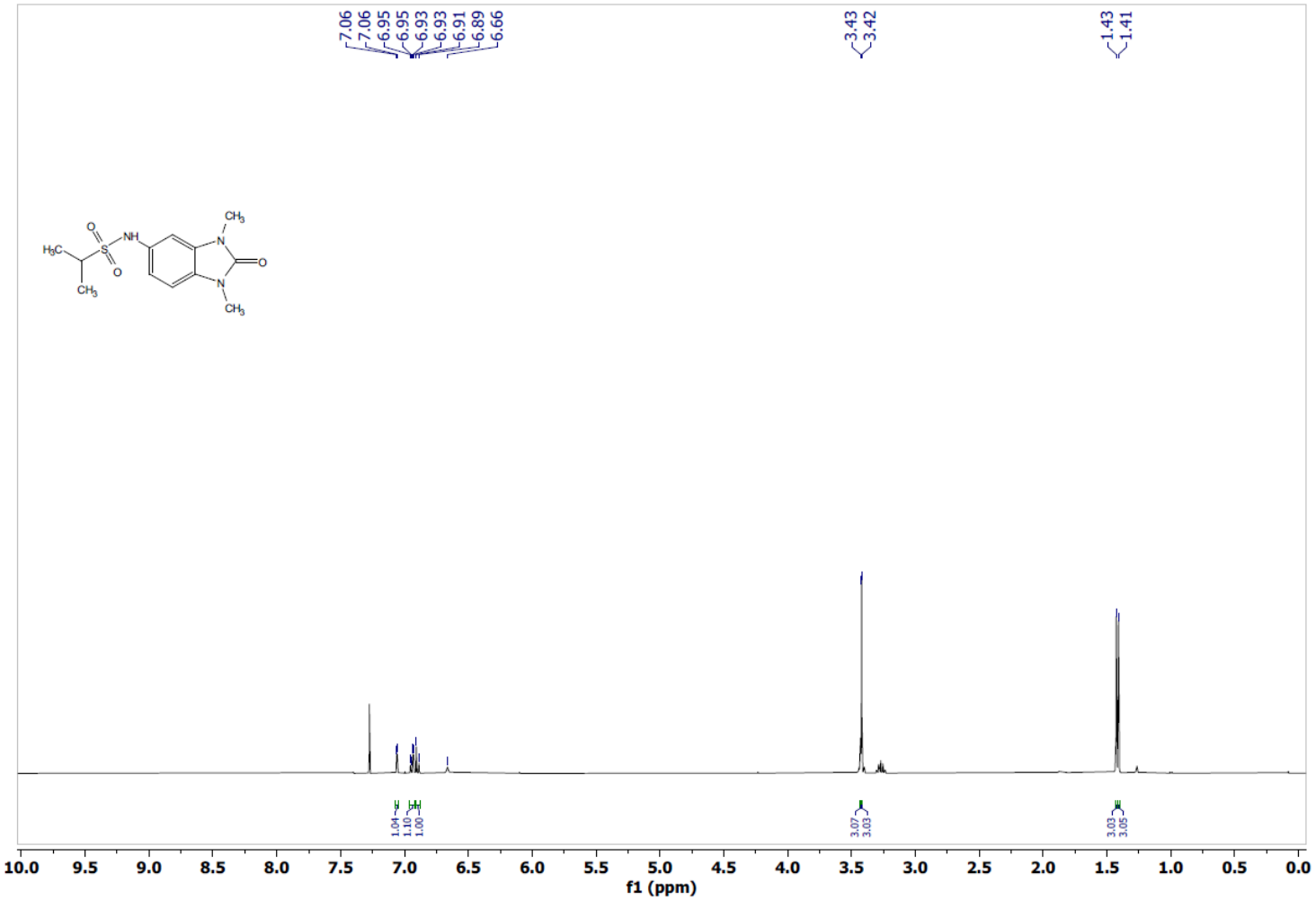
7.06
7.06
6.95
6.95
6.93
6.93
6.91
6.89
6.66
3.43
3.42
1.43
1.41
1.04
1.10
1.00
3.07
3.03
3.03
3.05
10.0
9.5
9.0
8.5
8.0
7.5
7.0
6.5
6.0
5.5
5.0
4.5
4.0
3.5
3.0
2.5
2.0
1.5
1.0
0.5
0.0
f1 (ppm)

^{13}C NMR BL-X17

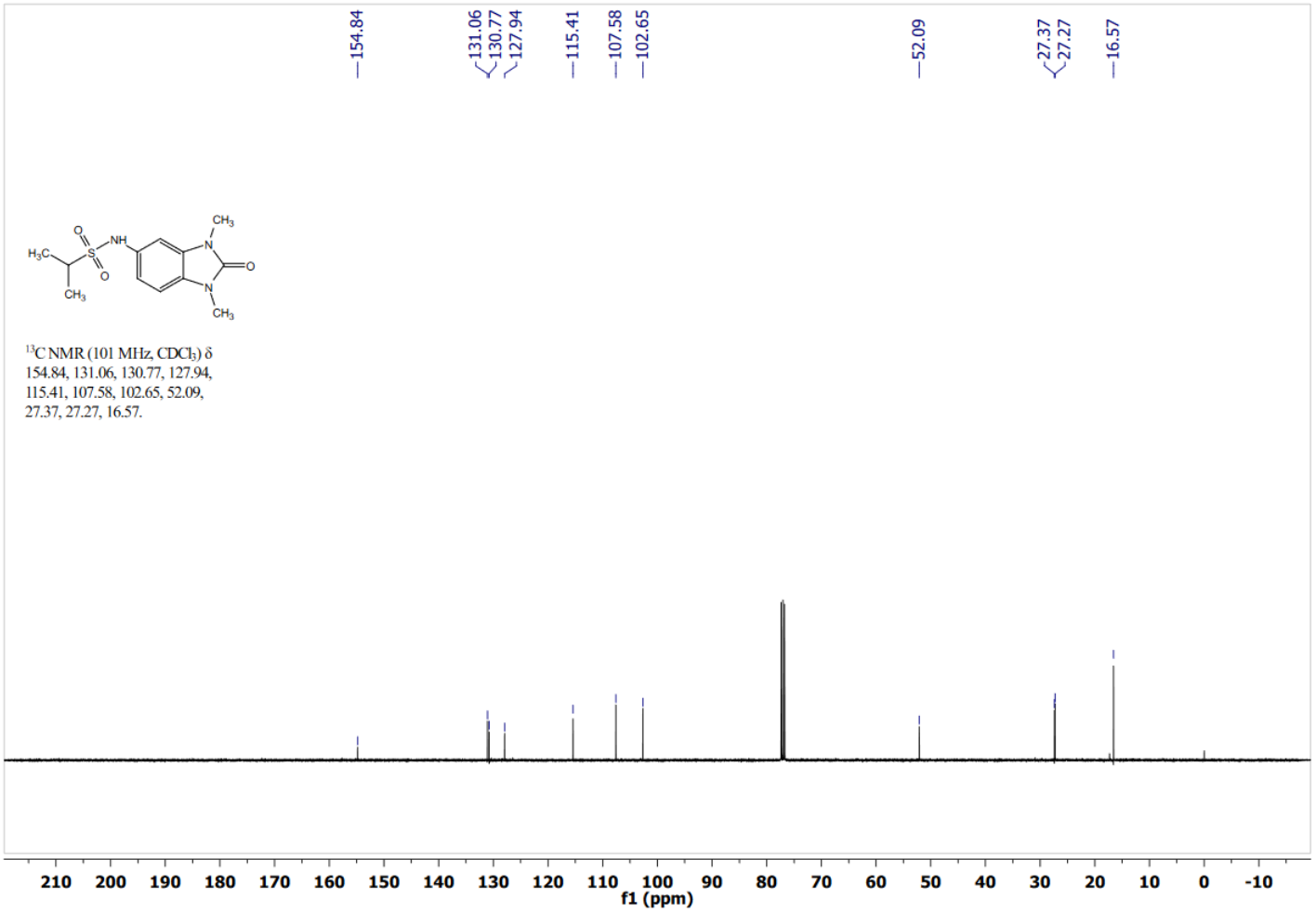

^{1}H NMR BL-X30

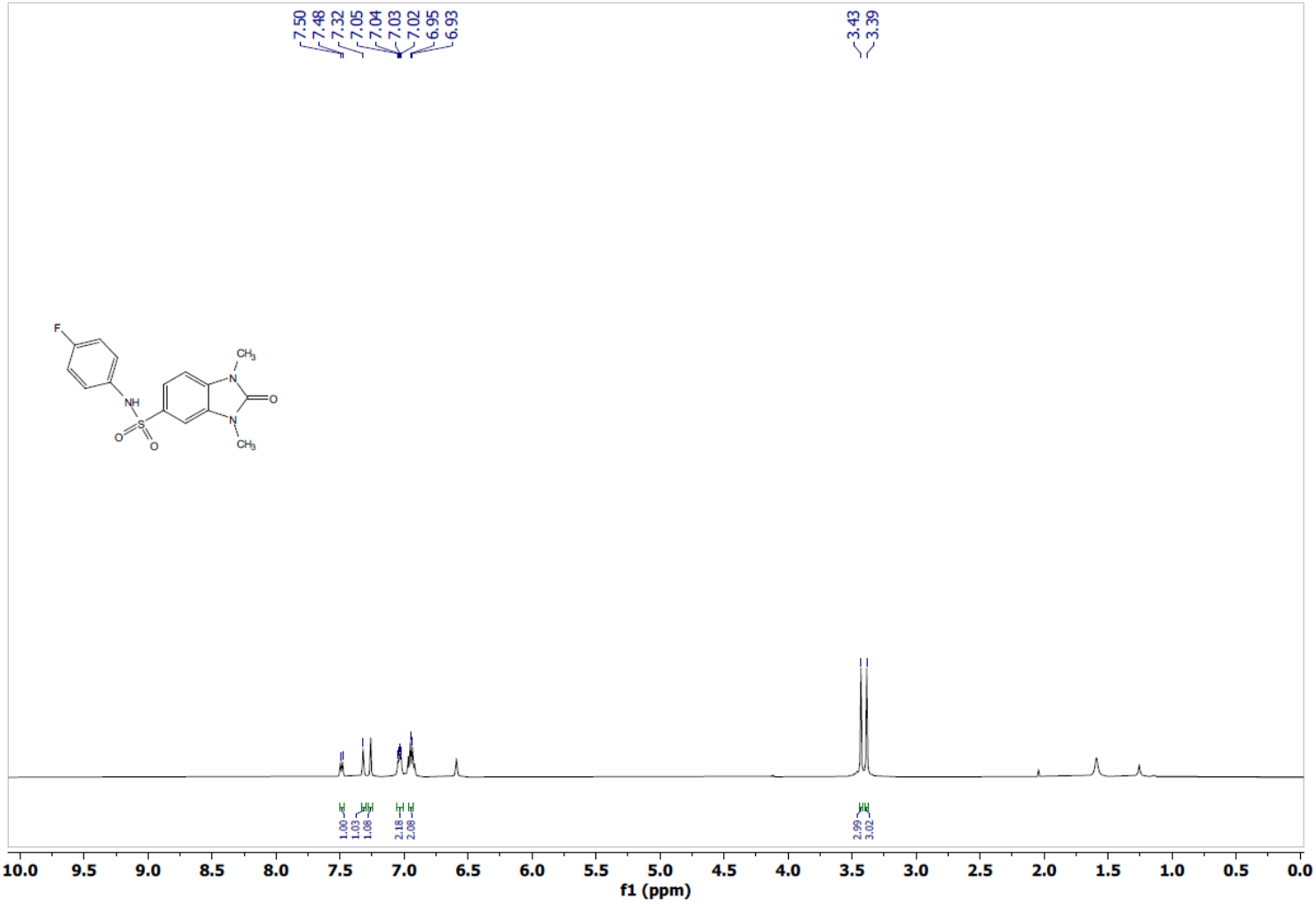
7.50
7.48
7.32
7.05
7.04
7.03
7.02
6.95
6.93
3.43
3.39
F
NH
S
O
O
N
CH3
N
CH3
O
1.00
1.03
1.08
2.18
2.08
2.99
3.02
10.0
9.5
9.0
8.5
8.0
7.5
7.0
6.5
6.0
5.5
5.0
4.5
4.0
3.5
3.0
2.5
2.0
1.5
1.0
0.5
0.0
f1 (ppm)

^{13}C NMR BL-X30

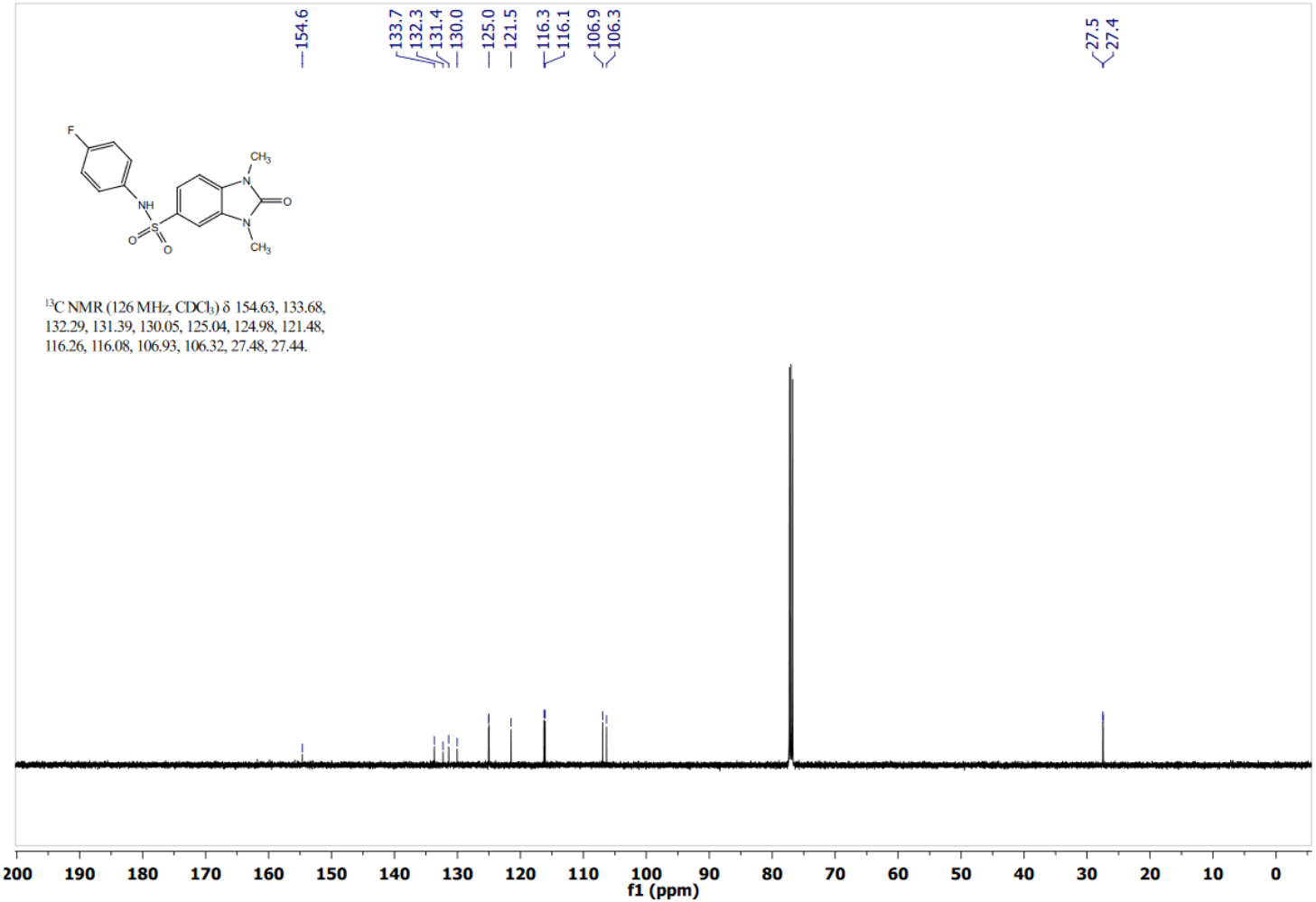

REFERENCES

1. Colon, N., Chung, D., Neuroblastoma. *Adv Pediatr* **2011,** *58* (1), 297-311.

2. Maris, J. M.; Hogarty, M. D.; Bagatell, R.; Cohn, S. L., Neuroblastoma. *Lancet* **2007,** *369* (9579), 2106-2120.

3. Park, J. R.; Eggert, A.; Caron, H., Neuroblastoma: Biology, Prognosis, and Treatment. *Hematology/Oncology Clinics of North America* **2010,** *24*, 65-86.

4. Wong, S. Y.; Hynes, R. O., Lymphatic or hematogenous dissemination: how does a metastatic tumor cell decide? *Cell cycle (Georgetown, Tex.)* **2006,** *5* (8), 812-7.

5. Monclair, T.; Brodeur, G. M.; Ambros, P. F.; Brisse, H. J.; Cecchetto, G.; Holmes, K.; Kaneko, M.; London, W. B.; Matthay, K. K.; Nuchtern, J. G.; von Schweinitz, D.; Simon, T.; Cohn, S. L.; Pearson, A. D. J., The International Neuroblastoma Risk Group (INRG) staging system: an INRG Task Force report. *Journal Of Clinical Oncology: Official Journal Of The American Society Of Clinical Oncology* **2009,** *27* (2), 298-303.

6. Duffy, D. J.; Krstic, A.; Halasz, M.; Schwarzl, T.; Konietzny, A.; Iljin, K.; Higgins, D. G.; Kolch, W., Retinoic acid and TGF-β signalling cooperate to overcome MYCN-induced retinoid resistance. *Genome Medicine* **2017,** *9*, 1-22.

7. Long, G.; Peiguo, C.; Robert, L.; Heather, M.; Steven, K.; Robert, J. H.; Zheng, L.; Yate-Ching, Y.; John, A. S.; Gregg, B. F.; Linda, H. M., The Mechanism by Which MYCN Amplification Confers an Enhanced Sensitivity to a PCNA-Derived Cell Permeable Peptide in Neuroblastoma Cells. *EBioMedicine* **2015,** (12), 1923.

8. Ratner, N.; Brodeur, G. M.; Dale, R. C.; Schor, N. F., The "neuro" of neuroblastoma: Neuroblastoma as a neurodevelopmental disorder. *Annals Of Neurology* **2016,** *80* (1), 13-23.

9. Kholodenko, I. V.; Kalinovsky, D. V.; Doronin, I. I.; Deyev, S. M.; Kholodenko, R. V., Neuroblastoma Origin and Therapeutic Targets for Immunotherapy. *Journal of Immunology Research* **2018**, 1-25.

10. O'Rahilly, R.; Müller, F., The development of the neural crest in the human. *Journal of Anatomy* **2007,** *211* (3), 335-351.

11. Chan, H. S.; Gallie, B. L.; DeBoer, G.; Haddad, G.; Ikegaki, N.; Dimitroulakos, J.; Yeger, H.; Ling, V., MYCN protein expression as a predictor of neuroblastoma prognosis. *Clinical Cancer Research* **1997,** *3* (10), 1699-1706.

12. Vega-Lopez, G. A.; Cerrizuela, S.; Aybar, M. J., Trunk neural crest cells: formation, migration and beyond. 2017; Vol. 61, pp 5-15.

13. Abzhanov, A.; Tzahor, E.; Lassar, A. B.; Tabin, C. J., Dissimilar regulation of cell differentiation in mesencephalic (cranial) and sacral (trunk) neural crest cells in vitro. 2003; Vol. 130, pp 4567-4579.

14. Garner, E. F.; Beierle, E. A., Cancer Stem Cells and Their Interaction with the Tumor Microenvironment in Neuroblastoma. 2016; Vol. 8.

15. Reynolds, C. P., Differentiating agents in pediatric malignancies: retinoids in neuroblastoma. *Current Oncology Reports* **2000,** *2* (6), 511-518.

16. Sidell, N.; Altman, A.; Seeger, R. C.; Haussler, M. R., Effects of retinoic acid (RA) on the growth and phenotypic expression of several human neuroblastoma cell lines. *Experimental Cell Research* **1983,** *148* (1), 21-30.

17. de Thé, H., Differentiation therapy revisited. *Nature Reviews Cancer* **2017,** *18*, 117.

18. Dela Cruz, F.; Matushansky, I., Solid Tumor Differentiation Therapy - Is It Possible? 2012; Vol. 3, pp 559-567.

19. R B Livingston, a.; Hart, J. S., The Clinical Applications of Cell Kinetics in Cancer Therapy. *Annual Review of Pharmacology and Toxicology* **1977,** *17* (1), 529-543.

20. Tubiana, M., Tumor cell proliferation kinetics and tumor growth rate. *Acta oncologica (Stockholm, Sweden)* **1989,** *28* (1), 113-21.

21. Hoshi, N.; Hitomi, J.; Kusakabe, T.; Fukuda, T.; Hirota, M.; Suzuki, T., Distinct morphological and immunohistochemical features and different growth rates among four human neuroblastomas heterotransplanted into nude mice. *Medical Molecular Morphology* **2008,** *41* (3), 151-159.

22. Khoury, K. A.; Floch, M. H.; Hersh, T., Small intestinal mucosal cell proliferation and bacterial flora in the conventionalization of the germfree mouse. *The Journal of experimental medicine* **1969,** *130* (3), 659-670.

23. Yang, N. S.; Kube, D.; Park, C.; Furmanski, P., Growth of human mammary epithelial cells on collagen gel surfaces. *Cancer Res* **1981,** *41* (10), 4093-100.

24. Pahlman, S.; Ruusala, A. I.; Abrahamsson, L.; Mattsson, M. E.; Esscher, T., Retinoic acid-induced differentiation of cultured human neuroblastoma cells: a comparison with phorbolester-induced differentiation. *Cell differentiation* **1984,** *14* (2), 135-44.

25. Ponzoni, M.; Bocca, P.; Chiesa, V.; Pistoia, V.; Raffaghello, L.; Rozzo, C.; Montaldo, P. G.; Decensi, A., Differential Effects of N-(4-Hydroxyphenyl)retinamide and Retinoic Acid on Neuroblastoma Cells: Apoptosis versus Differentiation. *Cancer Research* **1995,** *55* (4), 853-861.

26. Michaela, S.; Veronica, P.; Shannon, W.; Liqin, D., MicroRNAs in neuroblastoma differentiation and differentiation therapy. *Advances in Modern Oncology Research* **2017,** (5), 213.

27. Zhao, Z.; Ma, X.; Hsiao, T.-H.; Lin, G.; Kosti, A.; Yu, X.; Suresh, U.; Chen, Y.; Tomlinson, G. E.; Pertsemlidis, A.; Du, L., A high-content morphological screen identifies novel microRNAs that regulate neuroblastoma cell differentiation. 2014; Vol. 5, pp 2499-2512.

28. Chlapek, P.; Slavikova, V.; Mazanek, P.; Sterba, J.; Veselska, R., Why Differentiation Therapy Sometimes Fails: Molecular Mechanisms of Resistance to Retinoids. *International Journal of Molecular Sciences* **2018,** *19* (1), 132.

29. Pession, A.; Trerè, D.; Perri, P.; Rondelli, R.; Montanaro, L.; Mantovani, W.; Derenzini, M.; Paolucci, G., N-myc amplification and cell proliferation rate in human neuroblastoma. *The Journal of Pathology* **1997,** *183* (3), 339-344.

30. Beltran, H., The N-myc Oncogene: Maximizing its Targets, Regulation, and Therapeutic Potential. 2014; Vol. 12, pp 815-822.

31. Wenzel, A.; Schwab, M., The mycN/max protein complex in neuroblastoma. Short review. *European Journal Of Cancer (Oxford, England: 1990)* **1995,** *31A* (4), 516-519.

32. Ruiz-Perez, M. V.; Henley, A. B.; Arsenian-Henriksson, M., The MYCN Protein in Health and Disease. 2017; Vol. 8.

33. BET Bromodomain Inhibition as a Therapeutic Strategy to Target c-Myc. *Cell* **2011,** *146* (6), 904-917.

34. Das, B. C.; Thapa, P.; Karki, R.; Das, S.; Mahapatra, S.; Liu, T.-C.; Torregroza, I.; Wallace, D. P.; Kambhampati, S.; Van Veldhuizen, P.; Verma, A.; Ray, S. K.; Evans, T., Retinoic acid signaling pathways in development and diseases. *Bioorganic & Medicinal Chemistry* **2014,** *22* (2), 673-683.

35. Janesick, A.; Wu, S. C.; Blumberg, B., Retinoic acid signaling and neuronal differentiation. *Cellular and Molecular Life Sciences* **2015,** *72* (8), 1559.

36. Jeon, J.; Kwon, H.; Cho, E.; Kim, K. S.; Yun, J.; Lee, Y. C.; Kim, D. H., The effect of coniferaldehyde on neurite outgrowth in neuroblastoma Neuro2a cells. *Neurochemistry International* **2019,** *131*.

37. Mihaylova, M. M.; Shaw, R. J., The AMPK signalling pathway coordinates cell growth, autophagy and metabolism. 2011; Vol. 13, pp 1016-1023.

38. Dickey, A.; Schleicher, S.; Leahy, K.; Hu, R.; Hallahan, D.; Thotala, D. K., GSK-3β inhibition promotes cell death, apoptosis, and in vivo tumor growth delay in neuroblastoma Neuro-2A cell line. *Journal Of Neuro-Oncology* **2011,** *104* (1), 145-153.

39. Suebsoonthron, J.; Jaroonwitchawan, T.; Yamabhai, M.; Noisa, P., Inhibition of WNT signaling reduces differentiation and induces sensitivity to doxorubicin in human malignant neuroblastoma SH-SY5Y cells. 2017; Vol. 28, pp 469-479.

40. Armstrong, J. L.; Taylor, G. A.; Thomas, H. D.; Boddy, A. V.; Redfern, C. P. F.; Veal, G. J., Molecular targeting of retinoic acid metabolism in neuroblastoma: the role of the CYP26 inhibitor R116010 in vitro and in vivo. *British Journal Of Cancer* **2007,** *96* (11), 1675-1683.

41. BROMODOMAIN INHIBITORS FOR TREATING DISEASE. 2016.

42. Heinemann, A.; Cullinane, C.; De Paoli-Iseppi, R.; Wilmott, J. S.; Gunatilake, D.; Madore, J.; Strbenac, D.; Yang, J. Y.; Gowrishankar, K.; Tiffen, J. C.; Prinjha, R. K.; Smithers, N.; McArthur, G. A.; Hersey, P.; Gallagher, S. J., Combining BET and HDAC inhibitors synergistically induces apoptosis of melanoma and suppresses AKT and YAP signaling. 2015; Vol. 6, pp 21507-21521.

43. Dowden, H.; Munro, J., Trends in clinical success rates and therapeutic focus. *Nature Reviews Drug Discovery* **2019,** *18* (7), 495.

44. Galloway, W. R. J. D.; Isidro-Llobet, A.; Spring, D. R., Diversity-oriented synthesis as a tool for the discovery of novel biologically active small molecules. *Nature Communications* **2010,** *1*, 80.

45. Prueksaritanont, T.; Tang, C., ADME of Biologics-What Have We Learned from Small Molecules? 2012; Vol. 14, pp 410-419.

46. Van Vleet, T. R.; Liguori, M. J.; Lynch, J. J., 3rd; Rao, M.; Warder, S., Screening Strategies and Methods for Better Off-Target Liability Prediction and Identification of Small-Molecule Pharmaceuticals. *SLAS Discovery: Advancing Life Sciences R & D* **2019,** *24* (1), 1-24.

47. Doogue, M. P.; Polasek, T. M., The ABCD of clinical pharmacokinetics. *Therapeutic advances in drug safety* **2013,** *4* (1), 5-7.

48. Reinhold, A. K.; Rittner, H. L., Barrier function in the peripheral and central nervous system-a review. *Pflugers Archiv: European Journal Of Physiology* **2017,** *469* (1), 123-134.

49. Liu, H.; Chen, Y.; Huang, L.; Sun, X.; Fu, T.; Wu, S.; Zhu, X.; Zhen, W.; Liu, J.; Lu, G.; Cai, W.; Yang, T.; Zhang, W.; Yu, X.; Wan, Z.; Wang, J.; Summerfield, S. G.; Dong, K.; Terstappen, G. C., Drug Distribution into Peripheral Nerve. 2018; Vol. 365, pp 336-345.

50. Zheng, W.; Thorne, N.; McKew, J. C., Phenotypic screens as a renewed approach for drug discovery. *Drug Discovery Today* **2013,** *18* (21-22), 1067-1073.

51. Moffat, J. G.; Rudolph, J.; Bailey, D., Phenotypic screening in cancer drug discovery - past, present and future. *Nature reviews. Drug discovery* **2014,** *13* (8), 588-602.

52. Johnston, P. A.; Trask, O. J., *High content screening : a powerful approach to systems cell biology and phenotypic drug discovery*. New York, NY : Humana Press, [2018].

Second edition.: 2018.

53. Radio, N. M.; Breier, J. M.; Shafer, T. J.; Mundy, W. R., Assessment of chemical effects on neurite outgrowth in PC12 cells using high content screening. *Toxicological sciences : an official journal of the Society of Toxicology* **2008,** *105* (1), 106-18.

54. Du, L., Research Plan.

55. Decarolis, B.; Simon, T.; Krug, B.; Leuschner, I.; Vokuhl, C.; Kaatsch, P.; von Schweinitz, D.; Klingebiel, T.; Mueller, I.; Schweigerer, L.; Berthold, F.; Hero, B., Treatment and outcome of Ganglioneuroma and Ganglioneuroblastoma intermixed. 2016; Vol. 16.

56. DeSimone, R. W.; Currie, K. S.; Mitchell, S. A.; Darrow, J. W.; Pippin, D. A., Privileged structures: applications in drug discovery. *Combinatorial chemistry & high throughput screening* **2004,** *7* (5), 473-94.

57. Welsch, M. E.; Snyder, S. A.; Stockwell, B. R., Privileged scaffolds for library design and drug discovery. *Current Opinion in Chemical Biology* **2010,** *14* (3), 347-361.

58. Zanella, F.; Lorens, J. B.; Link, W., High content screening: seeing is believing. *Trends in Biotechnology* **2010,** *28* (5), 237-245.

59. Overington, J. P.; Al-Lazikani, B.; Hopkins, A. L., How many drug targets are there? *Nature reviews. Drug discovery* **2006,** *5* (12), 993-6.

60. Hann, M. M., Molecular obesity, potency and other addictions in drug discovery. 2011; Vol. 2, pp 349-355.

61. Pharmacophore Perception, Development and Use in Drug Design. *Molecules* **2000,** *5* (7), 987.

62. Dearden, J., The History and Development of Quantitative Structure-Activity Relationships (QSARs): Addendum. *International Journal of Quantitative Structure-Property Relationships* **2017,** *2* (2), 36.

63. Punj, S.; Kopparapu, P.; Jang, H. S.; Phillips, J. L.; Pennington, J.; Rohlman, D.; O'Donnell, E.; Iversen, P. L.; Kolluri, S. K.; Kerkvliet, N. I., Benzimidazoisoquinolines: A New Class of Rapidly Metabolized Aryl Hydrocarbon Receptor (AhR) Ligands that Induce AhR-Dependent Tregs and Prevent Murine Graft-Versus-Host Disease. 2014; Vol. 9.

64. Chopra, A. S.; Kuratnik, A.; Giardina, C.; Scocchera, E. W.; Wright, D. L., Identification of novel compounds that enhance colon cancer cell sensitivity to inflammatory apoptotic ligands. *Cancer Biology and Therapy* **2013,** *14* (5), 436-449.

65. Kao, R. Y. T.; Jenkins, J. L.; Olson, K. A.; Key, M. E.; Fett, J. W.; Shapiro, R., A small-molecule inhibitor of the ribonucleolytic activity of human angiogenin that possesses antitumor activity. *Proceedings of the National Academy of Sciences* **2002,** *99* (15), 10066-10071.

66. Kujawski, J., The log P Parameter as a Molecular Descriptor in the Computer-aided Drug Design – an Overview. *COMPUTATIONAL METHODS IN SCIENCE AND TECHNOLOGY* **2012**.

67. Lipinski, C. A.; Lombardo, F.; Dominy, B. W.; Feeney, P. J., Experimental and computational approaches to estimate solubility and permeability in drug discovery and development settings. *Advanced Drug Delivery Reviews* **2012,** *64* (Supplement), 4-17.

68. Prasanna, S.; Doerksen, R. J., Topological Polar Surface Area: A Useful Descriptor in 2D-QSAR. 2009; Vol. 16, pp 21-41.

69. Smolyar, N. N.; Pankina, O. Y.; Bondarenko, A. I.; Borodkin, Y. S.; Khizhan, A. I., Synthesis of 1,3-dialkyl-5-(hetaryl-1-yl)-1,3-dihydrobenzimidazol-2-ones. *Russian Journal of Organic Chemistry* **2011,** *47* (8), 1190.

70. Feng, M.; Tang, B.; Liang, S. H.; Jiang, X., Sulfur Containing Scaffolds in Drugs: Synthesis and Application in Medicinal Chemistry. 2016; Vol. 16, pp 1200-1216.

71. Scozzafava, A.; Owa, T.; Mastrolorenzo, A.; Supuran, C. T., Anticancer and antiviral sulfonamides. 2003; Vol. 10, pp 925-953.

72. Wang, Y.; Tong, J.; Wu, W.; Xu, Z.; Lu, Y., Organic fluorines as halogen bond donors: Theoretical study and crystallographic evidence. *International Journal of Quantum Chemistry* **2015,** *115* (14), 884-890.

73. Wilcken, R.; Zimmermann, M. O.; Lange, A.; Joerger, A. C.; Boeckler, F. M., Principles and Applications of Halogen Bonding in Medicinal Chemistry and Chemical Biology. 2013; Vol. 56, pp 1363-1388.

74. Chopra, D.; Row, T. N. G., Role of organic fluorine in crystal engineering. *CrystEngComm* **2011,** *13* (7), 2175-2186.

75. Horiuchi, D.; Anderton, B.; Goga, A., Taking on challenging targets: making MYC druggable. *American Society Of Clinical Oncology Educational Book. American Society Of Clinical Oncology. Annual Meeting* **2014**, e497-e502.

76. Puissant, A.; Frumm, S. M.; Alexe, G.; Bassil, C. F.; Qi, J.; Chanthery, Y. H.; Nekritz, E. A.; Zeid, R.; Gustafson, W. C.; Greninger, P.; Garnett, M. J.; McDermott, U.; Benes, C. H.; Kung, A. L.; Weiss, W. A.; Bradner, J. E.; Stegmaier, K., Targeting MYCN in Neuroblastoma by BET Bromodomain Inhibition. 2013; Vol. 3, pp 308-323.